BARRIER LAYERS OF THE ATLANTIC WARM POOL: FORMATION MECHANISM AND INFLUENCE ON WEATHER AND CLIMATE

A Dissertation

by

KARTHIK BALAGURU

Submitted to the Office of Graduate Studies of
Texas A&M University
in partial fulfillment of the requirements for the degree of

DOCTOR OF PHILOSOPHY

May 2011

Major Subject: Oceanography

BARRIER LAYERS OF THE ATLANTIC WARM POOL: FORMATION MECHANISM AND INFLUENCE ON WEATHER AND CLIMATE

A Dissertation

by

KARTHIK BALAGURU

Submitted to the Office of Graduate Studies of
Texas A&M University
in partial fulfillment of the requirements for the degree of

DOCTOR OF PHILOSOPHY

Approved by:

Chair of Committee,	Ping Chang
Committee Members,	Ramalingam Saravanan
	Benjamin Giese
	Robert Hetland
Head of Department,	Piers Chapman

May 2011

Major Subject: Oceanography

ABSTRACT

Barrier Layers of the Atlantic Warm Pool: Formation Mechanism and Influence on Weather and Climate. (May 2011)

Karthik Balaguru, B.Tech, Indian Institute of Technology - Madras;
M.Tech, Indian Institute of Technology - Madras

Chair of Advisory Committee: Dr. Ping Chang

The aim of this research is to study the formation mechanism of Barrier Layers (BL) in the western tropical Atlantic and their influence on the tropical Atlantic climate at both short and long timescales. Many Coupled General Circulation Models (CGCMs) tend to overestimate the salinity in the Atlantic warm pool or the Northwestern Tropical Atlantic (NWTA) and underestimate the surface salinity in the subtropical salinity maxima region. Most of these models also suffer from a sea-surface temperature (SST) bias in the NWTA region, leading to suggestions that the upper ocean salinity stratification may need to be improved in order to improve the BL simulations and thus the SST through BL-SST-Intertropical Convergence Zone (ITCZ) feedbacks. We used a CGCM to perform a set of idealized numerical experiments to understand the sensitivity of the BL and consequently SST in the NWTA region to freshwater flux and hence the upper ocean salinity stratification. We find that the BL of the western tropical Atlantic is quite sensitive to upper ocean salinity changes in the Amazon River discharge region and the subtropical salinity maxima region. The BL phenomenon is further manifested by the formation of winter temperature inversions in our model simulations. However, in the region of improved BL simulation, the SST response is not statistically significant.

SST response to Tropical Cyclones (TCs) is studied for the Atlantic region using a high-resolution coupled regional climate model (CRCM) and observational data

sets. The presence of a BL, defined as the layer below the mixed layer that separates the base of the isothermal layer from the base of the isohaline layer, is found to modulate the SST response. The amplitude of TC-induced surface cooling is reduced by more than 35% in the presence of a BL, as a consequence of the weak thermal stratification. Furthermore, in locations when the BL exhibits a temperature inversion, TC-induced mixing can result in weak surface warming. BLs considerably reduce the rightward bias for tropical storms, but the effect is less conspicuous for TCs. The enthalpy flux into the atmosphere at the air-sea interface is enhanced by 16 % and the increase in upper ocean potential energy due to TC-induced mixing is reduced by 25 % in the presence of BLs. The results from the coupled model are supported by an observational analysis performed using re-analysis data sets, as well as data from Argo floats and TRMM satellite. As previous modeling and observational studies have indicated that the surface cooling caused by TC-induced mixing acts as a negative feedback for its intensity, results from our study suggest that BLs may have potential implications for TC intensity prediction.

To my mother Pushpalatha, my father Ravinder

and my sister Ujwala

ACKNOWLEDGMENTS

I would like to take this opportunity to thank Prof. Ping Chang for providing me with financial support during the years of my doctoral study. Under his tutelage I have understood the true spirit of scientific research. I have learned that in the pursuit of scientific truth, the journey is as enriching and satisfying as the ultimate destination. His passion for science and determination are qualities which have truly inspired me, and I hope to be able to emulate them. I'm also very thankful to him for giving me complete freedom in choosing the direction of my research and for backing me all the way.

Next, I would like to thank Prof. R. Saravanan who, along with Prof. Chang, has been my teacher and mentor. He has given me much needed encouragement several times during my study when situations looked bleak and progress difficult. He has been very patient with me at various times when I needed help and has always been very kind and understanding. I would not have reached the stage I'm in currently without his generous support.

I would like to extend my gratitude to my committee members Prof. Benjamin Giese and Prof. Robert Hetland for their encouragement and kind support. I would also like to thank Dr. Jen-Shan Hsieh and Dr. Link Ji who have helped me at various points during my period of study. Finally, last but not the least, I would like to thank my family and friends who have stood by me through thick and thin and whose contribution to the successful completion of my doctoral study is ineffable.

TABLE OF CONTENTS

CHAPTER Page

LIST OF FIGURES

FIGURE Page

FIGURE Page

FIGURE Page

FIGURE Page

CHAPTER I

INTRODUCTION

The upper ocean interacts with the atmosphere, exchanging heat, momentum and buoyancy fluxes. These fluxes jointly determine the climate of the coupled system. The density structure of the upper ocean determines the extent to which the atmospheric forcing gets mixed downward into the ocean interior. Mixing occurs when the turbulent kinetic energy imparted by wind mixing or convective instability caused by surface cooling or evaporation is sufficiently strong to overcome the potential energy barrier imposed by density stratification. Mixing affects the SST by regulating the mixed layer heat budget through entrainment of sub-surface water into the mixed layer and in this way exerts a certain degree of control on the climate of the coupled system.

The tropics are regions of strong air-sea coupling and thus it is very important to understand the role played by the various factors that determine the upper ocean density structure. Salinity is an important variable of the ocean, which plays a pivotal role along with temperature in determining the density and hence the stratification of the ocean. Traditionally, the importance of salinity has always been recognized in the high-latitude deep-water formation regions of the world, in the context of the thermohaline circulation, but not so much so in the tropics.

The importance of the role played by salinity in the tropics was first recognized by Miller (1976), who extended the thermally-mixed upper ocean layer theory originally developed by Kraus and Turner (1967) and later by Denman (1973) to include the effects of salinity and found that it has a significant influence on the heating

---

This dissertation follows the *Journal of Climate*.

characteristics of the upper ocean mixed layer and is essential for the formation of temperature inversions. But the real interest in salinity began with the focus on the El Nino and Southern Oscillation (ENSO) gaining momentum, when it was recognized that the upper ocean salinity in the western pacific warm pool region might have a role to play in the onset of El Nino. This eventually led to the discovery of the salt-stratified Barrier Layer (Godfrey and Lindstrom, 1989; Lukas and Lindstrom, 1991).

The BL mechanism is perhaps one of the most important mechanisms through which salinity directly plays a role in air-sea coupling. The BL occurs when the Mixed Layer Depth (MLD), which is homogenous in density, is shallower than the Isothermal Layer Depth (ILD), which is homogenous in temperature. In this situation, the distance separating the top of the pycnocline from the top of the thermocline is known as BL, as it acts like a 'barrier' to vertical mixing. Fig. 1 is a schematic which illustrates this mechanism. The BLs in the various oceanic regions can be distinguished into three basic types. In the equatorial and western tropical Atlantic and Pacific, the Bay of Bengal and parts of the eastern equatorial Indian ocean, the Labrador sea and the southern ocean, the BLs are almost permanent. In the southern Indian ocean, the Arabian sea and in the northern sub-polar basins, the BLs are seasonal. However, between 25^0 and 40^0 latitude in each basin, BLs are never found(de Boyer Montégut et al., 2007).

A. Significance

Even though the BL occurs in many oceanic regions, its significance is amplified in the tropics due to the effect of strong air-sea coupling in the region. In the tropics, the three important regions of BL formation are the western Pacific warm pool, northwest-

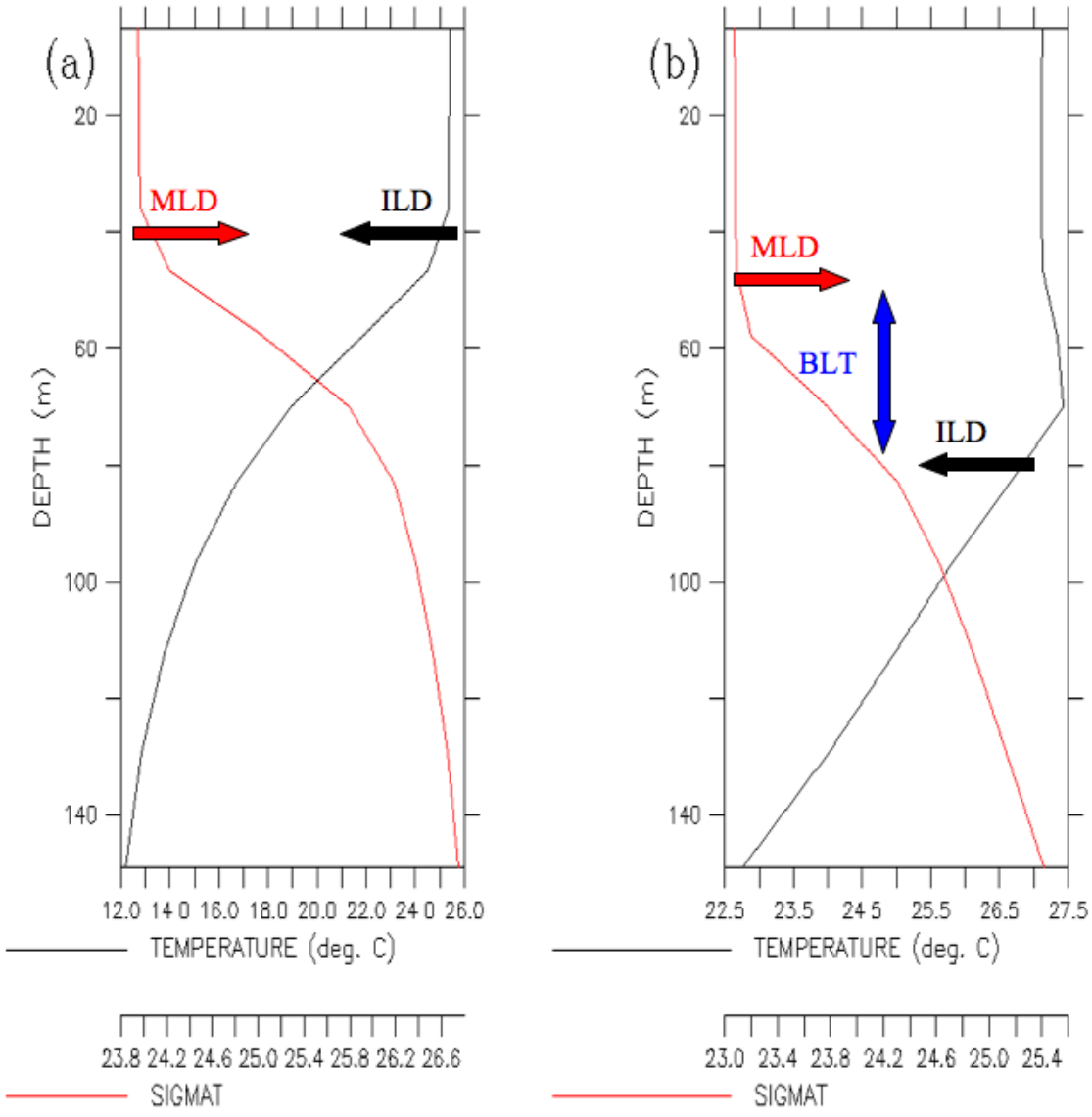

Fig. 1. Upper ocean stratification (a) Typical view where MLD and ILD coincide with each other (b) Non-typical view with a Barrier Layer where the MLD is shallower than the ILD with a BL separating the two.

ern tropical Atlantic and the Bay of Bengal in the Indian Ocean(de Boyer Montégut et al., 2007). Studies in the past confirm the importance of the BL. In the western pacific, BLs decouple wind mixing from entrainment cooling and thus help in not only the heat build-up in the upper ocean but also the migration of the warm pool under the influence of westerly wind bursts. During westerly wind events, as the momentum of the wind forcing is confined to a shallow mixed layer due to the freshwater BL-effect, the warm pool slides over the salty central equatorial waters and thus begins the onset of ENSO. Maes et al. (2006), using data obtained from TAO/TRITON moorings, demonstrate the significance of upper ocean salinity in the western pacific warm pool in controlling air-sea interactions. They show that the BL at the eastern edge of the warm pool is very well correlated with the 28^0C isotherm near the dateline. Using a regional ocean-atmosphere coupled model, Maes et al. (2002) illustrate the importance of salinity BLs for the heat build-up in the pacific warm pool, which possibly triggers the ENSO. They performed two experiments with their model, one a control case and another, a perturbed case by excluding the effects of salinity on density in the warm pool, in essence removing the BL-effect. It is found that the ENSO in the perturbed experiment is weaker than in the control case.

In the Indian ocean, the BLs of the south-eastern Arabian are instrumental in the early onset of monsoon (Masson et al., 2005). The combined effect of the oceanic anticyclonic circulation feature which deepens the thermocline and the winter monsoon current which brings freshwater from the Bay of Bengal gives rise to BL formation in the south-eastern Arabian. These BLs in turn cause the springtime SST to increase by about 0.5^0C, which leads to a statistically significant increase of precipitation in May, paving the way for an early onset of monsoon. Also, all the three tropical regions of BL formation are regions of TCs. The BLs in these regions help in maintenance of warm SSTs and could potentially aid in the formation or

intensification of TCs.

These BLs potentially play a role in marine-ecosystem dynamics. In the latitude band of the subtropical gyres, there are certain regions of upwelling that occur primarily along the western boundaries of the continents and are regions of enhanced biological productivity and consequently are very important for fisheries. However, in the western Pacific warm pool and in the eastern equatorial Indian ocean, despite considerable upwelling, the productivity is low due to the freshwater BL effect at the base of the mixed layer as it acts as a barrier to nutrients from below (Sarmiento et al., 2004).

B. Formation Mechanism

Based on analysis of Levitus data, Sprintall and Tomczak (1992) conclude that the BL formation mechanism varies from one tropical ocean region to another. We now examine the BL extent and magnitude in the three tropical regions using the observational climatology of Mignot et al. (2007). This observational BL climatology, which was based on more than 500,000 instantaneous temperature and salinity profiles collected between 1967 and 2002 obtained from the National Oceanographic Data Center (NODC) and from the World Ocean Circulation Experiment (WOCE) profiles obtained from the Argo Global Data Centers (GDAC), was downloaded from (`http://www.lodyc.jussieu.fr/~cdblod/blt.html`).

The BLT is computed as the difference between the ILD and the MLD. The ILD is defined as the depth where the potential temperature decreases by 0.2^0C from its value at 10 m. That is, ILD $= z(\theta_{10m} - 0.2)$. The MLD is defined as the depth where the potential density increases by a value, which corresponds to a drop in potential temperature by 0.2^0C, with respect to its value at a depth of 10 m. That is, MLD =

$z(\sigma(S_{10m}, \theta_{10m}) - 0.2)$. Then,

BLT = ILD - MLD (de Boyer Montégut et al., 2007).

1. Western Tropical Pacific Ocean

Fig. 2 shows the annual mean BLT in the western tropical Pacific ocean. We see that the maximum magnitude of BLT is about 20-25 m with one peak centered at around 170^0E and 5^0S and another peak centered on the equator at about 160^0E . From Papua New Guinea in the west, the 10 m contour extends until 180^0W and from there until 170^0W through two branch like structures. The northern and southern limits are 10^0N and 15^0S respectively. The E-P (Evaporation-Precipitation) balance of the warm pool is heavily influenced by the intense precipitation under the ITCZ and SPCZ (South Pacific Convergence Zone). Fig. 3 shows the annual mean precipitation for the western tropical Pacific region obtained from GPCP (Global Precipitation Climatology Project)(Huffman et al., 1997). From these two figures, it can clearly be seen that the BLT in this region coincides very well with the maxima in precipitation. The southern branch of the BLT is aligned with the SPCZ along its Northwest-Southeast axis and the respective maxima coincide with each other. The northern branch of the BLT is aligned along the ITCZ with the other peak in BLT coinciding with the maxima in precipitation at about 160^0E and between the equator and 5^0N. Thus, to the west of 160^0W, the excess of precipitation over evaporation is mainly responsible for the BL formation. To the east of 160^0W, the BLT is less than 10 m and forms due to the combined influence of freshening at the surface and also the subduction of salty central equatorial Pacific waters (Sprintall and Tomczak, 1992).

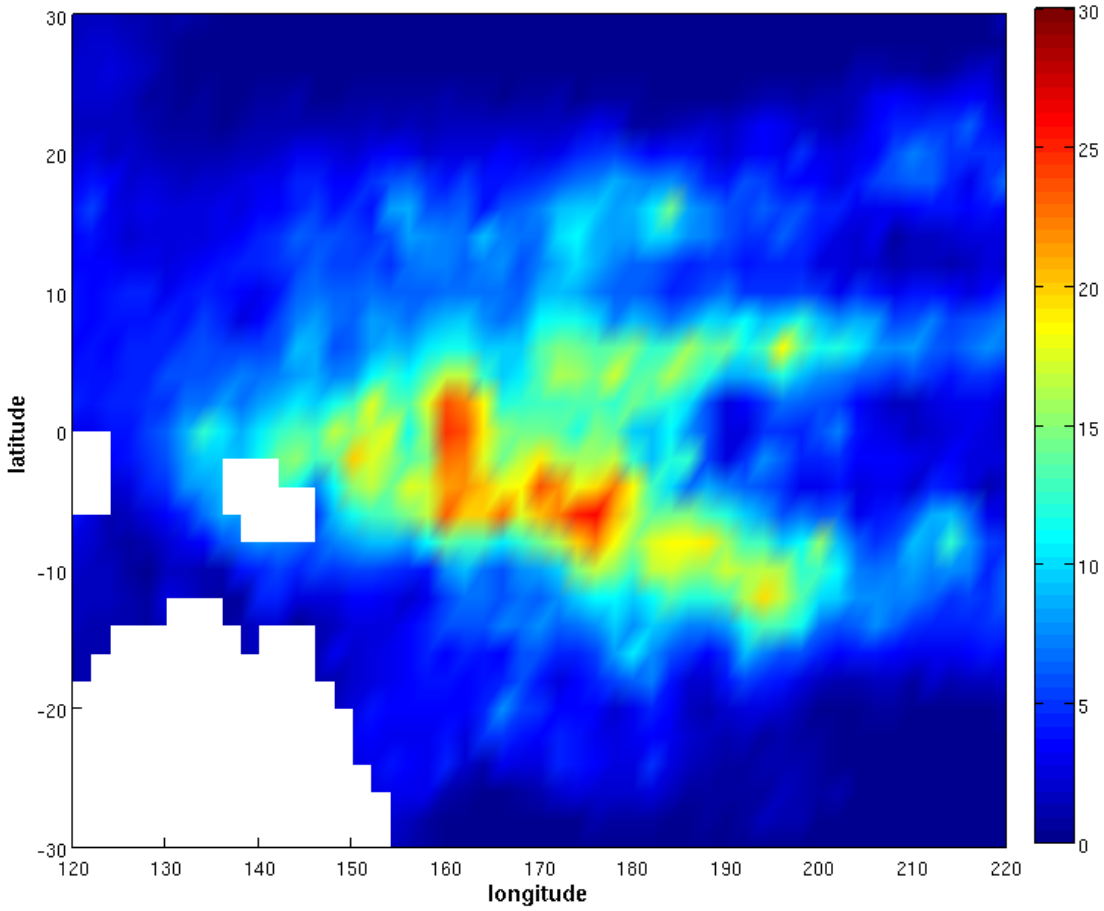

Fig. 2. Annual mean BLT (m) - western tropical Pacific.

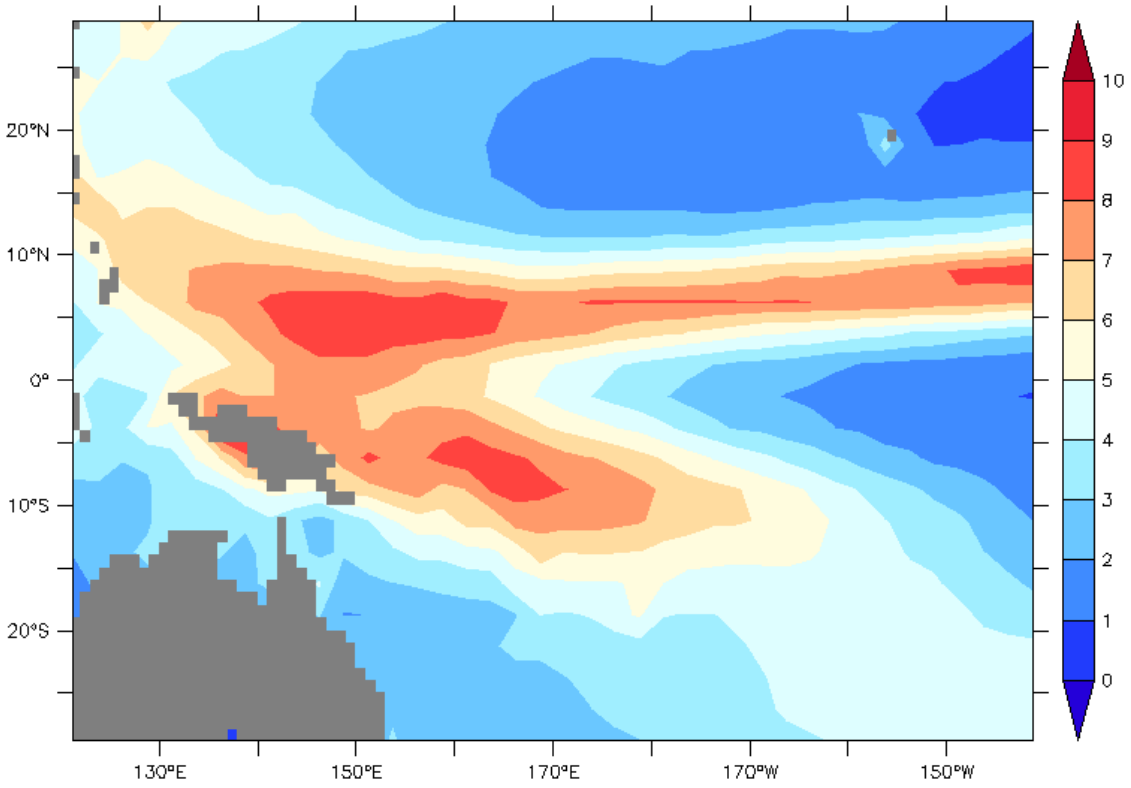

Fig. 3. Annual mean precipitation (mm day^{-1}) - western tropical Pacific.

2. Northwestern Tropical Atlantic Ocean

The annual mean BLT for the tropical Atlantic region is shown in Fig. 4. Thick BLs occur in the Caribbean sea or the northwestern part of the basin with a maximum thickness of 20-25 m and centered at 60^0W and 12^0N. The 10 m contour extends from the northeastern coast of south america until about 20^0N with the westernmost and eastern boundaries being 70^0W and 40^0W. BLT exceeding 10 m can also be found at 30^0W and 5^0N and near the equator at 40^0W. Unlike the western tropical Pacific, the BL formation in the northwestern tropical Atlantic is not attributable to an excess of precipitation.

The E-P balance analysis for this region indicates that this is a region of net loss of freshwater(Dorman and Bourke, 1981). The surface salinity in the western tropical Atlantic is heavily influenced by the Amazon and Orinoco River systems. The Amazon, with its mouth located at around 50^0W and 0^0N discharges about 1.7 Sv of freshwater while the Orinoco River discharges about 0.02 Sv of freshwater from its mouth located at around 60^0W and 10^0N. Most of the discharged water is carried northwestward initially by the strong North Brazil Current (NBC) and later by the Guiana current until it reaches the islands of Lesser Antilles. Also every year, beginning in summer, the NBC retroflects to give rise to the North Equatorial Counter Current (NECC) which develops as a continuous eastward flow. Every now and then, the NBC closes in on itself and spawns anticyclones. Due to potential vorticity conservation, these anticyclones intensify as they propagate northwestward along the coast and become NBC rings. There are approximately 6-7 ring shedding events per year (Jochum and Malanotte-Rizzoli, 2003). Along with the Guyana current, these NBC rings form the chief mode of transport of freshwater from the Amazon and Orinoco River systems into the Caribbean sea through several passages between

the Lesser Antilles islands (Hellweger and Gordon, 2002). From here the Caribbean

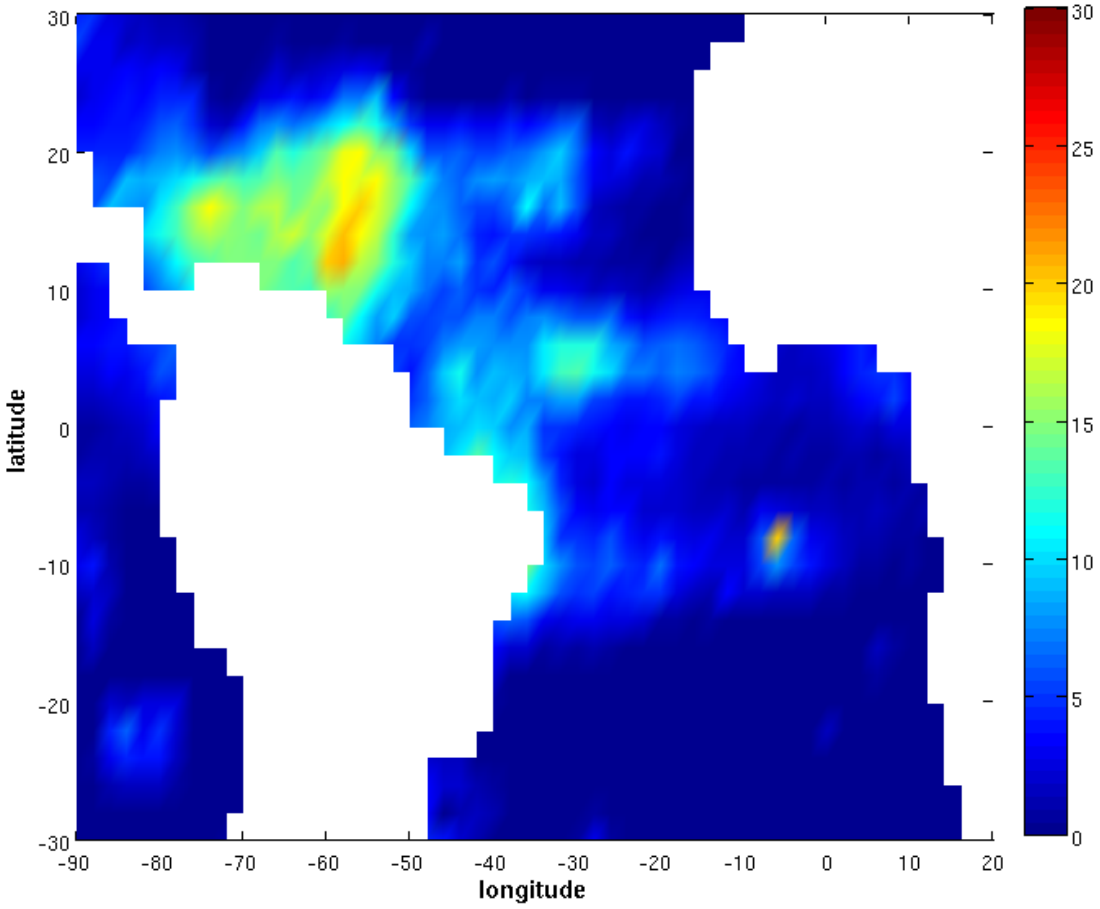

Fig. 4. Annual mean BLT (m) - northwestern tropical Atlantic.

current transports the freshwater further into the Caribbean sea and finally some of the freshwater exits through the Yucatan channel. As a result of these processes, a lens of freshwater forms on the ocean surface in the western tropical Atlantic.

While the surface ocean salinity is heavily influenced by river discharge, the sub-surface salinity is controlled by the remote mechanism of subduction. High salinity water forms at the centers of the northern and southern subtropical gyres, partly in

response to the massive rates of evaporation. After formation at the surface, these water masses then subduct and flow equatorwards as a shallow subtropical salinity maxima. The North Equatorial Current (NEC) approximately transports 10 Sv of the northern salinity maxima waters, of which 8 Sv go through the Caribbean and the South Equatorial Current (SEC) transports 6 Sv of the southern salinity maxima waters (Blanke et al., 2002). The presence of the sub-surface salinity maxima water in the northwestern tropical Atlantic was noted by Defant (1961) during the *Meteor* cruises of 1936 and during the Barbados Meteorological and Oceanographic Experiment (BOMEX) cruises in 1969. These high salinity waters in the sub-surface play a pivotal role in the maintenance of the strong haline stratification and in concert with the freshwater at the surface give rise to BLs in the northwestern tropical Atlantic. As noted earlier, centered at 30^0W and 5^0N, there is BL formation in a small region. Beginning in May, the NECC develops as a continuous eastward flow and carries part of the fresh Amazon river discharge eastwards and is responsible for the formation of BLs in that region(Sprintall and Tomczak, 1992). These BLs, which are a focal point of this dissertation, will be studied in great detail in the remaining chapters.

3. Eastern Equatorial Indian Ocean

The eastern equatorial Indian ocean is another tropical oceanic region where the BLs are prominent. As can be seen from Fig. 5, the 10 m BLT contour extends from the west coast of Sumatra at about 100^0E until about 60^0E in the zonal direction while 10^0S and continental land mass of the Indian subcontinent serve as the southern and northern limits respectively. The maximum BLT is about 25 m and occurs near the northern and eastern boundaries of the Bay of Bengal. The region adjacent to the west coast of Sumatra receives an annual freshwater flux of about 1800 mm year^{-1} (Oberhuber, 1988). Fig. 6 shows the annual mean precipitation for this region,

generated using GPCP climatology. It can clearly be seen that the region to the west of Sumatra has a local maximum in precipitation and thus it is very likely that rainfall is the chief contributor for BL formation in this region. On the other hand, even though precipitation could be responsible for part of the freshening, the major factor for the formation of thick BLs in the Bay of Bengal seems to be river discharge (Sprintall and Tomczak, 1992). Three major rivers of this region, Ganges, Brahmaputra and Irrawaddy contribute 455, 1070 and 1020 mm of freshwater on an average per year respectively into the northern and eastern sides of the Bay of Bengal(Baumgartner et al., 1975). The reflection of the seasonal cycle of southwest monsoons in the seasonality of BLT also strongly supports the fact that river discharge dominates over other factors which could contribute to BL formation(Sprintall and Tomczak, 1992).

In the southeastern part of Arabian sea, an oceanic anticyclonic feature develops between late winter and early spring. This is associated with a high in the sea-level known as the Lakshwadeep High which deepens the thermocline. Also, during winter, the Winter Monsoon Current transports freshwater from the Bay of Bengal into this region. The combined effect of these two oceanic features results in BLs with a mean thickness exceeding 10m and centered at about 72^0E and 7^0N.

C. Layout of Dissertation

The layout of the dissertation is as follows. An inter-comparison of BL simulation between coupled and uncoupled versions of a model is made in Chapter II. Chapter III deals with numerical simulations performed with a CGCM to study the formation mechanism of BLs in the northwestern tropical Atlantic and their influence on the mean climate. The modulation of SST response to TC induced mixing by BLs

is examined in Chapter IV using satellite data, data from Argo floats and various assimilation data products. In Chapter V, we re-examine the same problem from Chapter IV but within the framework of a regional coupled model. Finally the main conclusions and discussion have been given in Chapter VI.

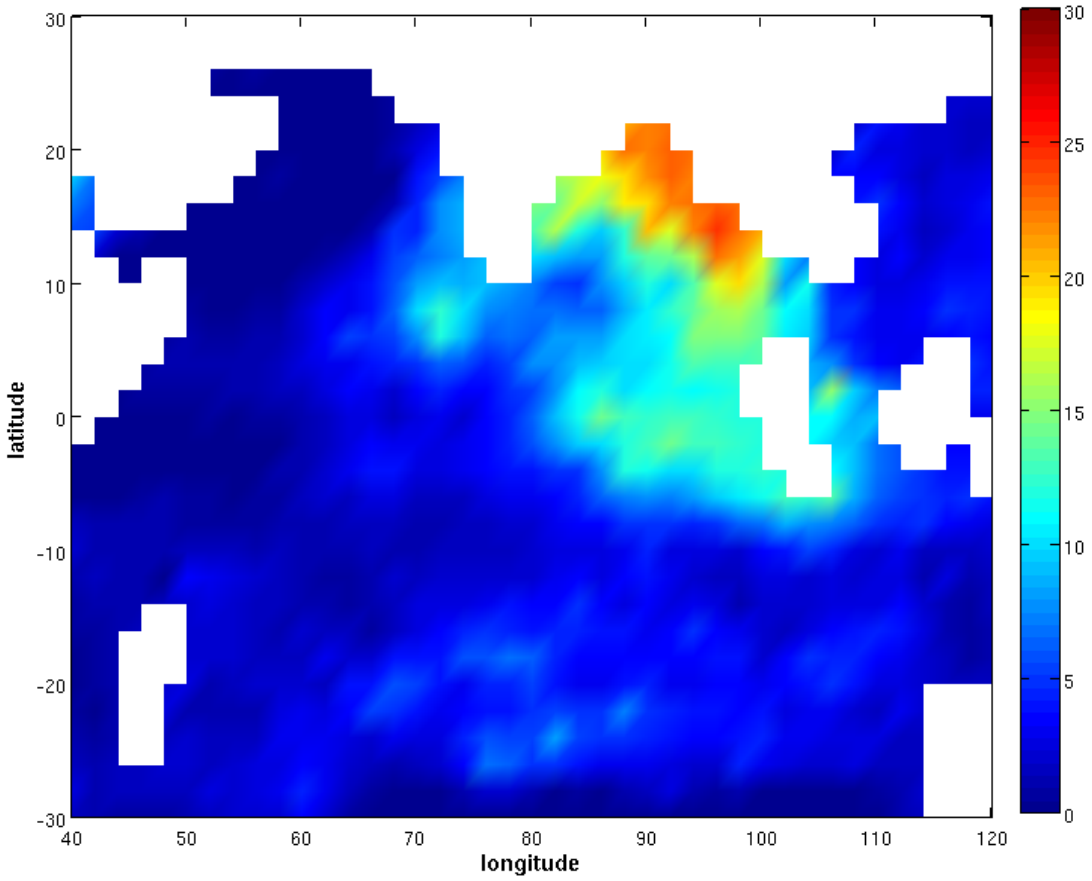

Fig. 5. Annual mean BLT (m) - eastern equatorial Indian Ocean.

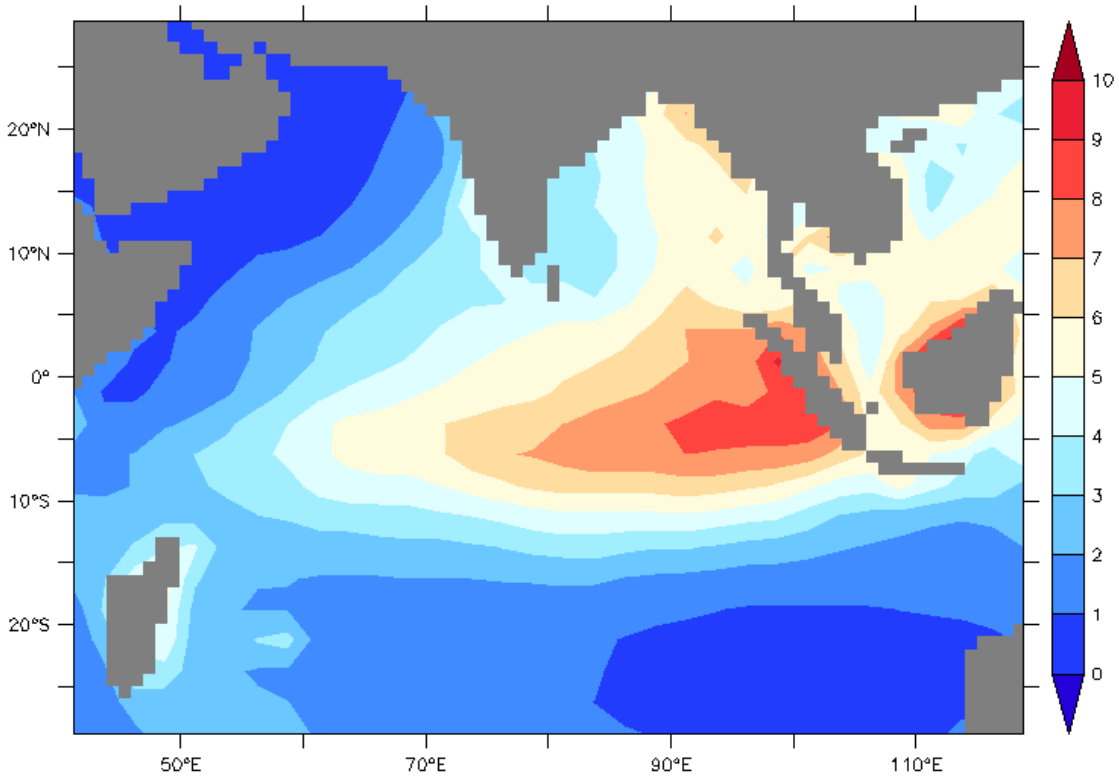

Fig. 6. Annual mean precipitation (mm day^{-1}) - eastern equatorial Indian Ocean.

CHAPTER II

SIMULATION OF BARRIER LAYER IN THE TROPICS: A QUALITATIVE COMPARISON OF UNCOUPLED VS COUPLED SIMULATIONS

In the previous chapter we briefly looked at the spatial structure and magnitude of BLs in the three different tropical oceanic regions using an observational data set. The aim of this chapter is to study the simulated spatial structure and magnitude of tropical BLs by a state-of-the-art Ocean General Circulation Model (OGCM) in its stand-alone configuration and when it is part of a CGCM and perform an inter-comparison between the two.

The OGCM we use for this study is the Parallel Ocean Program (POP) version 2.0 developed at Los Alamos National lab, (LANL). The model is used at a configuration of gx1v3 which means a longitudinal resolution of 1.125^0 and a variable latitudinal resolution of 0.27^0 at the equator to 0.64^0 at far northwest Pacific. There are 40 vertical levels increasing monotonically from 10m near the surface to about 250m in the deep ocean. The north pole in this model is displaced into Greenland. The model uses the isopycnal transport parametrization of Gent and Mcwilliams (1990) and the K-profile parametrization (KPP) of vertical mixing (Large et al., 1994). The output data for an ocean only simulation of this model with prescribed atmospheric and sea ice forcing is obtained from National Center for Atmospheric Research (Dr.Susan Bates, personal communication, NCAR). Further description of this simulation has been given in Large and Danabasoglu (2006) and the forcing used for this simulation is described in Large and Yeager (2004). We used 10 years of model data for this analysis. We also used ocean model output data from the control simulation of Community Climate System Model (CCSM) 3.0, the CGCM developed at NCAR, whose ocean component is POP 2.0 at the same resolution of gx1v3. 10 years of model data

was used. As we have used the CGCM extensively to perform numerical experiments, a subject of the following chapter, the description of the model would be given there.

For the remaining part of this chapter, we refer to the POP stand alone simulation as "uncoupled" while POP simulation as part of the CGCM would be called "coupled".

A. Western Tropical Pacific Ocean

Fig. 7a shows the annual mean BLT from the uncoupled simulation. In the western tropical Pacific, the BLs are underestimated both in terms of magnitude as well as spatial extent. The 10 m contour extends eastwards from Papua New Guinea only until about 180^0E and from 10^0S to the equator. As noted in Chapter I, the BL in this region extends into two branches on either sides of the equator as a result of intense convection under the ITCZ and SPCZ. The model is able to simulate to a little extent the southern branch but the northern branch is totally underestimated. The maximum model simulated BLT in this region is only about 15 m while it is nearly 25 m in observations.

The annual mean BLT from the coupled simulation is shown in Fig. 8a. It can be readily seen that BLs are grossly underestimated in this simulation. Spurious BLs of upto 15m are created to the north of Papua New Guinea between 0^0 and 5^0N. To the east of 150^0E, in the main formation region, BLs are almost nonexistent. Thus, for the western tropical Pacific region, both the uncoupled and coupled simulations of BLs are poor compared to observations but the uncoupled simulation of BLs is much better than the coupled simulation.

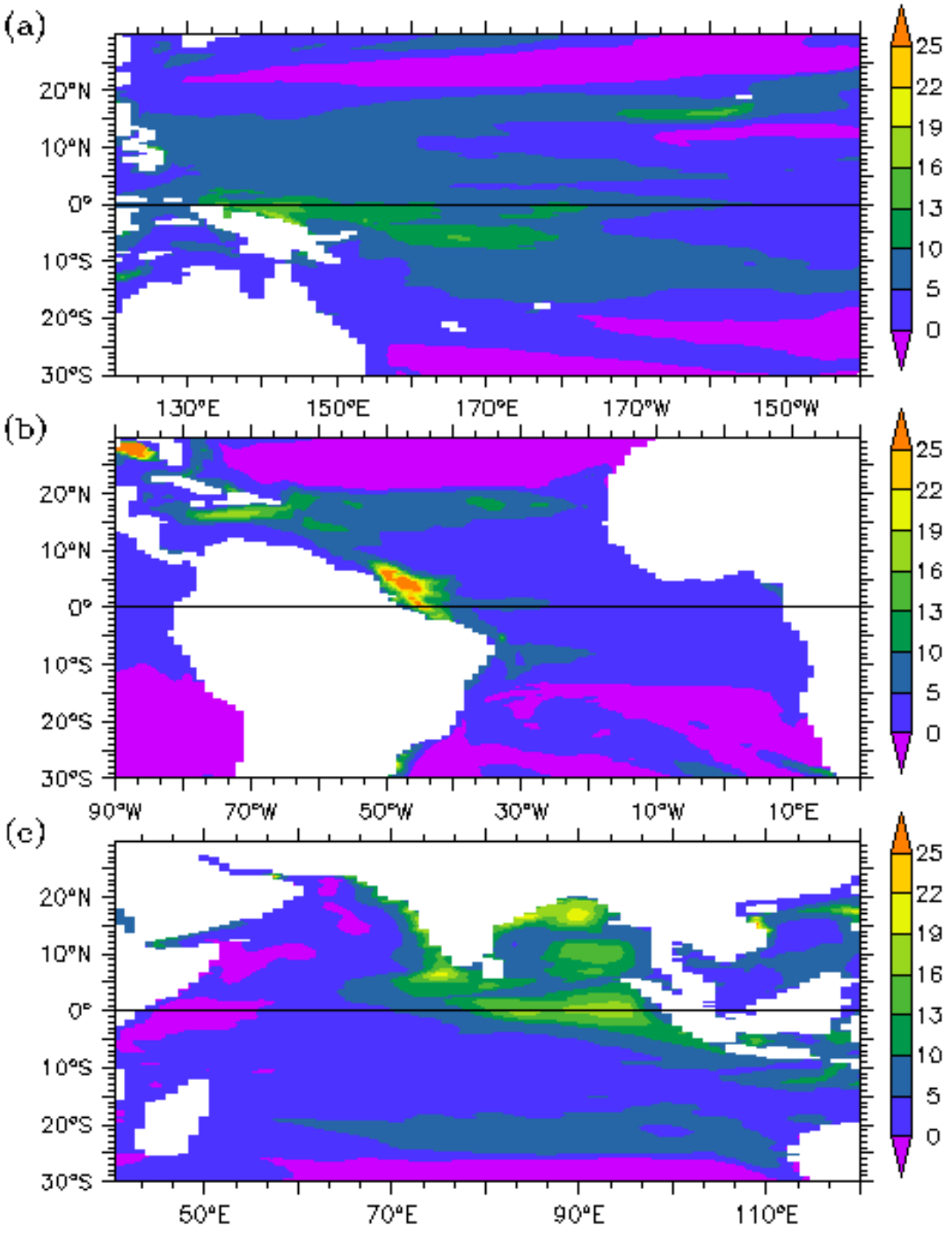

Fig. 7. Annual mean BLT (m) in POP (uncoupled mode) for a) Western tropical Pacific b) Northwestern tropical Atlantic c) Eastern equatorial Indian Ocean.

B. Northwestern Tropical Atlantic Ocean

The annual mean BLT from the uncoupled simulation is shown in Fig. 7b. The most striking aspect is the BL near the Amazon river mouth. The simulated BLT in this region is in excess of 25 m, centered at 45^0W and 5^0N, while the actual BLT in this region is only about 10 m - 15m. This probably implies that the swift western boundary currents like the NBC, which transport Amazon river discharge westwards, could be weak. This also perhaps explains the lack of BL formation in the model at about 30^0W and 5^0N, which could be due to a weak NECC which fails to advect Amazon river discharge eastwards during boreal summer and fall. An examination of the mean surface currents in the uncoupled simulation and a comparison of them with those from the GFDL re-analysis data set (Zhang et al., 2009) reveals that the model indeed under-estimates the strength of the Guyana current and the NECC by about 10-20 cm s^{-1}. To the west of 50^0W, which is the main region of formation, we find that except for a small region to the south of Haiti and Dominican republic where BLs of upto 20 m thick are simulated, the BLs are underestimated to a considerable extent.

When it comes to the coupled simulation (Fig. 8b), we find that it is much poorer than the uncoupled simulation for this region. The BLs near the Amazon mouth and in the central tropical Atlantic, at about 30^0W and 5^0N are nonexistent. To the south of Haiti and Dominican republic, centered at 70^0W and 15^0N, BLs with a maximum thickness exceeding 25 m form, which is clearly an overestimation. But the most glaring error occurs in the tropical north Atlantic. Stretching between 60^0W and 20^0W and between 20^0N and 30^0N, erroneous BLs with thickness exceeding 25 m are created. Another grave error in the coupled simulation occurs in the eastern part of the basin in the Gulf of Guinea region, centered at 5^0E and 5^0N, where spurious

BLs in excess of 20m are created. The misrepresentation of tropical Atlantic BLs in CGCMs is a topic which is examined in great detail in the following chapter.

C. Eastern Equatorial Indian Ocean

Simulation of BLs in the uncoupled and coupled modes have been shown in Figs. 7c and 8c respectively. The BLs of the eastern equatorial Indian ocean are simulated reasonably well in the uncoupled mode. From the west coast of Sumatra extending westwards until 80^0E, BLs with maximum thickness of about 20 m are found. These BLs extend northwards into the Bay of Bengal maintaining a thickness of 16m. However, when it comes to the Bay of Bengal, even though the spatial extent of BLs is reasonably well simulated, the maximum magnitude of BLs is slightly underestimated. BLs are severely underestimated along the northeastern boundary of the Bay while the maximum magnitude near the northern boundary of the basin is about 22 m. The model is also able to simulate quite well the BL in the southeastern Arabian sea. Centered at 80^0E and 5^0N, it has a peak magnitude of about 22 m.

Again, even in this region, the performance in the coupled mode is very poor. The BLs extending from the west coast of Sumatra are nonexistent. Even in the Bay of Bengal, except for along the northern and western boundaries of the Bay, BLs are not simulated. But the most glaring error is the simulation of spurious BLs, between 70^0E and 112^0E and between 30^0S and 50^0S, extending from the west coast of Australia all the way till Madagascar. The maximum thickness of these BLs is about 20m, centered at 110^0E and 30^0S. But in the southeastern Arabian sea, the coupled simulation is able to reproduce BL formation, with the maximum thickness being about 15 m.

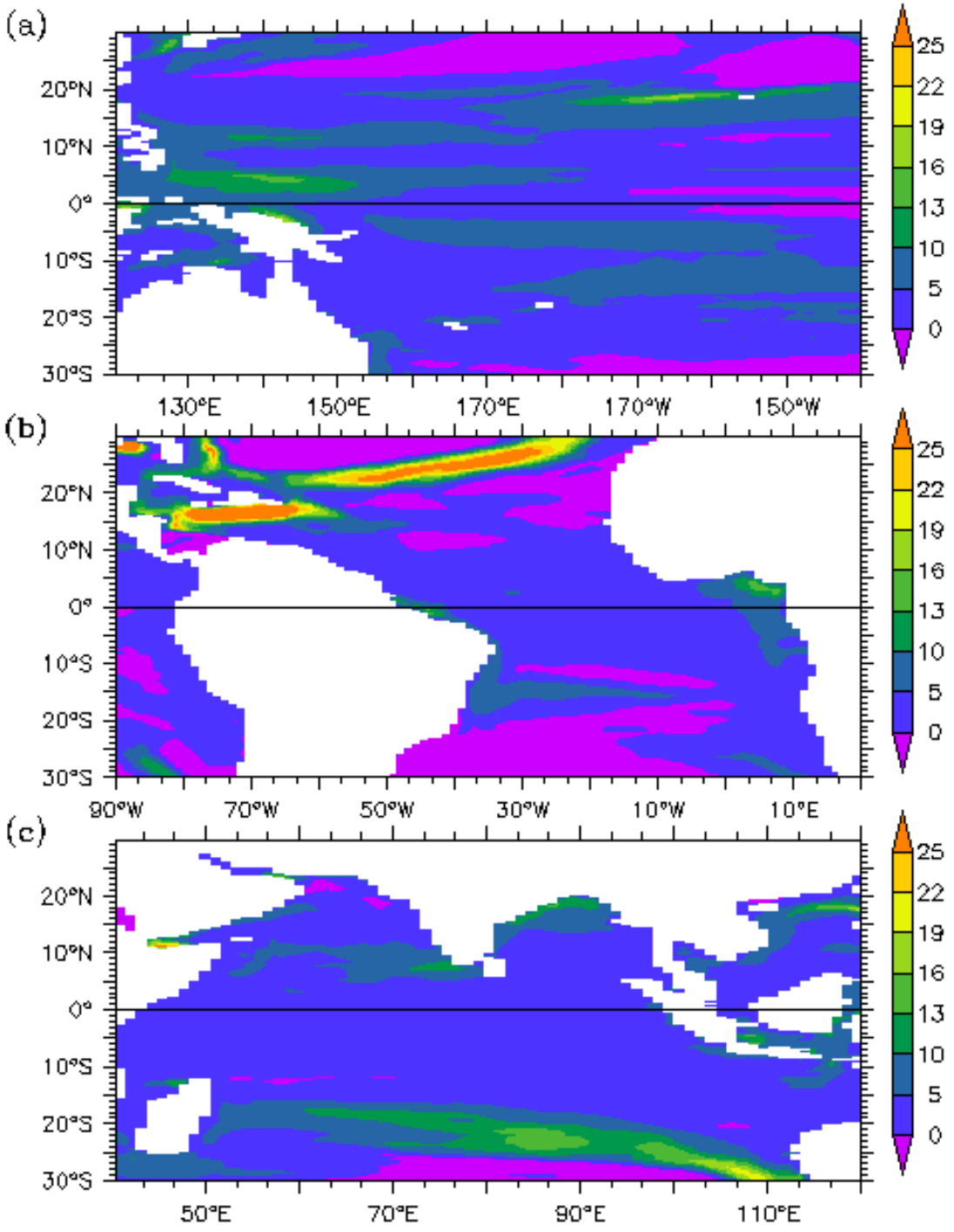

Fig. 8. Annual mean BLT (m) in POP (coupled mode) for a) Western tropical Pacific b) Northwestern tropical Atlantic c) Eastern equatorial Indian Ocean.

CHAPTER III

A NUMERICAL STUDY OF THE BARRIER LAYERS IN THE NORTHWESTERN TROPICAL ATLANTIC

In the previous chapter, we looked at the ability of a state-of-the-art OGCM in simulating BLs in the tropical oceanic regions. We saw that the simulations were closer to observations when the model was used in an uncoupled mode when compared to a coupled mode. In this chapter, we explore the inability of CGCMs in simulating BLs in the northwestern tropical Atlantic using a state-of-the-art CGCM.

A. The Tropical Atlantic Bias Problem

Most CGCMs fail to accurately simulate the tropical Atlantic climate. A notable feature of CGCM simulations is the bias in SST, with a warm bias over the southeast equatorial Atlantic and a cold bias over the northwestern tropical Atlantic. The tropical Atlantic SST is a very important factor in determining the regional climate of the Atlantic sector and is affected by phenomena, such as ENSO, North Atlantic Oscillation (NAO), etc., through atmospheric and oceanic teleconnections (Saravanan and Chang, 2000; Xie and Philander, 1994; Chang et al., 2006). It also plays a prominent role in the tropical Atlantic hurricane activity (Emanuel, 2005). This underscores the need to understand the sources of these biases in the coupled model simulations.

Carton and Zhou (1997) studied the seasonal cycle of tropical Atlantic and they attribute the SST cycle in the southeast equatorial Atlantic to the combined effect of coastal upwelling and the changes in latent and sensible heat fluxes due to variation in the trade winds. DeWitt (2005), using an ocean model forced with observed winds, attributes the SST bias primarily to the bias in the zonal wind stress that causes

an error in the thermocline and associated entrainment. The erroneous zonal wind pattern not only causes an error in the slope of the thermocline but also causes weak mixing in the east and strong mixing in the west and thus causes the zonal SST bias. Hazeleger and Haarsma (2005) have demonstrated the sensitivity of the SST in southeast equatorial Atlantic to upper-ocean mixing and thus the entrainment efficiency using both an ocean model as well as a coupled model. Richter and Xie (2008), after an analysis of an ensemble of CGCMs and their atmospheric components, suggest that the bias in coupled model simulations appears to originate from the atmospheric component, particularly convective parameterizations over the Amazon and northwestern tropical Atlantic. The failure to simulate good precipitation over tropical South America may be responsible for the weaker-than-observed zonal winds in the eastern equatorial Atlantic, which in turn does not allow the cold tongue to develop during boreal summer. Huang et al. (2007) attribute the SST bias to the models inability to simulate stratus clouds in the southeast equatorial Atlantic region along with the zonal windstress bias in the equatorial Atlantic.

The BLs of the northwestern tropical Atlantic, according to Mignot et al. (2007), is one of the most prominent structures of the global tropics and sub-tropics. These BLs, when they form during late fall and early winter, weaken entrainment and do not allow atmospheric cooling to penetrate into deeper waters. Thus, this region is usually associated with a temperature inversion during the winter, the magnitude of inversions being as high as 0.5^0C. It is shown that the BLT indeed has an impact on SST in the tropical Atlantic (Foltz and McPhaden, 2009). They examine data from three mooring buoys of the Pilot Research Array in the Tropical Atlantic (PIRATA) in the central tropical north Atlantic and based on a heat budget analysis conclude that the BL may play an important role in the annual cycle of SST at those locations. As the BL plays a role in trapping the heat within the upper ocean layer, it may

also affect the Atlantic hurricane activity (Ffield, 2007; Vizy and Cook, 2010). The Amazon plume, which extends into the Caribbean Sea, has relatively high SSTs. The high SSTs are sustained for great distances in the plume due to the BL effect, which may significantly impact the air-sea coupling processes of hurricanes passing these regions by alleviating the SST cooling due to the more stable stratification of the BLs. Hence, such BL effects on the tropical climate and hurricane simulations in CGCMs may not be negligible. For long-term trend prediction in Atlantic hurricanes, we need realistic BL simulations in CGCMs.

As noted earlier, the tropical Atlantic annual (E-P) balance analysis indicates that precipitation cannot be the primary source of fresh-water at the surface in the northwestern tropical Atlantic and that the river discharge from the Amazon and Orinoco River systems plays a more dominating role. Pailler et al. (1999) examined data from nearly 2673 conductivity-temperature-depth profiles and concluded that river discharge plays a dominant role in the formation of thick BLs off the mouth of Amazon River extending northwestwards into the Caribbean. Hu et al. (2004), using data from Lagrangian drifters and ocean colour data from satellites also noted the important influence of river discharge. Subsurface warm and high salinity waters are formed in the subtropical gyres of the respective hemispheres and are subducted as salinity maximum water. The surface fresh-water along with the sub-surface salinity maxima water presumably forms the thick BLs observed here during boreal winter (Sprintall and Tomczak, 1992).

Many CGCMs underestimate the freshening due to river discharge in this region and also have a bias in precipitation due to an error in the mean position of the ITCZ. These two factors together contribute to the upper ocean salinity bias. This can potentially cause a bias in the density stratification and hence the BL formation. Breugem et al. (2008) analyze output from a suite of CGCMs and propose that

misrepresentation of BLs could potentially contribute to the mean bias of the climate simulation in the coupled system BL-SST-ITCZ feedback mechanism and that upper ocean salinity stratification needs to be improved in the model to allow a realistic representation of BL dynamics and associated feedbacks among BL, SST and ITCZ.

Most studies have focused on the effects of heat and momentum flux exchanges between the atmosphere and ocean, fewer studies have focused on feedbacks associated with freshwater changes. Masson and Delecluse (2001) have done a series of sensitivity experiments with varying river discharge to observe the effect of Amazon river discharge on the tropical Atlantic climate. They find that the river discharge considerably affects the upper ocean salinity and BL formation in the northwestern tropical Atlantic. But they find that a clear relationship between BL and SST does not exist. However, their experiments were carried out with an OGCM, thus leaving out the scope for potentially important air-sea interactions to play a role. Here, we have devised a set of idealized sensitivity experiments with a fully coupled general circulation model to examine not only the effect of freshwater flux on the upper ocean salinity stratification, but also its effect on the SST in the northwestern tropical Atlantic region through BL-SST-ITCZ feedbacks.

B. Model, Data and Experiments

The model we use for the present study is the fully coupled climate model CCSM 3.0 developed at NCAR. It consists of the Community Atmosphere Model (CAM), the Community Land Model (CLM), the Parallel Ocean Program (POP) and the Community Sea Ice Model (CSIM). These four component models interact with each other through a coupler (CPL). Analysis of its performance at high resolution is given by (Collins et al., 2006). We use the model at its standard resolution which has CAM

and CLM configured at a resolution of T42 ($2.8^0 \times 2.8^0$ approximately) while POP and CSIM are set at a resolution of gx1v3, as was described in the previous chapter.

First we consider the simulated climate of this model. Fig. 9 shows the model bias in SST, SSS and Precipitation. The model bias in SST and SSS is obtained by subtracting the annual averaged SST from NOAAs extended reconstructed SST (Smith and Reynolds, 2004) and SSS of Levitus data (Levitus, 1982) from the model control simulation. In the SST (Fig. 9a), the model shows a warm bias in the southeast tropical Atlantic and a cold bias in the northwestern tropical Atlantic region. The warm bias has a maximum value of about 5^0 C while the cold bias has a maximum value of about 3^0 C. On the other hand, the model shows a positive SSS bias (Fig. 9b) with a peak value of about 2 g kg^{-1} in the northwestern tropical Atlantic region. The peak value is centered just off the mouth of the Amazon river and extends into the northwestern tropical Atlantic region region. In the south tropical Atlantic, the SSS shows a negative bias with a peak value of about 4g kg^{-1}. Another negative SSS bias occurs near the northern subtropical salinity maxima region. The precipitation bias, shown in Fig. 9c, is obtained by taking the difference between the model annual mean precipitation in the Control Run (CR) and the annual mean precipitation from GPCP (Huffman et al., 1997). The most glaring error of the precipitation is the positive bias over the southeast tropical Atlantic region and the negative bias over the Amazon region. This error pattern is indicative of a southward shift of the ITCZ, which sparks the hypothesis by Breugem et al. (2008) that the erroneous BL simulation in this region may contribute to the bias in SST through the BL-SST-ITCZ feedback mechanism. The idea is that the overestimation of BLs in the southeast tropical Atlantic, near the Gulf of Guinea, reinforces the warm SST bias due to reduced entrainment cooling while in the northwestern tropical Atlantic the underestimation of BLs reinforces the cold bias due to enhanced entrainment cooling.

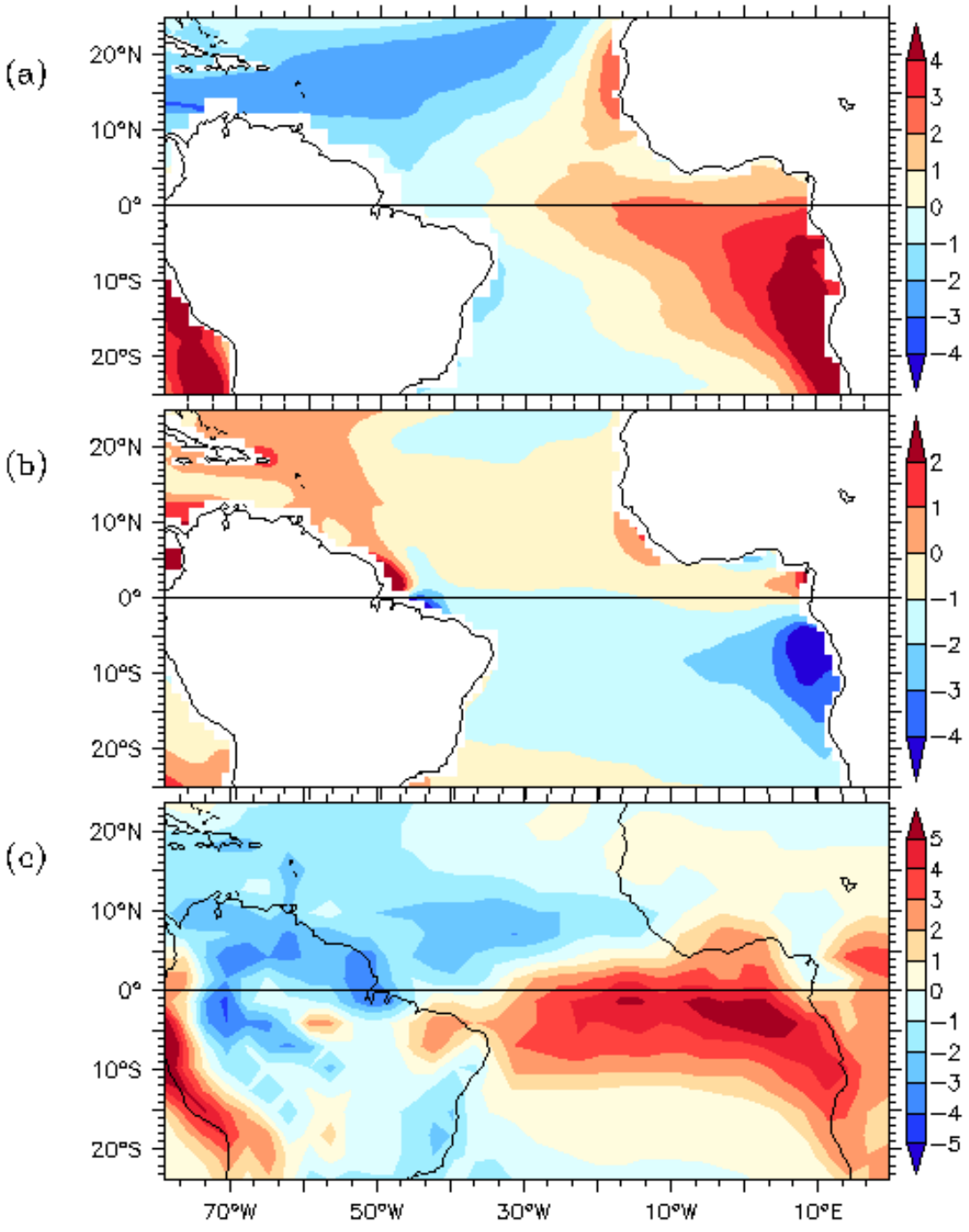

Fig. 9. Mean biases in the model simulation. (a) SST (^{0}C), (b) SSS (g kg^{-1}) and (c) Precipitation (mm day^{-1}).

In Fig. 10, the climatology of the BLT in the northwestern tropical Atlantic region is shown for both the model simulation and observations. The BLT is computed using the definition given by de Boyer Montégut et al. (2007), as discussed earlier. We take an index by averaging BLT in a region from 60^0W to 55^0W and 10^0N to 20^0N and compute its climatology. The observational climatology of BLT and MLD were obtained from Laboratoire d Oceanographie et du Climat at the following site (`http://www.lodyc.jussieu.fr/cdblod/blt.html`). As can be seen, the model under-estimates the BL in this region with most under-estimation occurring during the winter months. This region is known to have BLs exceeding 50 m in the boreal winter season (Mignot et al., 2007). Most existing coupled models under-estimate the BLs in the northwestern tropical Atlantic region to a large extent except for a small region in the Caribbean basin (Breugem et al., 2008).

To study factors that cause these biases, we conduct four ensembles of experiments with the coupled model. First, we perform a 50-year control simulation with an initial condition obtained from a spin up run. The restart file of the spin up run is obtained from NCAR at (`www.earthsystemgrid.org`). We then divide the 50-year long run into 5 sets of 10-year runs and use the first month of each of these 5 sets as our initial condition and perform simulations with each initial condition. With each of these 5 initial conditions, we then add a constant precipitation anomaly of +4mm day^{-1} in the region of Amazon discharge to the model and integrate the model for 10 years. The value of 4mm day^{-1} is estimated from the precipitation bias over Northern South America. This experiment is referred to as EXP1, where we attempt to emulate the Amazon-Orinoco river discharge and examine the effect of lowering the upper ocean salinity in this region. In the next set of experiments we add a constant precipitation anomaly of -4mm day^{-1} in the subduction region of the northern subtropical salinity maxima, along with the forcing described above in EXP1. We

refer to this experiment as EXP2. Since primarily subduction processes control the

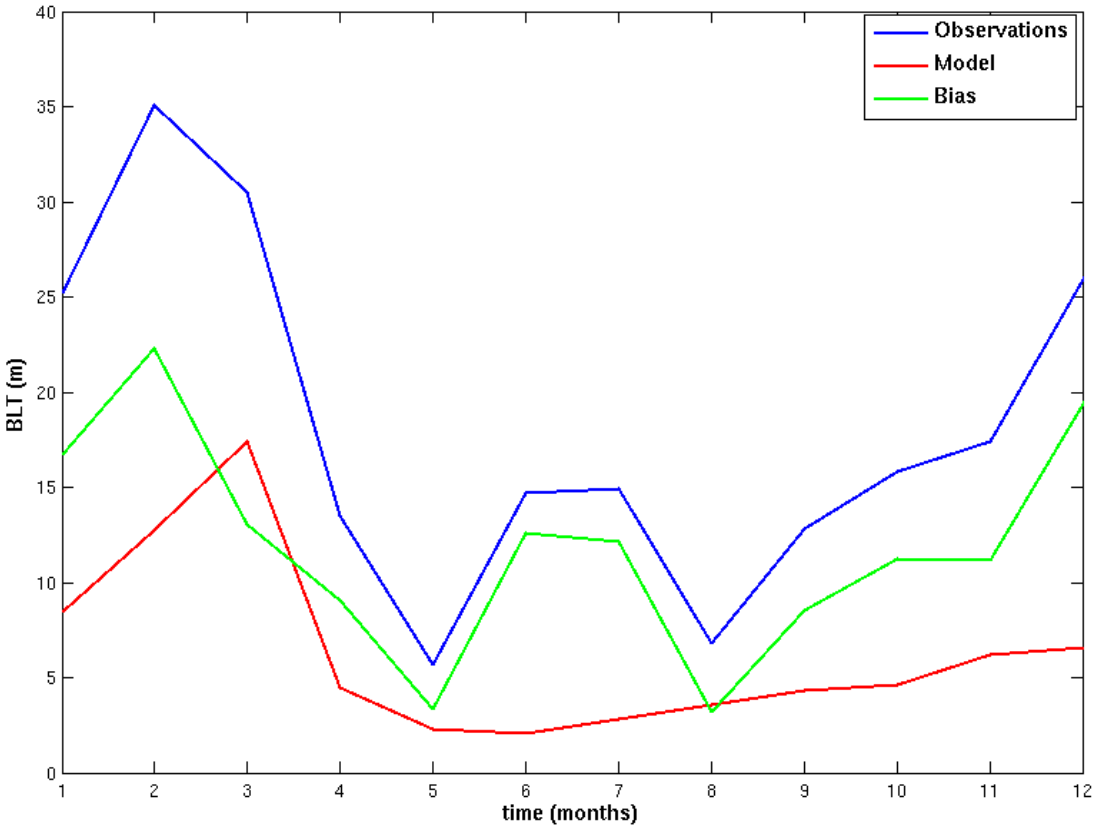

Fig. 10. The climatologies of BLT in northwestern tropical Atlantic: observations (blue), model (red) and the bias (green), obtained by subtracting the model values from the observations.

sub-surface salinity in the northwestern tropical Atlantic region, EXP2 allows us to examine the effect of correcting the bias in sub-surface salinity on improving the BL simulation in the northwestern tropical Atlantic region. Finally, to test the model sensitivity, we double both the forcings in EXP3. The regions of forcing are shown in Fig. 11.

Using different ocean and atmosphere initial conditions for each simulation allows

us to form an ensemble of runs subject to the same salinity forcing. An ensemble

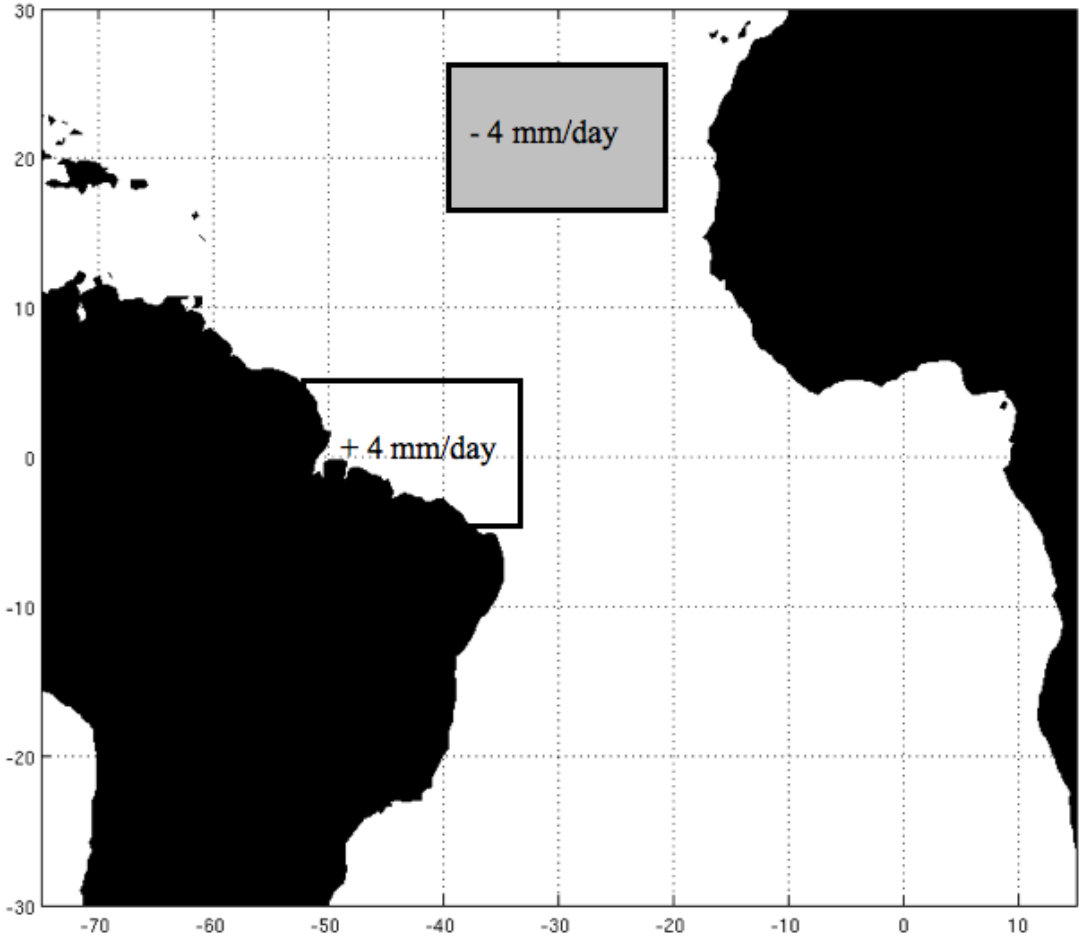

Fig. 11. Regions and the magnitudes of the forcing applied in model experiments.

average of these runs can reduce the influence of internal variability of the system, so that the response of the coupled system to the salinity forcing can be more clearly delineated. In each of these experiments, after we perform the simulations with each of the 5 initial conditions, we perform an ensemble average to generate a single time series of 10 years. We then analyze the ensemble averaged model simulations to

identify the factors controlling the extent and magnitude of BLs in the northwestern tropical Atlantic region.

C. Results

We begin by examining EXP1 in Fig. 12. The changes in mean SST and SSS are shown in Figs. 12a and 12b, while the mean changes in MLD and BLT are shown in Figs. 12c and 12d respectively. The change is obtained by taking the ensemble average of time mean for EXP1 and the CR and subtracting the latter from the former.

The Amazon river discharges about 0.17 Sv on an average from its mouth located at around 50^0W, 0^0N. The river discharge varies from about 112,000 m^3 in November to about 229,000 m^3 in May-June. Most of the discharged water is carried northwestward initially by the Guyana current. The maximum correlation of SSS occurs at Barbados with a lag time of 2 months. The water then flows further westward through the islands of Lesser Antilles into the Caribbean Sea. From there, the Caribbean current takes it northward and westward and the water finally exits through the Yucatan Channel (Hellweger and Gordon, 2002). Consistent with this depiction, we find that most of the freshening is carried northwestward towards the Caribbean islands with a peak freshening of about 1 g kg^{-1}. There is some eastward propagation of the surface freshening and this could be attributed to the seasonal NECC.

Let us now consider the SST change in Fig. 12a. A students t-test is performed to check for the statistical significance of the SST change and it is found that the t-value for any point in the basin does not satisfy the criterion for 99 % confidence level. Thus the SST change in this experiment is not statistically significant. To

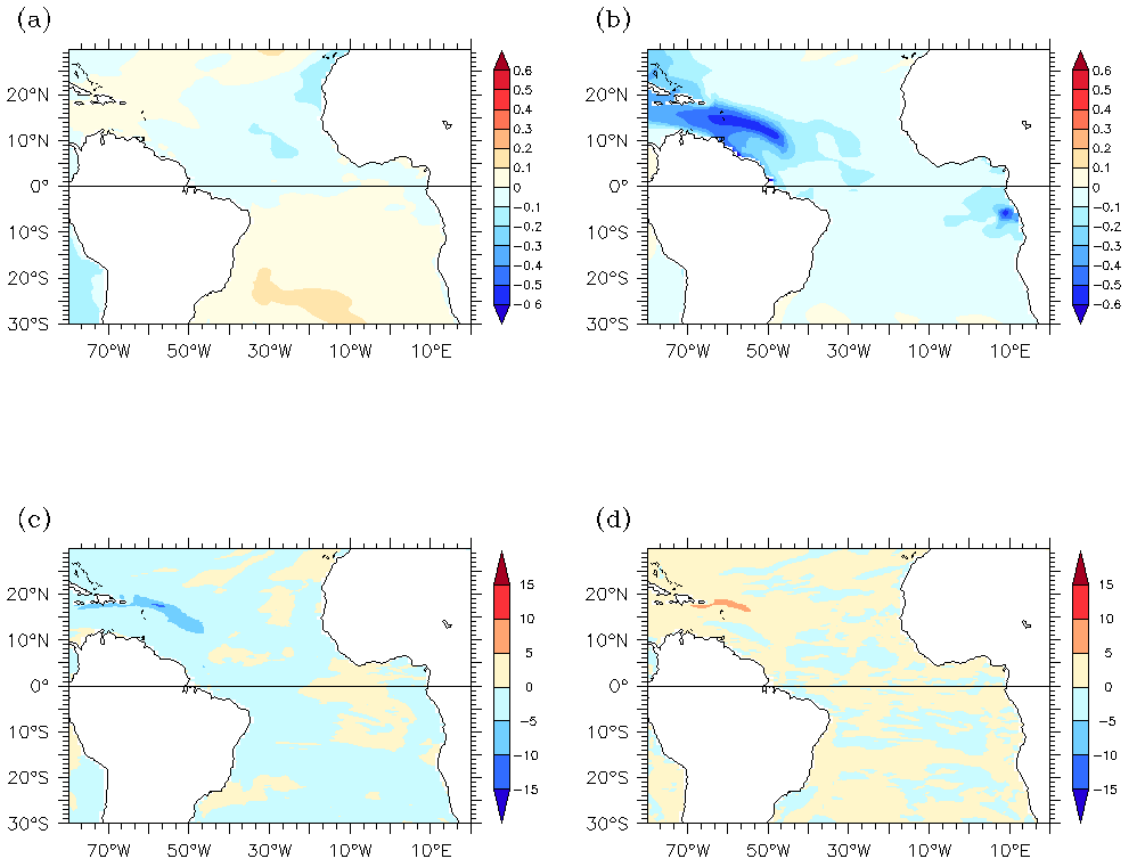

Fig. 12. Mean changes in EXP1 (a) SST (^{0}C), (b) SSS (g kg^{-1}), (c) MLD (m) and (d) BLT (m).

the east of the Caribbean Sea, between 50^0W and 65^0W and at around 18^0N, we find an increase of BLT with a maximum increase of about 10 m, as seen in Fig. 12c. Coinciding with this is the reduction in MLD with a maximum reduction of about 10 m (Fig. 12d). This indicates that the increase in BLT is brought about by the same factor that causes a decrease in MLD, which is surface freshening. This is especially evident when we consider that there is hardly any change in the ILD. A time-series analysis shows that the MLD and BLT are negatively correlated with a correlation coefficient of -0.65 at zero lag. Another interesting finding is that the region of maximum MLD change does not coincide with the region of maximum SSS change, but with the maximum gradient in SSS.

The mean changes in SSS, the meridional gradient in SSS anomaly $\frac{d\Delta SSS}{dy}$ and MLD , along 57^0W and between 10^0N and 25^0N, are shown in Figs. 13a, 13b and 13c respectively. The maximum decrease of salinity occurs at around 14^0N by about 0.6 g/kg while both $\frac{d\Delta SSS}{dy}$ and MLD change reach their maxima at around 18^0N. Increase in the salinity gradient occurs where the freshwater meets saltier water and slides over it, causing the increase in stratification and the reduction in MLD. The same can be seen when we look at the change in static stability (not shown).

As noted earlier, in the northwestern tropical Atlantic, while the surface salinity is heavily influenced by the river discharge from Amazon and Orinoco river systems the sub-surface salinity however is controlled primarily by the remote mechanism of subduction. The model fails to accurately simulate the sub-tropical salinity maxima region. In the Northern hemisphere the high SSS is not only lower but also displaced to the west of the actual region. The high SSS water subducts as a shallow subtropical salinity maximum and spreads both southward and westward. This high salinity water underlying the freshwaters of the Amazon-Orinoco river system is partially responsible for the formation of the shallow pycnocline. To validate our conjecture,

we further design a set of ensemble experiments, EXP2, as discussed in what follows.

The salinity change induced in EXP2 is shown in Fig. 14. The SSS change has been shown in Fig. 14a. In addition to the surface freshening from the Amazon mouth to the Caribbean as shown in the previous experiment, we also see high saline water flowing southwestwards from the region of subtropical salinity maxima. Fig. 14b shows subsurface salinity changes along a north-south transect at 60^0W while Fig. 14c shows the same along an east-west transect at 20^0N. From these two figures, it is clear that high salinity anomalies sink with the subtropical salinity maxima waters and flow southward and westward towards the Caribbean, where they lie beneath the low salinity anomalies propagating from the Amazon discharge region. Together they maintain the shallow pycnocline observed in this region. Every year, beginning in May, the NECC develops as a continuous eastward flow. Starting in November, the NECC weakens and by the end of boreal fall, it is almost non-existent.

Due to this, most of the subducted water is carried southwestward by the North Equatorial Current. This has been proposed to be a main cause for thick BLs to form during the winter months in the Caribbean (Sprintall and Tomczak, 1992).

Here we examine the response of the model to the salinity change shown in Fig. 14. The changes in mean SST and precipitation are shown in Figs. 15a and 15b, respectively. The closed contours show those regions where the SST change is statistically significant. Figs. 15c and 15d show the changes in mean MLD and mean BLT respectively. The first thing to note is that the regions of maximum change in BLT, MLD and SST coincide. The change in BLT is over 20 m and the MLD change is of the same order. This shows that not only a surface freshening but also a sub-surface salinity maximum is required for BL formation in this region. The relative extent to which the model responds to the changes in these two factors would depend upon the respective magnitudes of bias. There is a positive SST change in

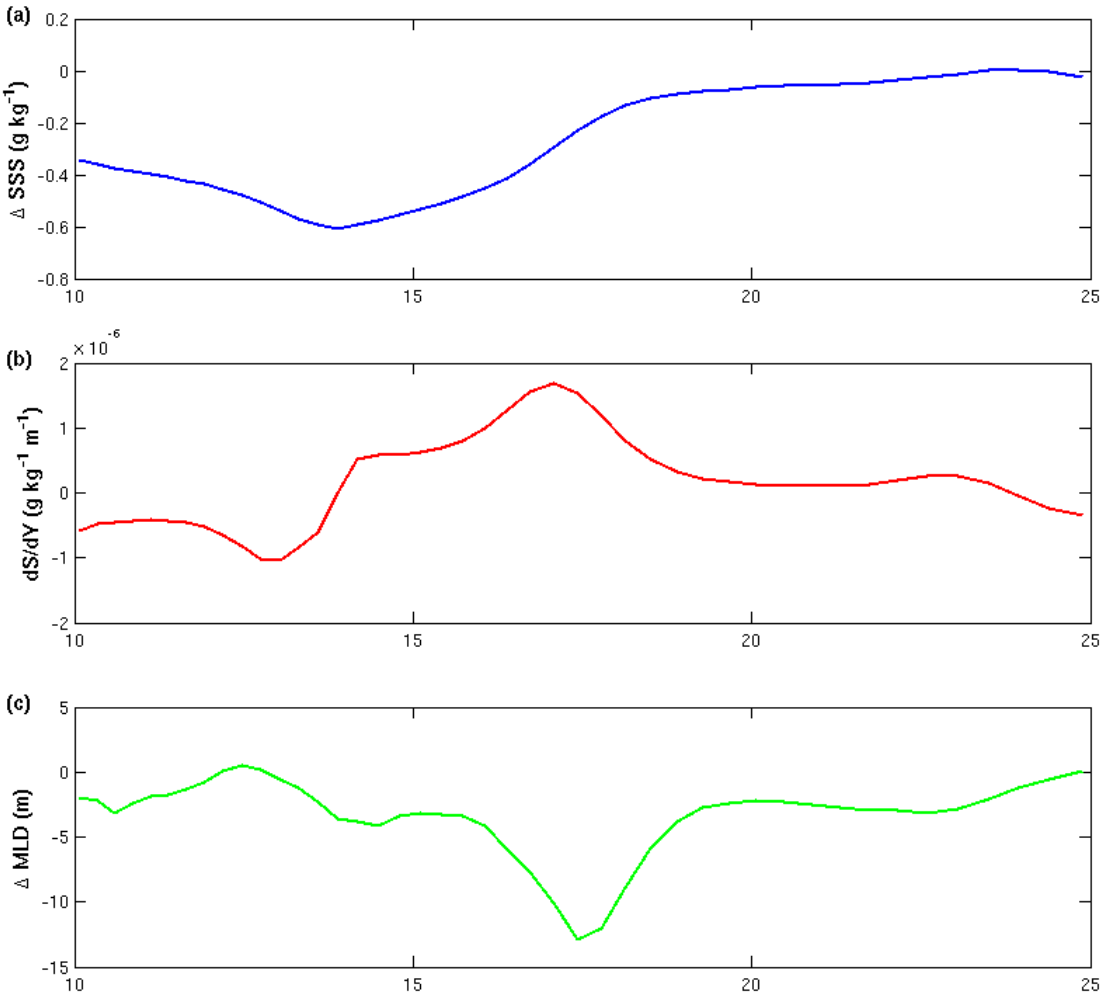

Fig. 13. The mean changes along 57^0W and between 10^0N and 25^0N for (a) SSS (g kg^{-1}), (b) $\frac{d(\Delta SSS)}{dy}$ (g kg^{-1}m^{-1}) and changes in (c) MLD (m).

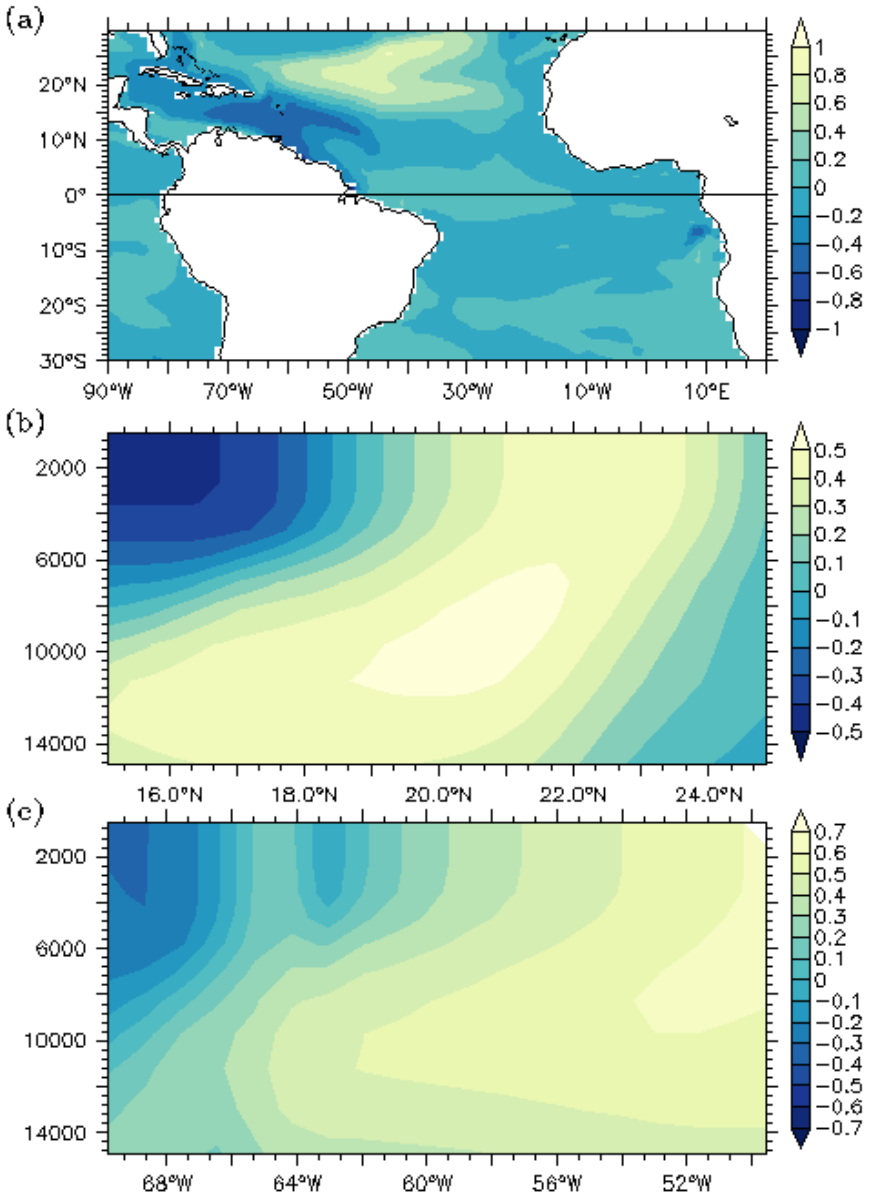

Fig. 14. Illustration of the mean salinity changes induced in EXP2. The change in surface salinity is shown in (a) the subsurface salinity change along 60^0W in (b) and along 20^0N in (c).

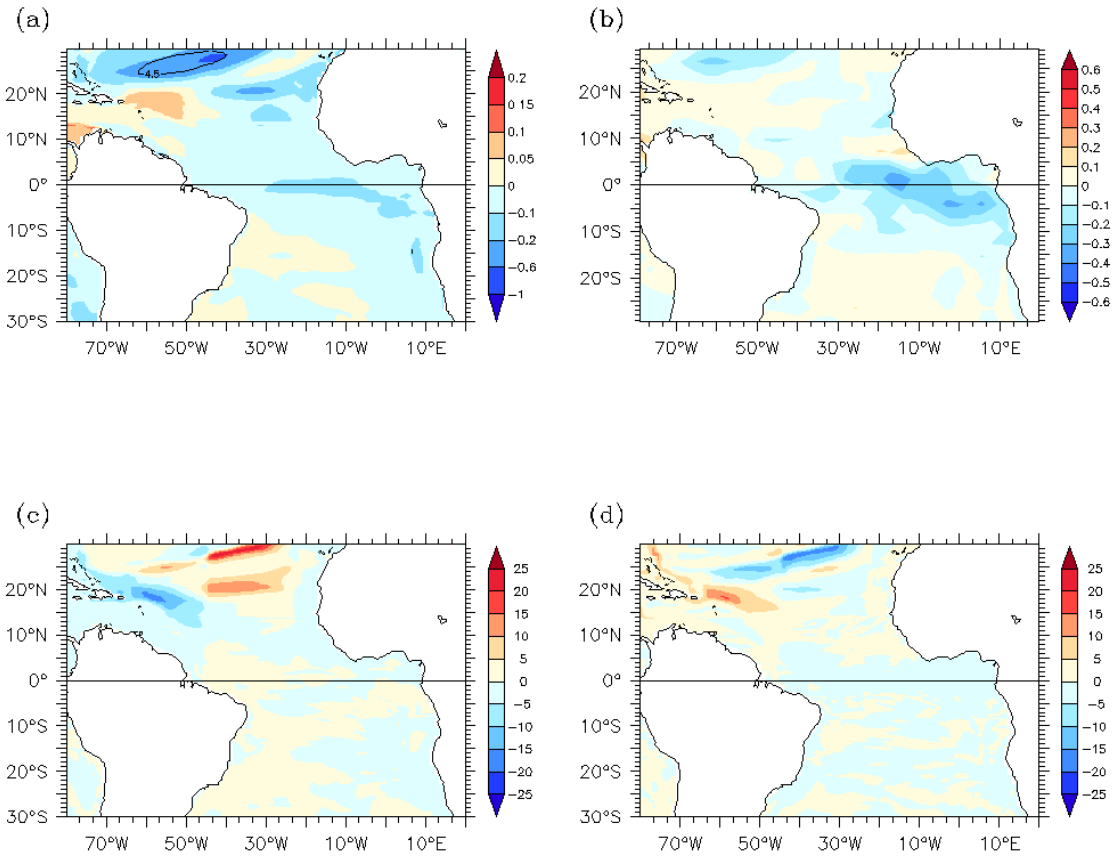

Fig. 15. The results from EXP2 are shown in this figure. The mean change in SST is shown in 15a, the mean SSS change in 15b, the MLD change in 15c and the mean BLT change in 15d (closed contours show those regions where the SST change satisfies the Student's t test for statistical significance at 99% confidence level).

the region of BL increase of about 0.1^0 C to 0.2^0 C, but the change does not satisfy the *t*-test and hence is not statistically significant. There is significant cooling of about 0.6^0 C in the region between 60^0W and 40^0W and between 25^0N and 30^0N. We shall discuss the source of these cold anomalies later in this section. Also, there is a reduction in precipitation of about 0.4 mm day^{-1} coinciding with the region of positive precipitation bias but the magnitude of change, which is about 10% of the mean bias, is not statistically significant.

To test the sensitivity of the model response to the forcing amplitude, we perform EXP3. The results are shown in Fig. 16. The salinity changes are regionally similar to the salinity changes in EXP2 but the magnitude of maximum salinity change is about 1.5 g kg^{-1}. Again, like in the previous experiment, we see a decrease of MLD and an increase of BLT in the Caribbean with the respective changes being higher than in EXP2 (about 25 m). There are significant cold anomalies with a maximum magnitude of about 1^0C to the north of the region of BL increase. There is also some cooling near the equator of about 0.2^0C to 0.6^0C that is statistically significant. The magnitude of precipitation anomalies straddling the equator in this experiment is also higher (about 0.8 mm day^{-1}) and is statistically significant. To establish the causal relationship between SST and precipitation, Singular Value Decomposition (SVD) analysis was performed. The region where maximum covariance occurs is between 35^0W and 20^0W and between 0^0 and 5^0N. Up to 47 % of the covariance can be explained by the first three empirical modes. For this region, the time series of SST and precipitation anomalies are correlated at 0.53. However, it is very difficult to establish lead-lag relationship using monthly data.

We have seen in EXP2 and EXP3 that there is cooling to the north and northeast of the region of BLT increase with a maximum magnitude of about 0.6^0C in EXP2 and about 1^0C in EXP3. There was no cooling found in EXP1. This leads us to the

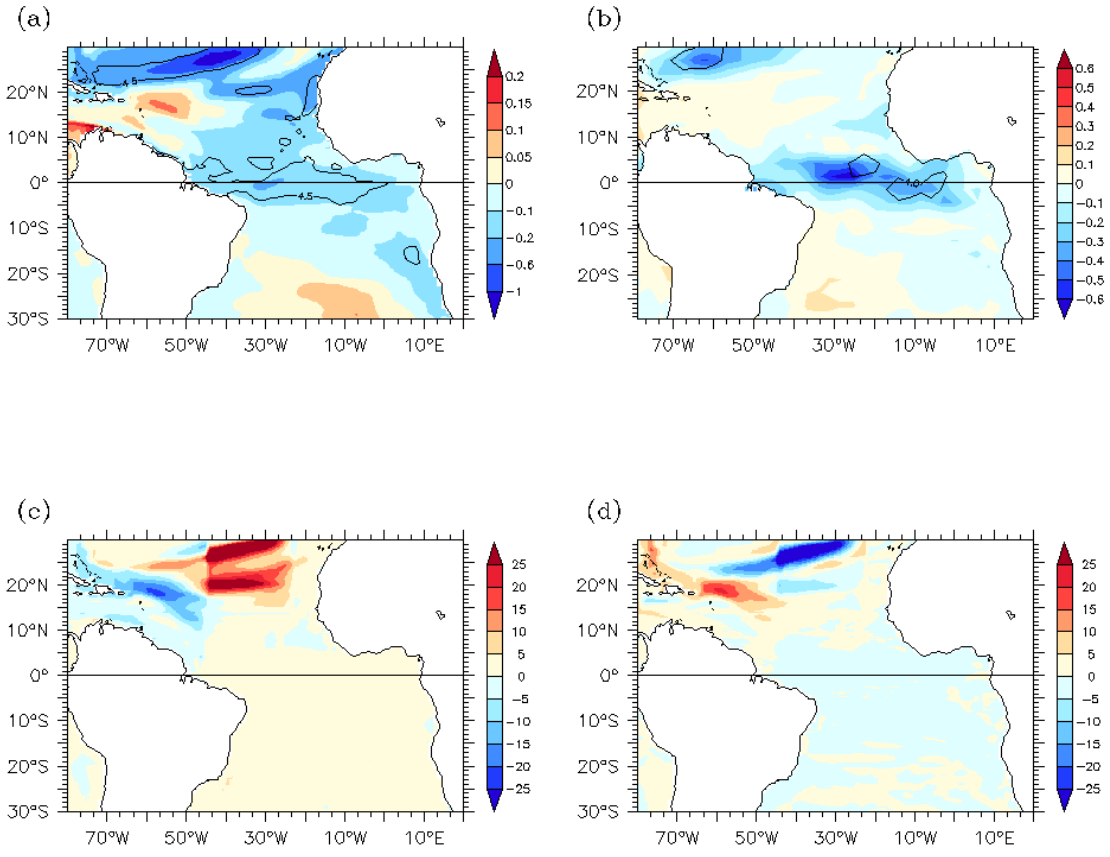

Fig. 16. As in Fig. 15 but for EXP3.

question as to what the source of this cooling could be. There are two important observations that are worth noting. The first is that the cooling occurs only in those experiments where we increase the salinity in the salinity maxima region. The second is that the magnitude of cooling responds almost linearly to forcing magnitude. This suggests that the cooling may be a direct response to the salinity changes in the subduction region. When we look at the evolution of SST (not shown), it is very clear that the cooling pattern resembles the pattern of salinity changes at the surface. Also, when we look at the change in MLD (Figs. 15 and 16), we can see that the regions of MLD increase coincide well with regions of cooling. To increase the salinity, we have added a positive E-P anomaly in this region. More evaporation occurs leading to an increase in surface salinity, which in turn destabilizes the water column, resulting in an enhanced mixing. The convection within the oceanic boundary layer in the KPP mixing scheme, which is employed in this model, can penetrate into the thermocline and cause an increase in the mixed layer (Large et al., 1994). Therefore, the evaporation forcing is likely to be responsible for the cooling.

Apart from the cooling in the forcing region, to explain the cooling in the equatorial region, we need to consider changes in atmospheric circulation. Fig. 17 shows the change in the mean circulation of the surface winds in EXP3. We find that there is an increase in equatorial divergence between 40^0W and 20^0W, which causes enhanced equatorial upwelling and cooling. Fig. 18 shows the mean changes in oceanic vertical velocity for EXP3 along the equator. We can clearly see that upwelling is increased, with maximum increase occurring between 34^0W and 30^0W. Vertical velocity averaged for this region and between the depths of 20 m and 40 m correlates significantly with surface zonal windstress for the same region at 0.41. Thus we suggest that when the forcing is strong, the response in the atmospheric circulation triggers a significant equatorial response in SST through changes in upwelling, which in turn causes the

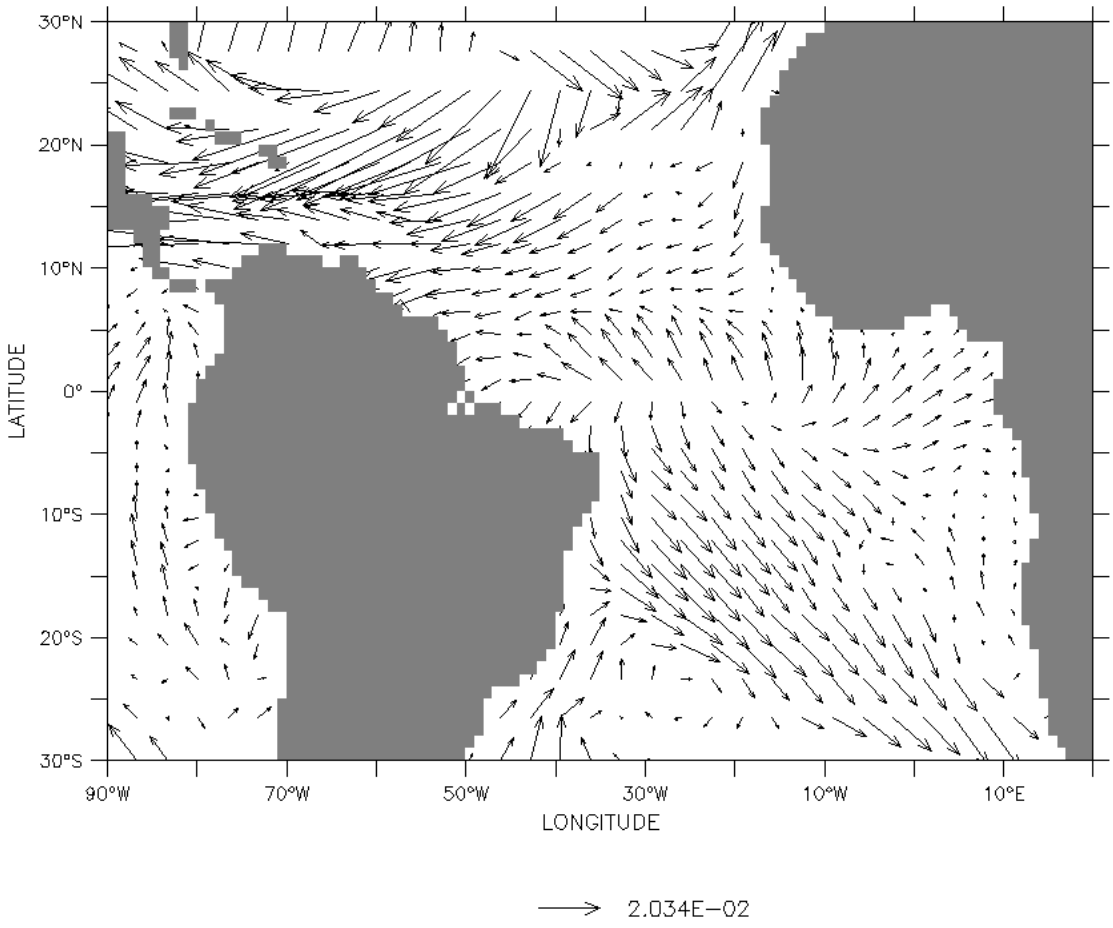

Fig. 17. The mean changes in circulation of surface winds in EXP3. The units are dyne cm^{-2}.

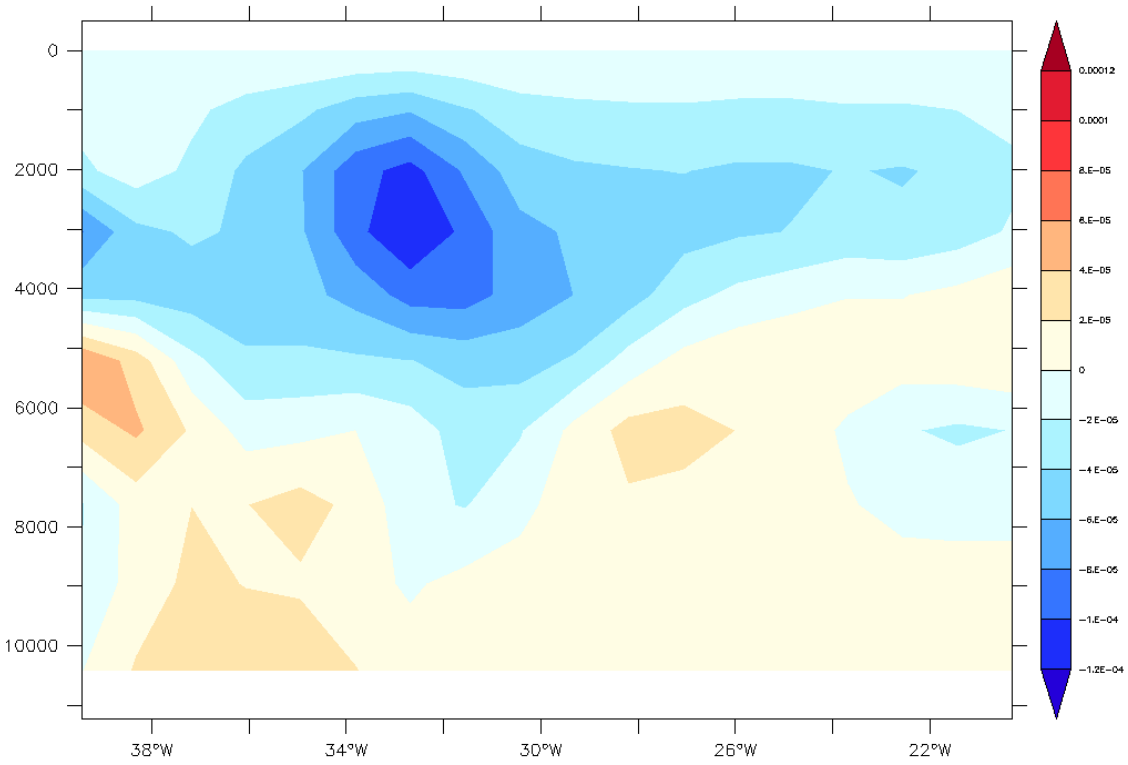

Fig. 18. Mean changes in vertical velocity (cm s^{-1})along the equator and between 40^0W and 20^0W . Velocity is positive downwards.

response in precipitation.

D. Temperature Inversions

One of the hallmarks or signatures of BLs in the western tropical Atlantic is the formation of temperature inversions during boreal fall and winter months. Beginning in fall, the atmosphere tends to cool the surface ocean. Normally, wind mixing would mix up the surface ocean and cause a uniform cooling of the mixed layer or isothermal layer. However, in the presence of a BL, the strong pycnocline below the mixed layer does not allow wind mixing to penetrate below the mixed layer. Consequently, the water below the density mixed layer is not cooled and is able to retain its temperature. As a result of this, temperature inversions begin to form. Temperature inversions could also form during summer and late spring seasons near the Amazon mouth where thick BLs arrest an important part of the penetrative solar radiation within them (Masson and Delecluse, 2001). Typically, entrainment would cause a cooling of the mixed layer but in cases where we have sub-surface temperature inversions, entrainment would cause a warming of the mixed layer temperature (Breugem et al., 2008). This process helps in alleviating the effect of atmospheric cooling on SST in the northwestern tropical Atlantic. The effect of improved BL simulation on the temperature inversions found in this region is now examined.

We take the ensemble averages for each experiment and compute the maximum subsurface temperature difference (ΔT) across the base of the mixed layer, averaged over the region between 65^0W and 50^0W and between 18^0N and 20^0N and for the winter seasons in each of the 10 years. $\Delta T = T_{-h} - T_{ml}$, where T_{-h} is the temperature below the mixed layer and T_{ml} is the temperature at the base of mixed layer. Thus a positive ΔT indicates an inversion in subsurface temperature. ΔS

is the corresponding salinity difference across the mixed layer. Fig. 19 shows the scatter between ΔT and ΔS. In EXP1, the increase in BLT is about 10 m and the vertical salinity stratification is not strong enough to support an inversion in temperature. However, in EXP2 the BLT increase is much larger (about 20 m) and the salinity gradients induced are substantial enough to induce temperature inversions. The maximum inversion in this experiment is about 0.07^0 C. The BLT increase in EXP3 is even larger (about 25 m) and thus the higher salinity gradients are able to support a stronger temperature inversion of about 0.2^0 C.

The effect of improved BL simulation on the formation of temperature inversions is illustrated in Fig. 20. The top panel (Fig. 20a), corresponding to the winter of year 4 from the 10 year CR, shows that the MLD is almost as deep as the ILD, as a result of which there are no thick BLs. This means that below the MLD, the haline stratification is not strong enough to sustain the formation of an inversion in temperature and thus no inversions develop. The middle panel (Fig. 20b) shows the development of the sub-surface salinity anomaly in year 4 of EXP3. The intrusion of a high salinity tongue, which can be seen centered at around 100m, is a result of the enhanced subduction as discussed earlier. This increased salinity in the subsurface is responsible for the shoaling of the pycnocline and the formation of thick BLs. From Fig. 20c, it is evident that the thick BLs result as a consequence of the sub-surface salinity anomaly, which in turn supports the formation of temperature inversions. It should be noted that the ILD in EXP3 is almost identical to the ILD in the control simulation, suggesting that the inversions are entirely induced by changes in MLD and consequently BLT.

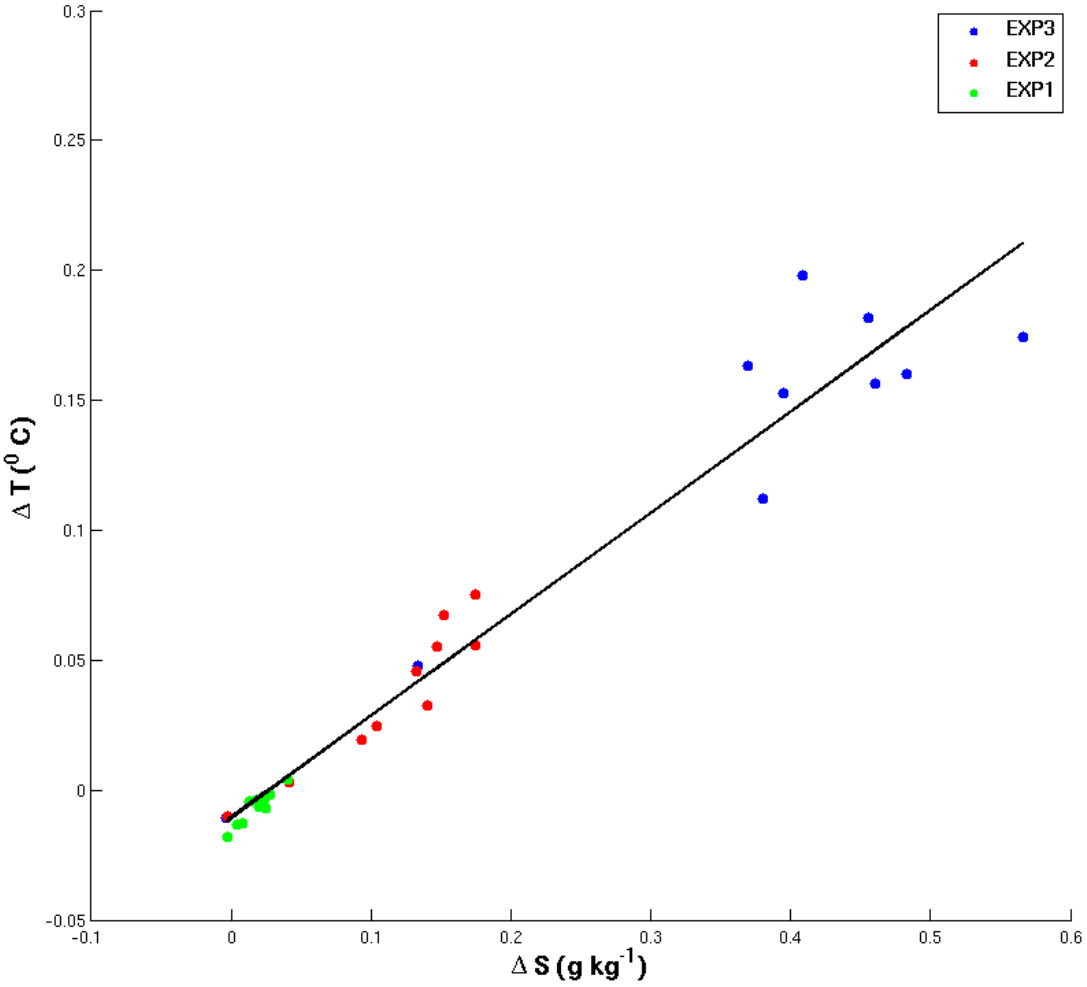

Fig. 19. Winter vertical subsurface temperature and salinity differences below the mixed layer plotted against each other for the three experiments. Values have been averaged over the region between 65^0W and 50^0W and between 18^0N and 20^0N.

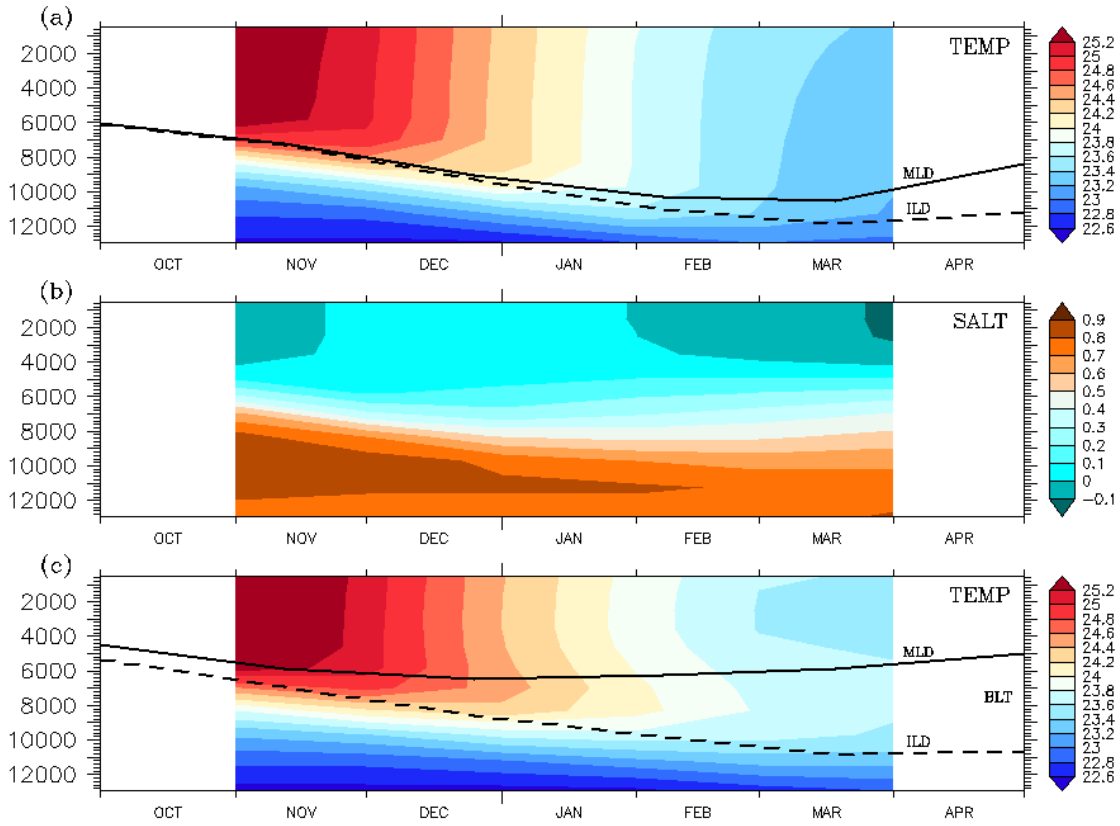

Fig. 20. The subsurface temperature during the winter of year 4 in the CR is shown in 20(a). 20(b) and 20(c) show the sub-surface salinity anomaly and the subsurface temperature respectively during the winter of year 4 in EXP3. Values have been averaged over the region between 65^0W and 50^0W and between 18^0N and 20^0N.

E. Heat Budget Analysis

To better understand the SST change in the region of BL increase, we consider a simplified mixed layer heat-budget equation (Moisan and Niiler, 1998), which can be written as

$$\rho C_p h \frac{\partial T}{\partial t} = q_0 - \rho C_p h\,(v.\nabla T) + q_{-h} + \epsilon$$

The above simplified mixed layer heat equation was also used by Foltz and McPhaden (2009) in the analysis of BL in the central tropical North Atlantic. Here ρ is the mixed-layer averaged density, C_p is the specific heat of sea-water (4000 J kg^{-1} K^{-1}), h is the depth of the mixed layer, T is the mixed-layer averaged temperature, q_0 represents the net surface heat flux corrected for the shortwave radiation penetration through the base of the mixed layer, v is the mixed-layer averaged velocity and q_{-h} represents the heat flux across the base of the mixed layer which includes heat flux due to entrainment and turbulent mixing. The term on the left hand side, $\rho C_p h \frac{\partial T}{\partial t}$, represents the rate of change of mixed-layer heat storage (MLH), the first term on the right hand side, q_0, represents the net surface heat flux corrected for the penetration of shortwave radiation at the base of the mixed layer (SHF), the second, $\rho C_p h\,(v.\nabla T)$, represents advective heat flux (AHF) and the third, q_{-h}, represents the heat flux due to entrainment and other turbulent processes at the base of the mixed layer (THF), which is obtained as a residue. The short-wave radiation penetrating the base of the MLD can be written as follows.

$$q_{pen} = q_{sfc}\,(1-a)\,[A_1\, e^{-B_1 h} + A_2\, e^{-B_2 h}\,]$$

Here the parameters A_1, A_2, B_1 and B_2 are Chlorophyll-based parameters, q_{sfc} is the shortwave radiation incident at the surface, a is the albedo and h is the MLD. The climatology of Chlorophyll distributions is based on SeaWIFS data and the chlorophyll based parameters A1, A2, B1 and B2 obtained from Ohlmann (2003). The

SeaWIFS chlorophyll climatology was obtained from NCAR (Nancy J. Norton, personal communication, 2009). We obtain the net surface heat flux directly as model output, calculate the penetrative heat flux as described above and subtract the latter from the former to obtain q_0.

Fig. 21 shows the evolution of the anomalies for each of the terms in the mixed layer heat budget in EXP1, EXP2 and EXP3 for the region averaged between 65^0W and 50^0W and between 18^0N and 20^0N. All terms are smoothed with a 5-month running mean and the corresponding error bars are indicated. Fig. 21a shows the MLH anomalies, 21b the SHF anomalies, 21c the AHF anomalies while 21d shows the THF anomalies. We caution that THF is calculated as a residue and thus may not be an accurate representation of entrainment and other turbulent processes at the base of the mixed layer.

In evaluating different components of the heat budget, we note that in MLH, AHF and SHF the long-term changes are comparable to the seasonal variations, whereas in THF the former are much weaker than the latter. Mean changes in MLH are 4.57 and 12.46 Watt m^2 respectively in EXP2 and EXP3 implying a slight increase in the mixed layer heat storage in the region of BL increase. The changes in mean SHF are estimated to be about -7.66 and -4.55 Watt m^{-2} in EXP2 and EXP3, respectively, suggesting that the atmosphere tends to cool the ocean surface. As we had seen earlier, the SST cooling induced by our forcing tends to reinforce the prevailing easterly trades in the region of BL increase. This causes an increase in latent and sensible heat loss from the ocean and is responsible for the reduction in SHF in EXP2 and EXP3. However, there is no such loss in EXP1 as there are no such changes in the surface windstress. The changes in mean AHF are estimated to be about 10.78 and 14.1 Watt m^{-2} in EXP2 and EXP3, respectively, but it is again small in EXP1.

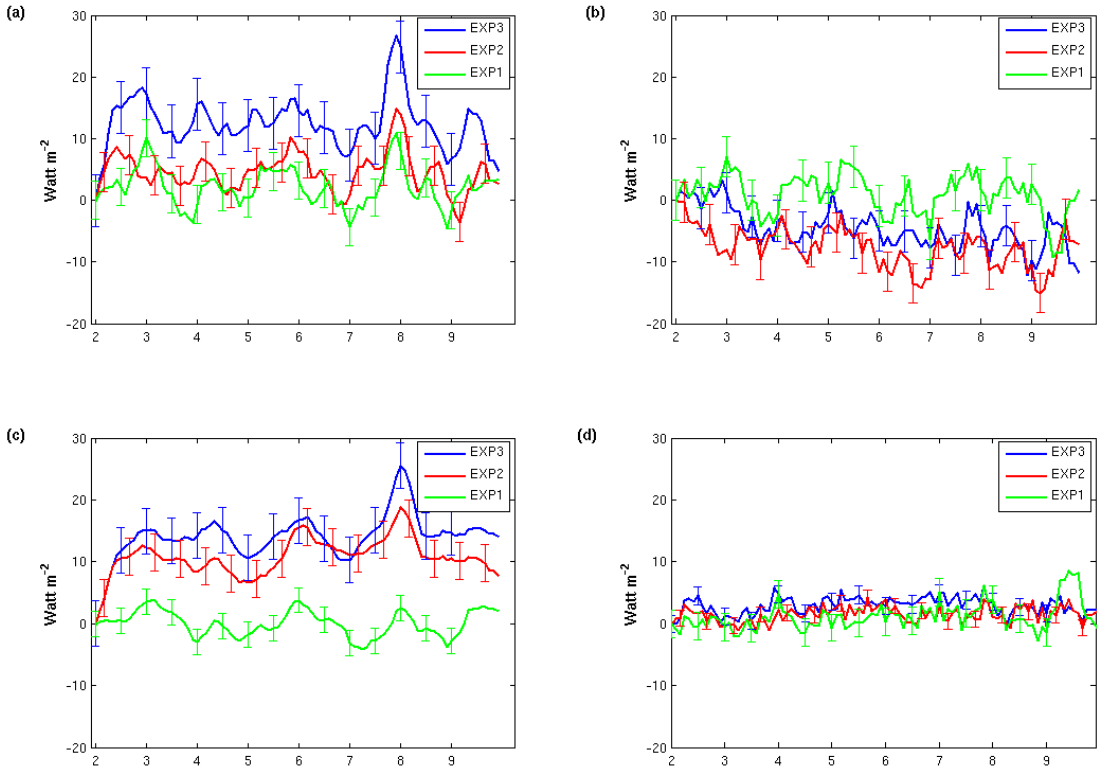

Fig. 21. Time evolution of the mixed layer heat budget terms with error bars indicated. The evolution of MLH in 21(a), SHF in 21(b), AHF in 21(c) and THF in 21(d) for the various cases as depicted in the legend. All time series are at a running mean of 5 months. The first and last years have been removed due to box-car smoothing. All values have been averaged over the region between 65^0W and 50^0W and between 18^0N and 20^0N.

F. Summary

Several theories have been advanced before suggesting various possible mechanisms for the BL formation in the northwestern tropical Atlantic region. While some felt that the main factor responsible was the freshening caused by Amazon-Orinoco river discharge, some others suggested that the remote mechanism of subduction could play a more dominant role. It has also been suggested that erroneous representation of BLs in coupled models could contribute to the well-known tropical Atlantic SST biases and that BL simulation needs to be improved in order to improve the mean climate of the coupled system through the BL-SST-ITCZ mechanism. Our goal in the present study is to identify the reasons responsible for the misrepresentation of BLs in the NWTA region in CGCM simulations and investigate the effects of improving the BL simulation on the coupled climate system within the framework of a state-of-the-art CGCM.

We have performed a series of idealized numerical experiments to test the various hypotheses. In the first experiment (EXP1), we examined the effect of freshening in the Amazon basin on the BL formation. Most of the low salinity water is carried northwestward by the strong Guyana current and there is a decrease in MLD and an increase in BLT (5-10 m) to the east of the Caribbean in the region where the meridional salinity gradient is a maximum. However, the increase in BLT fails to generate a statistically significant SST response.

Next we investigated the combined effect of improving not only the surface salinity but also the sub-surface salinity by increasing the salinity in the subtropical salinity maxima region (EXP2). It was found that high salinity water subducts as a shallow sub-tropical salinity maximum and flows southwestward into the Caribbean. This salty water mass raises the pycnocline and in that process results in thicker BLs (15-

20m). This shows that the BLT is controlled by both the freshening at the surface due to advection of low-salinity waters from the Amazon mouth and by the salinity maxima waters in the sub-surface. The extent to which the model responds to the forcing depends on the extent of model bias in the surface and sub-surface. In our present model, for the region between 65^0W and 50^0W and between 18^0N and 20^0N, the surface salinity bias is about 0.4 g kg^{-1} but in the subsurface, the bias is about 0.8 g kg^{-1}. There is not much improvement in the surface salinity but the sub-surface salinity bias is reduced by about 0.4 g kg^{-1} in EXP2. SST increases in the region of BL increase by about 0.1^0C to 0.2^0C, but is not statistically significant.

In the third set of ensemble experiments (EXP3), we tested the sensitivity of the model response to the forcing amplitude by doubling the forcing. In this case, the BLT increase was slightly larger than that in EXP2 (20-25 m). In the region of BL increase, the sub-surface salinity bias is almost completely removed. As in EXP2, we have an SST increase in the region of BL increase by about 0.1^0C to 0.2^0C, but the increase is not statistically significant. Also, both in EXP2 and EXP3, there is significant cooling to the north of the region of BLT increase (of the order of 1^0C), which increases with the forcing amplitude. It was found that evaporation along with increased mixing below the mixed layer contributes to the cooling to the north of the region of BL increase.

There is an increase in equatorial divergence causing enhanced equatorial upwelling and cooling of about 0.2^0C to 0.6^0C in EXP3. We speculate that these anomalous surface winds are a response to changes in convergence over continental South America. Coinciding with the cold SST anomalies are negative precipitation anomalies of about 0.8 mm day^{-1} in EXP3. The tropical Atlantic precipitation bias is improved by about 15-20 %. SVD analysis shows that the maximum covariance of SST and precipitation anomalies occurs in the region between 35^0W to 20^0W and

between 0^0 and 5^0N. However, a causal relationship cannot be established using time-series correlation as monthly data is used for the analysis. We suggest that under the influence of strong forcing, the atmospheric circulation response triggers a significant equatorial response in SST through changes in upwelling and consequently causes the response in precipitation.

In EXP1, even though there is a shoaling of the MLD due to freshening at the surface, no temperature inversions form, as the induced salinity gradient is not strong enough to sustain an inversion. Formation of a temperature inversion requires a strong salinity gradient below the MLD, which can compensate the instability caused by an increase in temperature. Temperature inversions form in EXP2 and EXP3, as the induced salinity gradients are strong enough to sustain inversions in temperature. Also, the magnitude of temperature inversions increases with the forcing amplitude. Thus, to improve the simulation of temperature inversions in the model, we need to not only improve the surface but also the sub-surface salinity, as both of them jointly determine the salinity stratification.

Heat budget analysis for the region of BL increase reveals that in EXP2 and EXP3, there is an increase in mixed layer heat storage rate (MLH) and advective heat flux tendency (AHF). Incase of surface heat flux (SHF), there is a reduction for the region of BL increase in EXP2 and EXP3. This is because the SST cooling induced by the positive E- P anomaly reinforces the easterly trades and causes an increased latent and sensible heat loss. This acts as a mechanism to damp the SST increase in the region of BL increase. Again, we do not find such a reduction in surface heat flux in EXP1 as there is no cooling to the north to cause the changes in surface windstress. Even though in EXP2 and EXP3, there is a slight increase in the mean turbulent heat flux (THF) at the mixed layer base, the signal to noise ratio is very low making it very hard to draw conclusions. Also, the THF is estimated as a

residue and thus is prone to errors in approximation.

Finally, there are certain caveats in our present study. One is that the forcing is artificial. Salinity biases result not only from biases in precipitation but also from biases in wind-stresses and circulation. Also in reality, the Amazon water that is discharged into the Atlantic has very high turbidity. This is due to the suspended particles found in riverine discharge. Thus it is capable of arresting the penetration of solar short wave flux and confining much of it to the very upper layers of the ocean. Because we have only changed the salinity and not the turbidity, we cannot exactly reproduce the effect of Amazon River discharge. This could be another possible reason as to why the response in SST in the region of BL increase was not very strong.

CHAPTER IV

EFFECT OF BARRIER LAYERS ON THE SURFACE OCEAN RESPONSE TO TROPICAL CYCLONES. PART 1: OBSERVATIONS

We studied the formation mechanism of BLs in the northwestern tropical Atlantic using a CGCM and we also looked at its potential role in the maintenance of the mean climate of tropical Atlantic. Now we explore their influence at shorter time scales. More specifically, we study how they modulate the upper ocean response to TC induced mixing. In this chapter, we analyze a string of observational data sets.

A. Introduction

A TC is a cyclone that forms over the tropical oceans. They are also known as typhoons (Pacific) or hurricanes (Atlantic) depending on which oceanic region they are found. TCs are natural hazards impacting human life and economy around the world. They constitute some of the most important geophysical phenomena, as along with floods they are known to cause most property damage globally.

Apart from the role they play in day to day weather, they may also play an important role in climate on longer time scales. This makes it very important for us to understand the factors responsible for the formation and intensification of TCs. The meridional overturning circulation (MOC) is an important feature of the earth's climate system as it relates to the global ocean heat transport. This MOC is a simplified conceptual view of the complex global ocean circulation. There are two basic physical mechanisms for explaining the MOC, one of which is related to diapycnal mixing. According to this mechanism, as explained by Munk and Wunsch (1998), the MOC is primarily maintained by diapycnal mixing. Mechanical energy is expended in the formation of deep water in the high latitudes which sinks to the bottom and trav-

els equatorwards. They find that nearly 2.1×10^{12} W of turbulent energy is required for the formation of 30 Sv of deep water. In the tropics the ocean receives heat from above and thus is highly stratified. Hence a strong mixing agent is required to cause diapycnal mixing. TCs mix the surface ocean down until 100-200 m depth, depending on their intensity. When the ocean is mixed, cold anomalies form in the surface ocean while warming occurs in the sub-surface. The atmosphere restores the surface cold anomalies while the sub-surface warm anomalies remain, which then act as a source of enthalpy. When we consider the net column integrated heating, in steady state there has to be a divergence of heat flux towards the poles and this according to Emanuel (2001) contributes to the poleward heat transport. Using observed TC tracks as well as data from coupled ocean-atmosphere models, Emanuel (2001) shows that TC induced mixing could be responsible for as much as 1.4 ± 0.7 PW of heat transport, which accounts for a significant fraction of the oceanic heat transport. Using several reanalysis data sets, Sriver and Huber (2007) estimate that the TCs are responsible for upto 15% of poleward heat transport and mixing in the surface ocean of the tropics. After having conducted a set of experiments with an OGCM where they vary the vertical mixing coefficient, Jansen and Ferrari (2009) conclude that the latitudinal extent of vertical mixing from the equator plays a critical role in the determination of ocean heat transport. Using a coupled model of intermediate complexity, Korty et al. (2008) show that enhanced poleward heat transport resulting from vigorous TC activity could have helped maintain the low pole-to-equator temperature gradient during warm equable climates of the past. Fedorov et al. (2010) using a variety of models including a downscaling hurricane model and GCMs show that the TC induced mixing plays a critical role in the temperature of water parcels which subduct in the tropics and surface in the eastern equatorial Pacific. They even suggest that TC extent and mixing induced by them in the upper ocean of the

Pacific could have caused the permanent El Nino-like situation during past climatic conditions like the early Pliocene epoch.

TCs could also play an important role in marine eco-system dynamics. Marine autotrophs like phytoplankton perform photosynthesis by acquiring solar energy from above and nutrients from below. This photosynthesis is a very important process for the maintenance of the food-chain and ultimately is the driver for the sustanence of all life on the planet. Typically, upwelling regions are the places which are biologically most productive because of the availability of nutrients. Especially, in the tropics, as the surface ocean is highly stratified, it is difficult to get nutrient upwelling without a strong mixing agent. There is mounting evidence in recent studies to indicate that TCs can perform this function to a considerable degree. Lin et al. (2003b) observed in the South China Sea that TCs could contribute to as much as 30% of the annual primary production. The hydrodynamic response of the ocean to TCs can also have a considerable effect on coral reefs (Madin and Connolly, 2006), which are a very important part of the marine eco-systems as they form a natural habitat for a host of aquatic flora and fauna.

The formation of a TC is characterized by the transformation of a randomly organized cold-core convective system into a warm-core system that can sustain itself with a cyclonic surface circulation. There are some pre-existing atmospheric conditions which are favorable for TC formation and intensification like low wind shear, significant planetary vorticity, diabatic heating source for initial convection etc. Low wind shear favors the formation of a TC as it helps concentrate the latent and sensible flux exchange at the air-sea interface. If the vertical wind shear is high, heat at the upper levels is advected away leading to reduced convection. This process is known as ventilation (DeMaria, 1996). It is also generally agreed that warm SSTs favour the formation of TCs by acting as a source of diabatic heating and moist convec-

tion. Several mechanisms have been proposed for the formation and intensification of a TC of which a well-accepted mechanism is that it is maintained primarily by the exchange of heat flux at the ocean-atmosphere interface (Emanuel, 1986). This heat flux exchange includes both latent and sensible heat fluxes. The sensible heat flux exchange depends on the wind speed and the air-sea temperature difference at the interface. The latent heat flux depends on the wind speed and the difference in humidity between air in contact with the ocean and air at a certain height above sea-level. Since the atmospheric humidity can also be expressed as a function of its temperature to first order, the latent flux also depends on the air-sea temperature difference.

Thermodynamically, a TC could be envisaged as being an idealized Carnot engine. In the energy cycle of a TC, the latent and sensible heat flux exchange at the air-sea interface form the energy source while the turbulent energy dissipation in the atmospheric boundary layer forms the energy sink. By considering an energy balance between the flux of momentum into the sea ($\mathrm{F}_m = -C_D\rho|V|V$), flux of enthalpy from the sea ($\mathrm{F}_k = C_K\rho|V|(k_0^* - k)$) and the column integrated dissipative heating of the atmospheric boundary layer ($\mathrm{D} = C_D\rho|V|^3$) in a circular region with the eye of the TC and making an approximation that this holds good within the radius of maximum winds, Emanuel (2003) shows that the potential intensity of a TC, which is the maximum attainable velocity (V_{max})is given as

$$V_{max} = \sqrt{\frac{C_K}{C_D}\,\frac{T_s - T_0}{T_0}\,(k_0^* - k)}$$

Here V is the near surface wind speed, ρ is the density of air, k is the specific enthalpy of surface-air and k_0^* is the specific enthalpy of air in contact with the sea-surface. C_D is the transfer coefficient of momentum while C_K is the transfer coef-

ficient of enthalpy. Finally T_s and T_0 are the temperatures of air in contact with the sea-surface and the outflow temperature respectively. From the above relationship, it is very clear that the potential intensity of a TC critically depends on the air-sea temperature difference. Thus any process that can affect the SST due to wind mixing can potentially play a role in TC intensification. This led Gallacher et al. (1989) to conclude that SST cooling produced by TC induced mixing could act as a negative feedback to its intensity. Using results from a coupled ocean-atmosphere model simulation, they conclude that a mere 2.5^0C decrease in SST could shut down the energy source to a TC completely.

Several other studies followed whose results concurred with them. Khain and Ginis (1991) performed a comparison of TC strength in two different numerical simulations. In one they use a 5-layer TC model coupled to a 3-layer ocean model and in the other simulation they use the uncoupled version of the same TC model. They find that the negative feedback effect of the ocean significantly reduced the TC intensity. Using an ax-symmetric hurricane model coupled to a 4-layer ocean model, Schade and Emanuel (1999) find that the SST feedback effect could reduce the TC intensity by as much as 50%. Results from real simulations of hurricanes in the Gulf of Mexico and the western tropical Atlantic using a nested mesh TC model coupled to a complex ocean model led Bender and Ginis (2000) to suggest that coupling significantly improves the TC intensity prediction skills of the model. An analysis of 23 Atlantic, Gulf of Mexico and Caribbean hurricanes using airborne expendable bathy thermograph (AXBT) data and buoy-derived SST data indicates that the inner-core SST change is a critical parameter for TC intensification (Cione and Uhlhorn, 2003). It is found that inner-core SST cooling on the order of 1^0C can alter the enthalpy flux exchange by upto 40% . By performing a 5-day cloud resolving simulation of Hurricane Bonnie (1998), Zhu and Zhang (2006) show that hurricane induced SST cooling reduces the

intensity considerably. They show that the reduction in intensity is about 25-hPa per 1^0 C cooling in SST. Using an analysis of data from various sources including satellites and a numerical model, Shay et al. (2000) show that Hurricane Opal (1995) intensified rapidly when passing over a warm-core eddy shed by the Loop current. Using an OGCM,Pasquero and Emanuel (2010) show that the feedback between TC activity and upper-ocean thermal structure could potentially amplify the modeled TC power dissipation. Analyzing remote sensing data sets for two typhoon events, Lin et al. (2003a) show that the surface winds significantly reduce in the presence of SST cooling. In the light of the above studies, it becomes vital to understand the factors controlling the upper ocean response to TCs.

The surface ocean SST response to TC induced mixing has been widely studied in the past. The non-linear response of a 2-layer baroclinic ocean to a stationary axi-symmetric hurricane was studied by O'Brien (1967). In a seminal work on upper ocean response to TC induced mixing, Price (1981) identified the wind speed, the storm translational speed and the oceanic thermal stratification to be the most important factors which determine the upper ocean response to TC induced mixing. He further suggested that when it comes to SST, the primary mechanism which determines SST change is entrainment and turbulent mixing at the base of the mixed layer and that the heat loss to the atmosphere plays a minor role. Using a coupled model with the Pennsylvania State University (PSU) - NCAR mesoscale model version 4 (MM4) as the atmospheric component and a mixed layer model as the ocean component, Chan et al. (2001) find that upper ocean features like warm core eddies and the vertical thermal stratification play an important role in TC intensification. Using results from a Gulf of Mexico TC simulation with an atmosphere boundary layer flux model coupled to the Navy Coastal Ocean Model (NCOM), Morey et al. (2006) show that the main factor responsible for SST cooling under the influence of TC induced

mixing in the open ocean is entrainment cooling while close to the coast, SST cooling is primarily due to latent heat loss to the atmosphere.

B. Potential Role of BLs

The oceanic mixed layer, which is typically defined as a layer of constant density and temperature, plays an important role as an interface for air-sea interaction mechanisms. It is normally assumed that the layer of uniform temperature is also the layer of uniform density. However, as noted earlier, in regions where the salinity dominates over temperature in the determination of the mixed layer density, the difference between the MLD and ILD is defined as the BL as it acts as a barrier to entrainment cooling and vertical mixing. When we consider the regions of BL formation in the tropics we also see that they are all regions of TC formation. Thus in these regions, the vigorous mixing under the action of TCs could be reduced. Consequently, the weakened entrainment could lead to reduced SST cooling which can help reduce the negative feedback effect of TCs. We also saw earlier that under certain conditions, the BL can also be associated with a sub-surface temperature inversion. In such situations, vertical mixing could bring warmer sub-surface water into the mixed layer and cause a slight SST warming, which could act as a positive feedback mechanism.

There have been some studies in the past which have hinted at the possible role of BLs in TC intensification. It is well known that the Amazon-Orinoco river discharge forms a fresh-water lens in the northwestern tropical Atlantic, resulting in the formation of salt-stratified BLs (Pailler et al., 1999; Hu et al., 2004). These BLs inhibit vertical mixing and entrainment cooling, and thus help to maintain the warmpool and favor the formation of TCs. The buoyant nature of the surface plume results in SSTs being considerably higher in the plume by up to 3^0C. These high

SSTs are maintained to a depth of about 60m due to the freshwater BL effect. A statistical study of Atlantic hurricane tracks by Ffield (2007) shows that 68% of all category 5 hurricanes passed over the historical Amazon plume region. Based on simulations using a regional atmospheric model, Vizy and Cook (2010) show that the Amazon/Orinoco plume SSTs are warm enough to significantly influence the Atlantic summer hurricane activity. In simulations where the warm plume SSTs are included, the hurricanes that form were found to be more intense and with more tendency to make land-fall when compared to those in which the warm plume SSTs were excluded. They attribute this to a westward shift in the North Atlantic subtropical anti-cyclone. In the eastern equatorial Indian Ocean, the Bay of bengal is a region of significant TC activity. We had seen earlier that the Bay is also a region where thick BLs result from the discharge of major river systems like the Ganges, Brahmaputra and Irrawaddy from the surrounding continental land mass and also monsoonal rain. Sengupta et al. (2008), by analyzing satellite SST products, show that the SST cooling induced by post-monsoon TCs in the Northern Indian Ocean is much lower than that induced by pre-monsoon TCs, and suggest that it could be due to BL formation in the Bay of Bengal. TC Nargis was one of the most devastating TCs ever in the Bay of Bengal. At its peak, it had sustained winds exceeding 215 km hr^{-1} and a storm surge of 3-4 m. It was responsible for the death of more than 130,000 people and an economic loss in the order of $10 billion. McPhaden et al. (2009), using a variety of satellite and in situ data sets, showed that TC Nargis intensified over a region with thick BLs and high SSTs. Due to the low salinities, the MLD was as shallow as 10 m and the SSTs exceeded 30^0 C.

These observational/reanalysis studies suggest that BLs may play a role in the SST response to TCs (Sengupta et al., 2008; McPhaden et al., 2009; Ffield, 2007), and that they might even have an impact on the intensification of TCs. Furthermore,

TCs may also in turn influence the BLs through a feedback loop. In the present study, we investigate how BLs modulate the upper ocean SST response to TCs by examining and analyzing the output from a high-resolution coupled regional climate model (RCM) combined with a variety of observational data including satellite data, reanalysis data, hurricane track data and data from Lagrangian drifters. In this chapter, we study using various observational data sets while in the following chapter output from the RCM is used.

C. Data and Methods

Daily SST data from TRMM satellite at a resolution of 0.25^0 for the years 1998−2007, obtained from (`ftp://ftp.misst.org`), is used to compute SST changes along hurricane tracks, which in turn are obtained from NOAA/AOML/HRD dataset (`http://www.aoml.noaa.gov/hrd/hurdat/Data_Storm.html`). Wind speed information for points along the tracks is obtained from the same data set. 5-day mean SODA (Simple Ocean Data Assimilation) re-analysis data for the same period at a resolution of 0.5^0, acquired from (`http://soda.tamu.edu/opendap/SODA_2.1.6/5DAY/contents.html`), is used to compute pre-existing BLT and MLD conditions for the hurricanes in the period between 1998 and 2007. Monthly mean SODA data for the period between 1958 and 2008, obtained from (`http://soda.tamu.edu/opendap/SODA_2.1.6/MONTHLY/contents.html`), is used to compute the BLT climatology and climatology for the probability for occurrence of temperature inversions in the northwestern tropical Atlantic. In addition, daily re-analysis SST data, obtained from the Naval Research Lab (NRL) using data assimilation with HYbrid Coordinate Ocean Model (HYCOM) at a resolution of 0.08^0, for the periods between 17^{th} and 23^{rd} September and between 15^{th} and 25^{th} October 2005, between 13^{th} and 18^{th} Octo-

ber 2008 and between August 15^{th} and 24^{th} 2009, is used to compute SST changes and pre-existing BLT along the tracks of Hurricanes Philippe, Wilma, Omar and Bill. This data, which has been obtained from (`http://tds.hycom.org/thredds/dodsC/glb_analysis.html`), is available starting from November 2003. Thus we pick four hurricanes after 2004, Hurricane Philippe (2005), Hurricane Wilma (2005), Hurricane Omar (2008) and Hurricane Bill (2009). With Omar and Bill, the added incentive was that we were able to find Argo floats in close proximity to their tracks. Data from Argo floats (AOML float numbers: 4900755, 4900360) from the site (`http://www.usgodae.org/cgi-bin/argo_select.pl`) is used to examine the sub-surface hydrographic conditions at locations close to the tracks of Hurricanes Omar and Bill.

The BLT was computed based on the definition of (de Boyer Montégut et al., 2007) as was described earlier. Also, a threshold BLT of 10 m is used, i.e., a region is assumed to have a BL only when BLT exceeds 10 m. SST change at each point along the hurricane tracks is evaluated as

$\Delta\text{SST} = \text{SST}_{T+2} - \text{SST}_{T-1}$, where SST_{T+2} is SST two days after the passage of the TC and SST_{T-1} is SST a day before the approach of the TC.

The maximum radius of a hurricane in the Atlantic ocean is around 360 km. A typical slow moving hurricane moves at a speed close to 5 ms^{-1}. At this speed, it travels a distance of 430 km in a day, which is larger than the maximum possible hurricane radius. As the SST data is available at a daily resolution, SST a day before would be the best possible SST estimate before the approach of the hurricane (Dr. Kerry Emanuel, personal communication). The SST cooling due to entrainment and turbulent mixing occurs at inertial timescales and we see that maximum cooling occurs after 2 days more or less. We calculate the TC translational speed as follows. If (x_i,y_i) and $(\text{x}_{i+1},\text{y}_{i+1})$ are the latitude-longitude positions of a TC at times t_i and

t_{i+1} respectively, then the storm translational speed at the i+1^{th} location is given as

$$speed_{i+1} = \sqrt{(x_{i+1} - x_i)^2 + (y_{i+1} - y_i)^2} \times \frac{109 \times 1000}{6 \times 3600}$$

We obtain this formulation by assuming that the path of the TC is approximately a straight line between two successive time steps. As the hurricane track information is available at a temporal resolution of 6 hours, the assumption is reasonable. We further assume that each degree is approximately 109 km. Hence the number of degrees traversed multiplied with 109×1000 would give the number of meters traversed and the the time taken is 6×3600 seconds.

D. Climatology of BLs and Temperature Inversions

Before we go further, let us briefly examine the climatology of BLs in the northwestern tropical Atlantic. Fig. 22 shows the climatology of BLs. As observed before, the two main factors responsible for the formation of BLs in the northwestern tropical Atlantic are the Amazon-Orinoco River plume and the subduction of subtropical salinity maxima waters. The signature of the Amazon-Orinoco River discharge is very clearly visible in the BL maps. The river discharge peaks every year during late spring-early summer and as a result we find thick BLs at the river mouths extending northwestwards into the Caribbean. Beginning in fall, the thickness of BL near the river mouth decreases and increases in extent and magnitude to the northwest. In winter, thick BLs are found in the region between 12^0N and 22^0N and between 80^0W and 40^0W. Subduction of subtropical salinity maxima water is mainly responsible for these BLs.

The probability of temperature inversion formation for each season is shown in

Fig. 23. First of all, from Figs. 22 and 23, it is clear that there is high spatial corre-

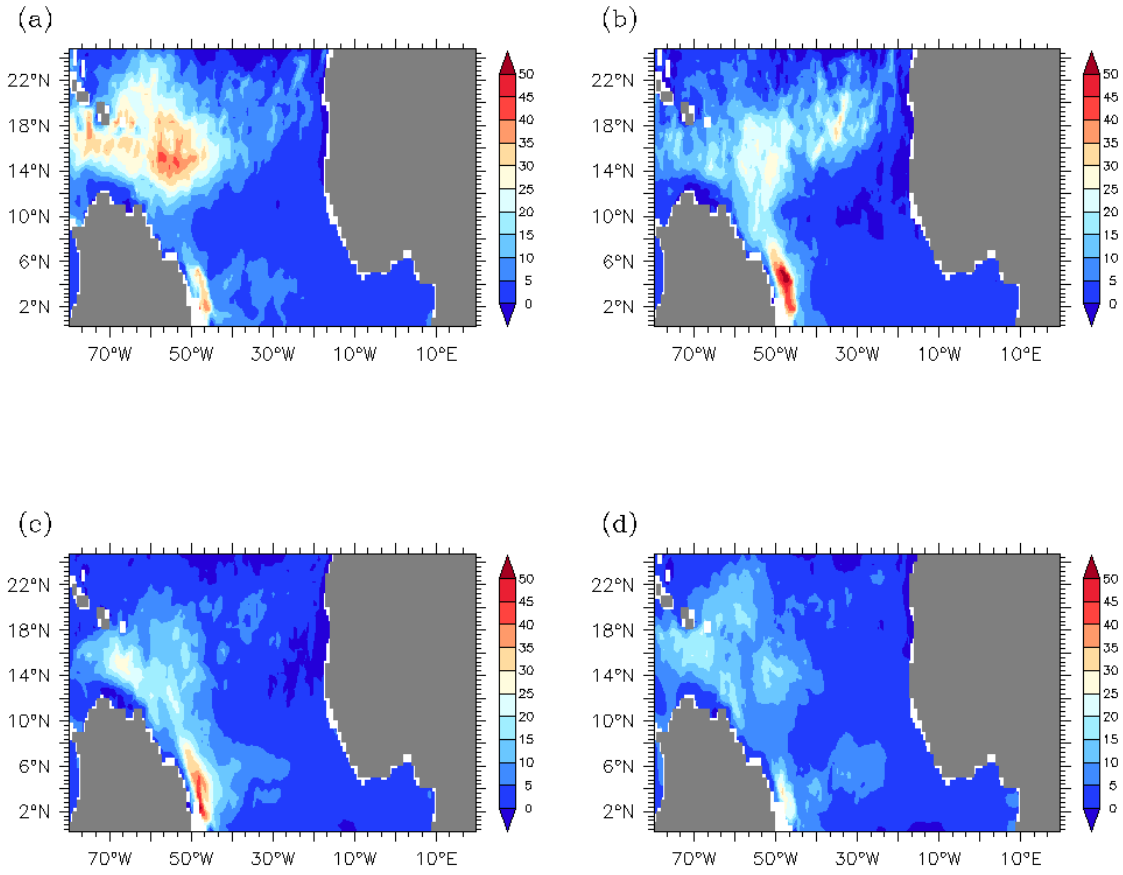

Fig. 22. BLT climatology in m (a) Winter (b) Spring (c) Summer (d) Fall.

lation between formation of BLs and temperature inversions. Even though maximum inversions occur during the winter season due to surface cooling, inversions also form during fall and winter seasons, which are the main seasons for the formation of TCs in the Atlantic. Thus, when TCs mix the upper ocean with a temperature inversion embedded in the thermal structure, the SST cooling might be reduced or there could even be some slight warming. This acts as a positive feedback mechanism for TC intensification. SST change in the wake of TCs was calculated by Sriver and Huber

(2007) using ERA-40 reanalysis data. Even though in majority of the cases, the SST

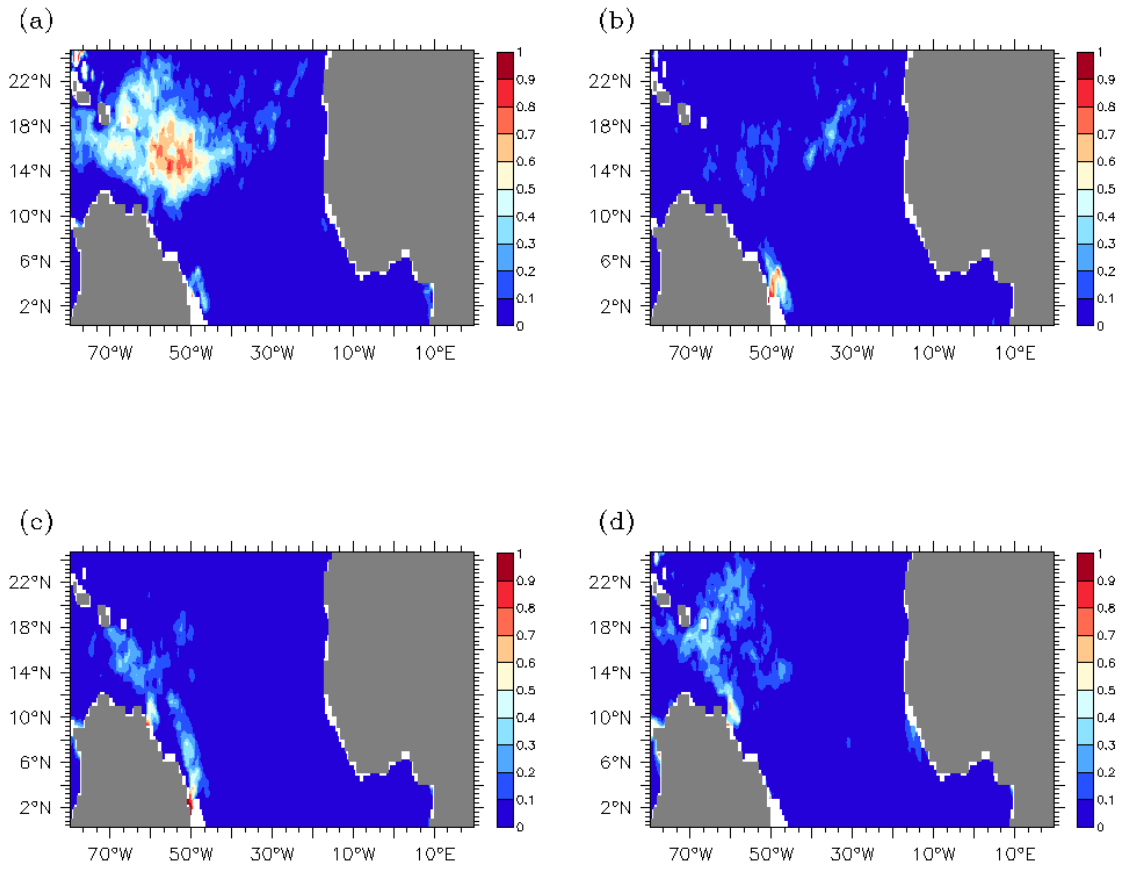

Fig. 23. Probability of formation of temperature inversions (a) Winter (b) Spring (c) Summer (d) Fall.

change is negative, there are regions where the SST change is alleviated or is even weakly positive. Thus it may be possible that some of the reduced cooling or slight warming of SST is caused due to temperature inversions associated with BLs.

E. Factors Affecting the Surface Ocean Response to TCs

There are three most important factors that govern the SST response to TC induced mixing in the open ocean (Price, 1981). The SST response is primarily a function of hurricane strength, its translational speed and surface ocean stratification. We use the hurricane windspeed as a measure of its strength. This is consistent with the Saffir-Simpson scale, which even though can be subjected to debate, is the most widely used scale to categorize hurricane strength. Fig. 24 is an illustration of all the hurricane tracks we have used for our analysis between 1998-2007. Of the three factors mentioned above, the first two concern the nature of the TC itself while the third factor concerns the prevailing hydrographic conditions of the upper ocean in contact with the TC.

Typically, the wind speed of a TC characterizes its intensity. The Saffir-Simpson scale is the commonly used criterion to classify the TCs based on their intensity. A TC is said to be a Tropical Storm when the surface wind speed reaches atleast 17 ms^{-1}. Category 1 hurricanes have a minimum speed of 32 ms^{-1} while Category 5 hurricanes have wind speeds exceeding 70 ms^{-1}. The strong winds in the boundary layer of the TC stir-up the ocean to depths of 100-200 m and cause a blast of mixing in the upper ocean. There are two ways in which the wind mixing influences the SST response to TCs. First, these winds acting on the surface act as a source of momentum transfer into the ocean. The upper ocean in contact with the wind has a much higher velocity when compared to the water beneath resulting in shear instability and turbulence. The higher the wind speed, the higher is the instability and mixing. The second effect of the wind is the latent and sensible heat flux transfer, both of which depend critically on the wind speed. The higher the windspeed, the more the flux of heat. Another factor which plays an important role in the SST response of the ocean is

the translational speed of the storm (stormspeed henceforth). Typically, the storm

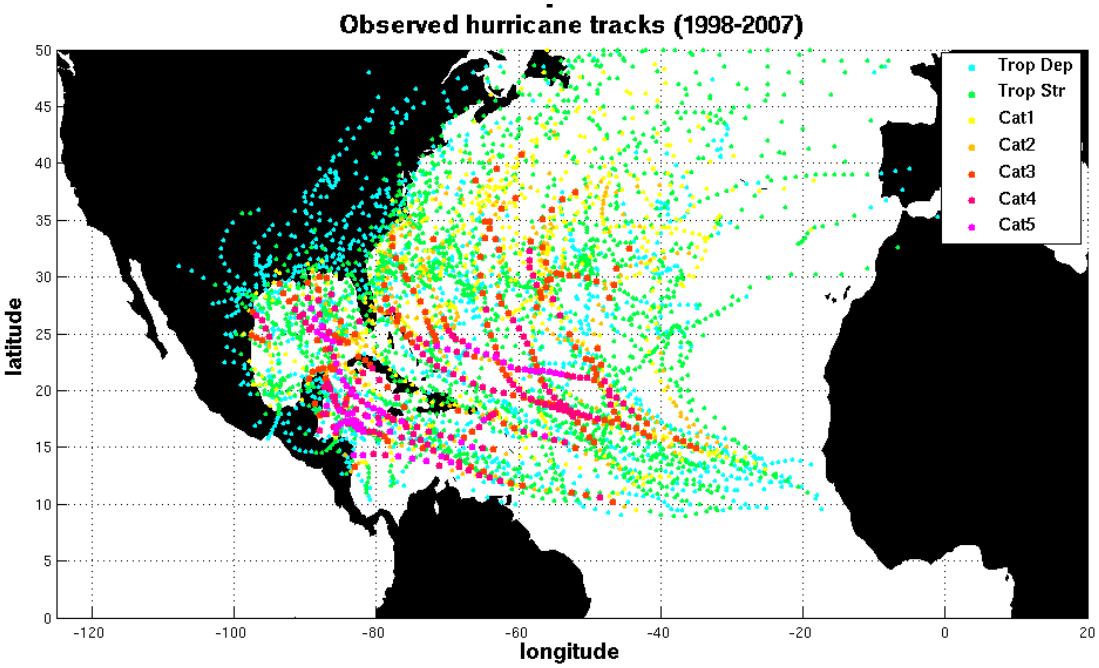

Fig. 24. Illustration of all the hurricane tracks used (1998-2007). The storms have been categorically differentiated according to the Saffir-Simpson scale.

speed ranges from about 5 ms^{-1} for the slow moving storms to up to 25-30 ms^{-1} for the faster moving storms. The slower the storm moves over the ocean, the more time it has to break through the stratification of the upper ocean and mix the cooler thermocline waters into the mixed layer and cause SST cooling. In essence, it is saying that strong and slow moving storms more effectively de-stratify the surface ocean stratification when compared to weaker and fast moving storms.

The third factor, which is the major focus of this study, is the upper ocean stratification. Typically, the surface ocean consists of the turbulent mixed layer below which the density (temperature) increases (decreases) rapidly in the pycnocline (thermocline) and beneath which we have the deep ocean where the density (tem-

perature) increases (decreases) more gradually. The depth of the mixed layer is a measure of the inertia of the upper ocean. The wind at the ocean surface transfers momentum into the upper ocean and the depth to which the mixing can penetrate depends on the MLD and the stratification below. When the MLD is deep, most of the wind momentum is trapped within the mixed layer and thus very little is available to cause turbulent mixing and entrainment at the base of the mixed layer. But when the MLD is shallow, the wind momentum is able to mix the cooler thermocline waters into the mixed layer to cause SST cooling. We shall now examine the effect of these three factors on SST cooling.

Fig. 25 shows the ΔSST plotted against the wind speed. The ΔSST is not continuous but rather in steps of nearly 0.15^0 C due to the precision of satellite data. Firstly, at low wind speeds, most of the SST cooling is less than 2^0C. This means that if the wind speed is low, irrespective of the storm translational speed and the surface ocean stratification, the SST cooling is low due to a reduced latent-sensible heat loss and because the wind momentum transfer into the ocean is not sufficient to break through the surface ocean stratification and cause entrainment cooling. But as the wind speed increases, so does the maximum SST cooling. This is consistent with the hypothesis of Price (1981). The maximum cooling is as high as 5^0C. At higher wind speeds, a range of SST cooling is possible depending on other factors.

The scatter plot (Fig. 26) between ΔSST and storm speed shows that at high storm translational speeds the SST cooling is very low and as the storm speed reduces, the magnitude of maximum SST cooling also increases. This suggests that when the storm speed is high, it does not spend sufficient time to cool the SST either through the latent and sensible heat flux exchange or through upwelling and entrainment. However, slower moving storms tend to cause more SST cooling as they stay at a location long enough to cause enhanced heat flux transfer and upwelling

and entrainment. Thus, at high storm speeds, the other factors have relatively weak

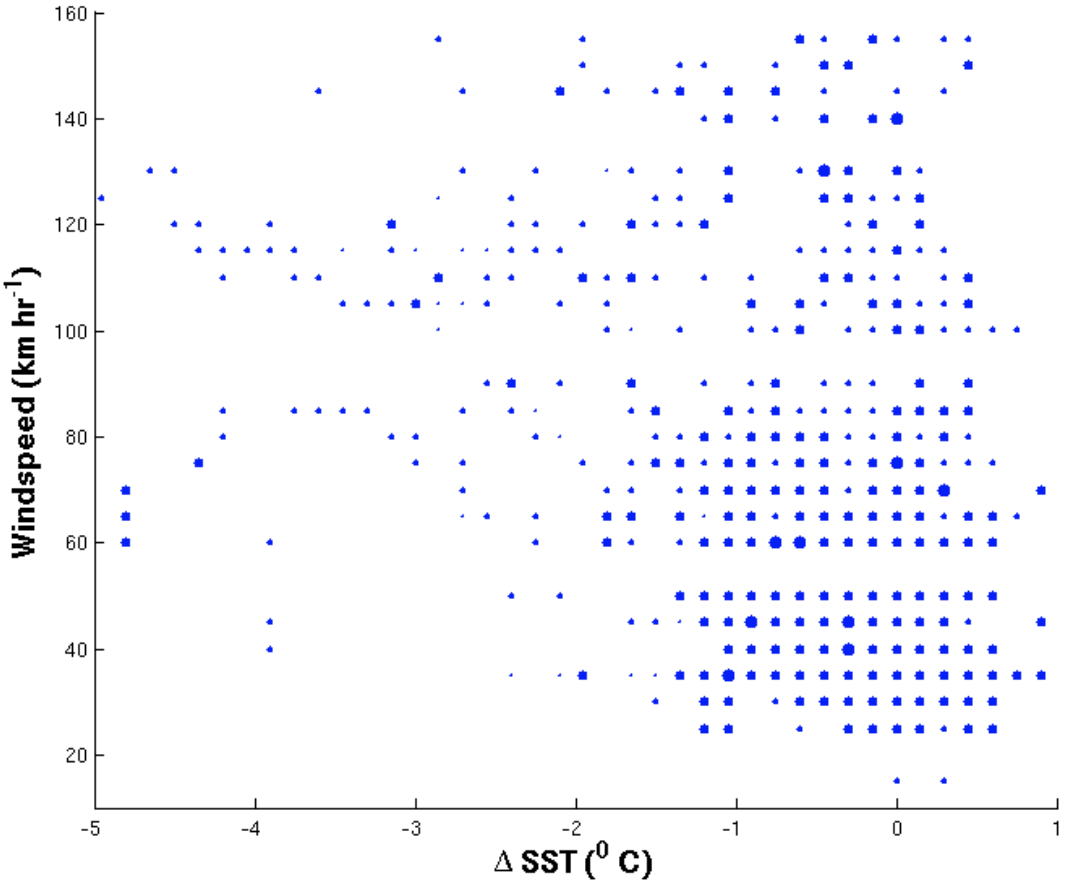

Fig. 25. Scatter plot between ΔSST (X-axis) and wind speed (Y-axis). The size of each dot is proportional to the initial MLD at that location.

influence on the surface ocean SST response. Again, this relationship between SST cooling and storm speed is consistent with the hypothesis of Price (1981).

Morey et al. (2006) show that the primary factor that influences the SST cooling near the center of the storm is the surface ocean stratification while surface fluxes are responsible 100-300 km away from the center. In this study we focus on the SST cooling within the high windspeed eye-wall regime and thus it becomes important

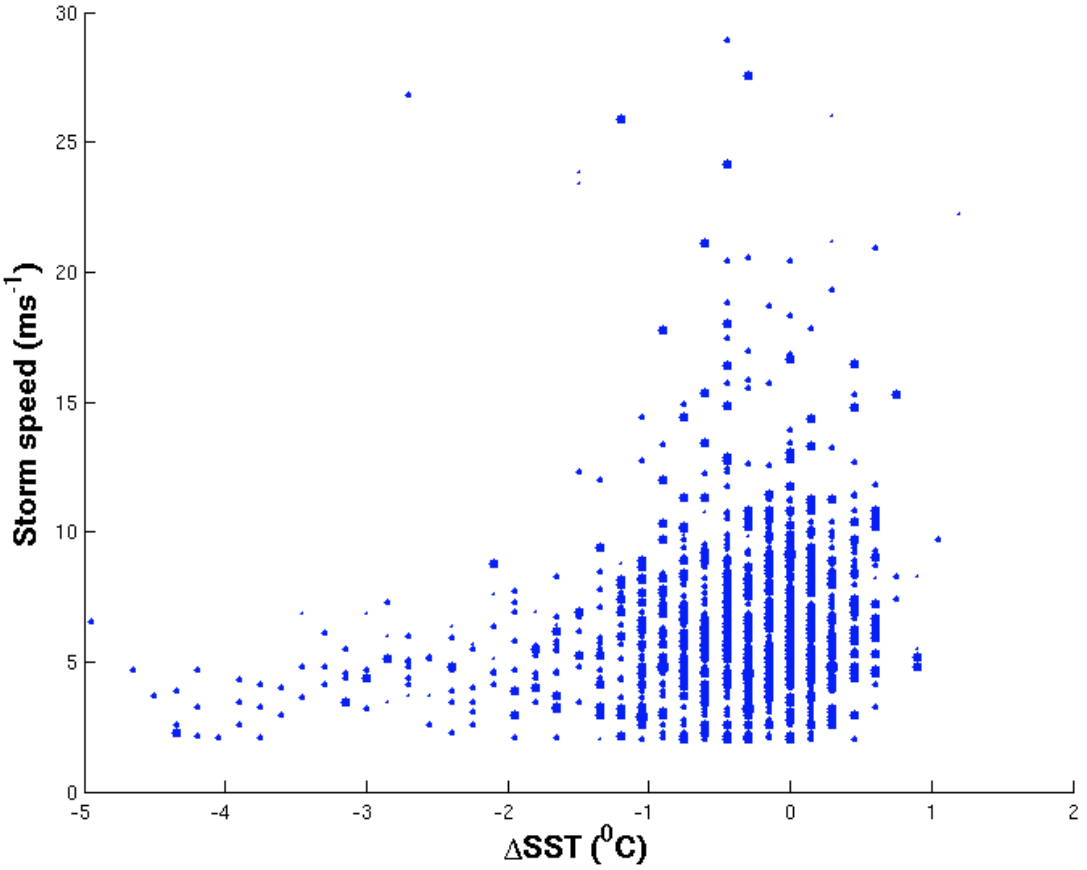

Fig. 26. Scatter plot between ΔSST (X-axis) and storm speed (Y-axis). The size of each dot is proportional to the initial MLD at that location.

to consider the effects of surface ocean stratification on SST cooling. Fig. 27 shows the scatter plot of ΔSST plotted against the MLD. When the mixed layer is deep, the magnitude of SST cooling is low and as the mixed layer gets shallower, the SST cooling increases. This means that when the mixed layer is very thick, the other factors become redundant and may play a minor role in the surface SST response. But as the mixed layer depth reduces, the SST cooling becomes a cumulative effect of the various factors. The surface ocean stratification typically refers to the mixed layer and the stratification beneath it. As noted earlier, usually the uniform density mixed layer is also the uniform temperature isothermal layer and the thermocline and pycnocline coincide with each other. But there are situations when either salinity or temperature plays a more dominant role in the determination of density. In such situations, discrepancies might arise between the mixed layer and isothermal layers. Thus, when the upper ocean is mixed by the intense winds of a TC, the SST cooling would depend not only on the mixed layer but also on the thermal stratification below the mixed layer making it very important to consider both the factors. If only the mixed layer defined by the density criterion is considered, then we are not taking into consideration the effect of the thermal stratification beneath the mixed layer. Also, if the mixed layer based on the temperature is considered, we are not taking into effect the salinity stratification within the isothermal layer.

Let us now put the effect of BLT on TC induced mixing in perspective. Sriver and Huber (2007) compute the depth of TC induced mixing in the following manner where K_v is the vertical mixing coefficient, L is the mixing length and τ is the time period of mixing.

$$K_v = \frac{L^2}{\tau}$$

The mixing length L is estimated as shown.

$$L = \frac{\Delta T}{\frac{\partial T}{\partial z}}$$

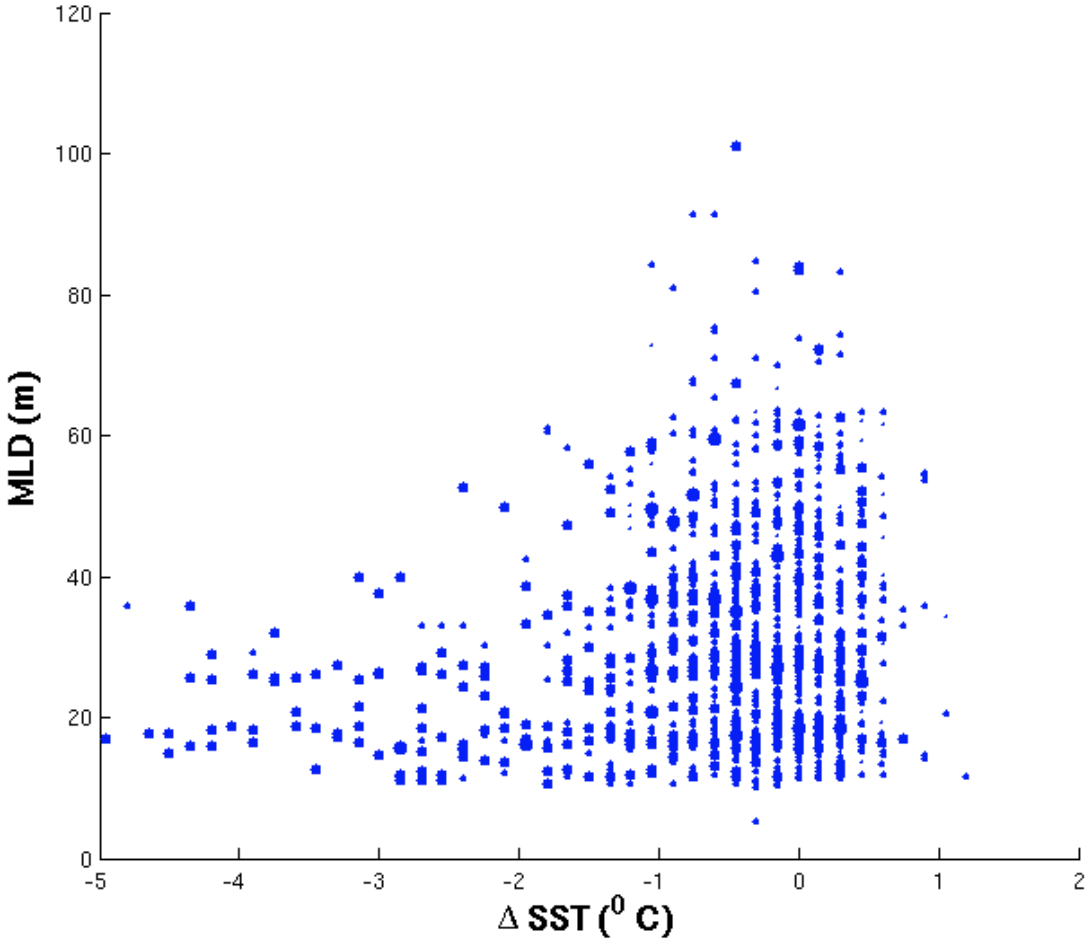

Fig. 27. Scatter plot between ΔSST (X-axis) and MLD (Y-axis). The size of each dot is proportional to the wind speed at that location.

The above formulation is justified based on the hypothesis of (Price, 1981) that the primary mechanisms responsible for the cooling of the surface ocean due to TC-induced mixing are entrainment and upwelling. The BL, which is the layer between the MLD and ILD, is an indicator of thermal stratification beneath the mixed layer. The BLT is inversely proportional to the thermal gradient at the mixed layer base $\frac{\partial T}{\partial z}$. The ILD is defined as the depth where the temperature drops by 0.2^0 C from its value at a depth of 10 m, which is typically the mixed layer temperature. Thus, the thermal stratification beneath the mixed layer could be written in terms of the BLT as follows

$$\frac{\partial T}{\partial z} = \frac{0.2}{BLT}$$

Using this, the vertical mixing coefficient could be rewritten as

$$K_v = \left(\frac{\Delta T \times BLT}{0.2}\right)^2 \times \frac{1}{\tau}$$

If the mixing is assumed to occur over a period of 1 day, then

$$K_v = \frac{1}{4 \times 24 \times 36} \times (\Delta T \times BLT)^2$$

This means that for a given amount of mixing, the SST cooling induced is inversely proportional to the BLT. Let us now consider the effect of BLT on SST cooling due to TC induced mixing. Fig. 28a is the same as Fig. 25 and Fig. 28b is the same as Fig. 27 except here all situations with a BL have been plotted in red while the situations without a BL have been plotted in blue. It can be immediately seen that most of the BL points are situated to the right side of the plots and there are very few points with a cooling of magnitude higher than 2^0C. When a TC passes over an oceanic region with a BL, the SST cooling is low meaning that when the thermal stratification beneath the mixed layer is low the water that entrains into the mixed layer is not significantly cooler than the mixed layer water and thus cannot cause substantial cooling.

To further illustrate the effect of BL on TC induced SST response, we have taken

the SST change along all the TC tracks and contrasted for situations when the TC passes over an ocean with a BL and without a BL. Fig. 29a shows the probability distribution function (PDF) of SST change for situations with a BL, 29b shows the PDF for situations without a BL and 29c the difference. When we consider the mean SST change, it is -0.28^{0}C for situations with a BL and about -0.53^0 C for situations without a BL which means that in the presence of BLs, the SST cooling is reduced by nearly 48%. A student's t-test confirms that this difference is statistically significant at 95 % confidence level.

Fig. 30 shows the scatter plot between MLD and BLT. There are almost no situations when both the MLD and BLT are high. Thus based on this, we can rule out the possibility that the reduced SST cooling due to thick BLs is due to a coincidence with deep mixed layers. This gives us further incentive to consider the role of BLs when looking at the SST response to TC induced mixing. In Fig. 31, the role played by various factors involved in the surface ocean response to TC induced mixing is summarized. Fig. 31a shows the average wind speed values for each range of SST change. As noted earlier large magnitudes of SST cooling are achieved at high wind speeds while the SST cooling is reduced at low wind speeds. From Fig. 31b, we see that on an average the storm speed is inversely proportional to the strength of SST cooling. Fig. 31c shows that the magnitude of SST cooling is high for shallow mixed layers and reduces with increasing MLD while Fig. 31d shows that the magnitude of SST cooling is low for high BLT and vice-versa.

Sriver and Huber (2007) adapted the formulation of Emanuel (2001) and computed the vertically integrated heat anomalies caused by TC induced mixing as follows.

$$Q = \int\int\int \rho C_p \Delta T dh dW dS$$

Here Q is the heat anomaly, ρ the density, C_p is the specific heat capacity, ΔT

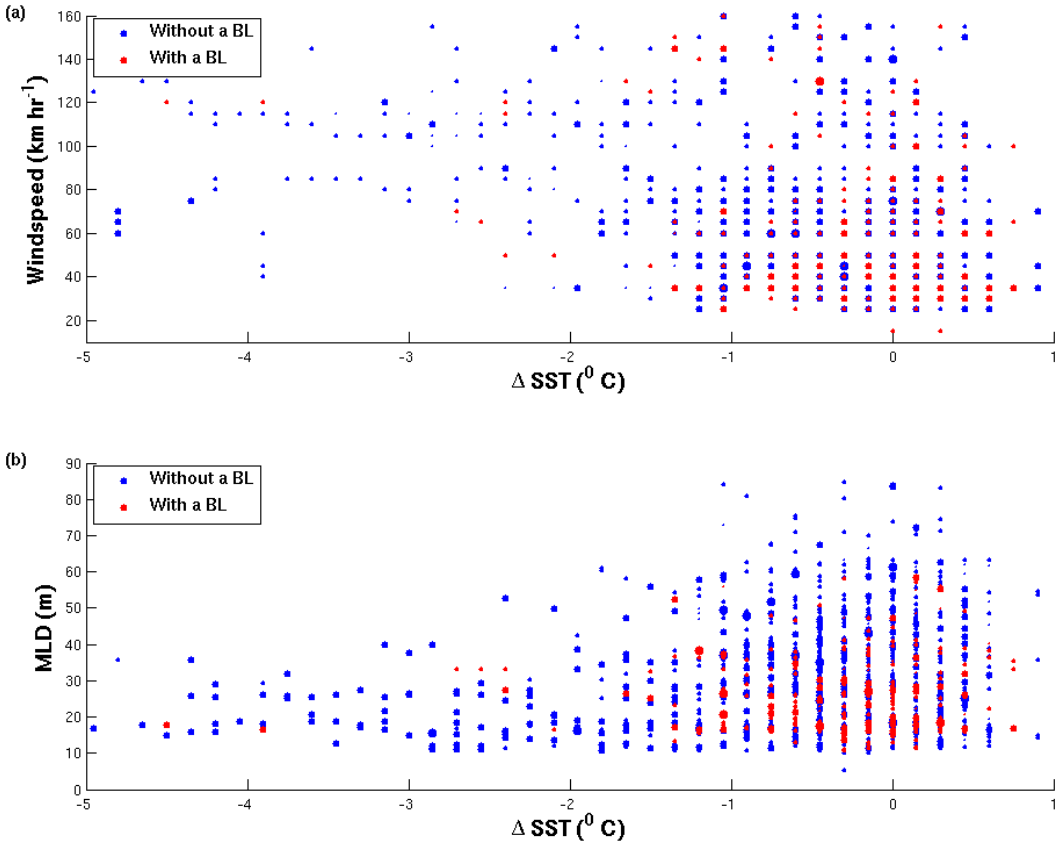

Fig. 28. Scatter plot between (a) ΔSST (X-axis) and wind speed (Y-axis) (b) ΔSST (X-axis) and MLD (Y-axis). The red points indicate situations with a BL and the blue points indicate situations without a BL.

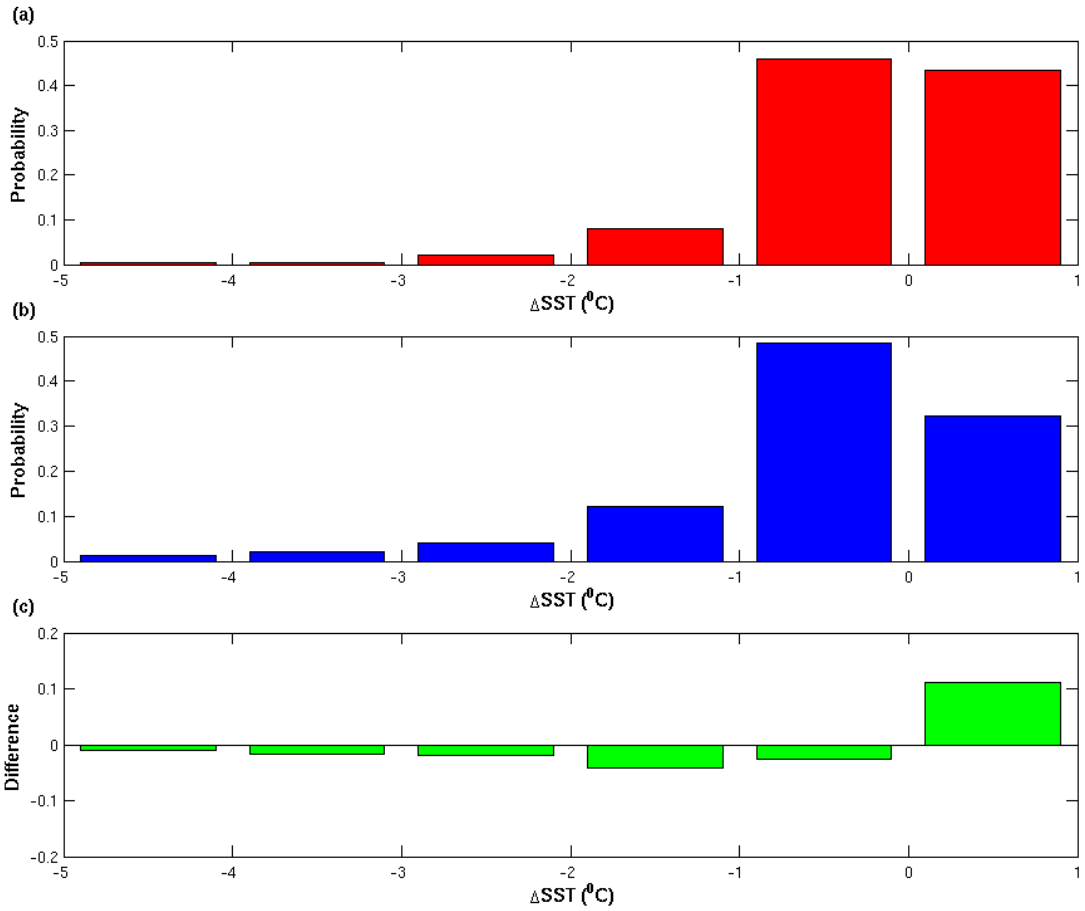

Fig. 29. PDF of ΔSST (a) Situations with a BL (b) Situations without a BL (c) Difference between the two.

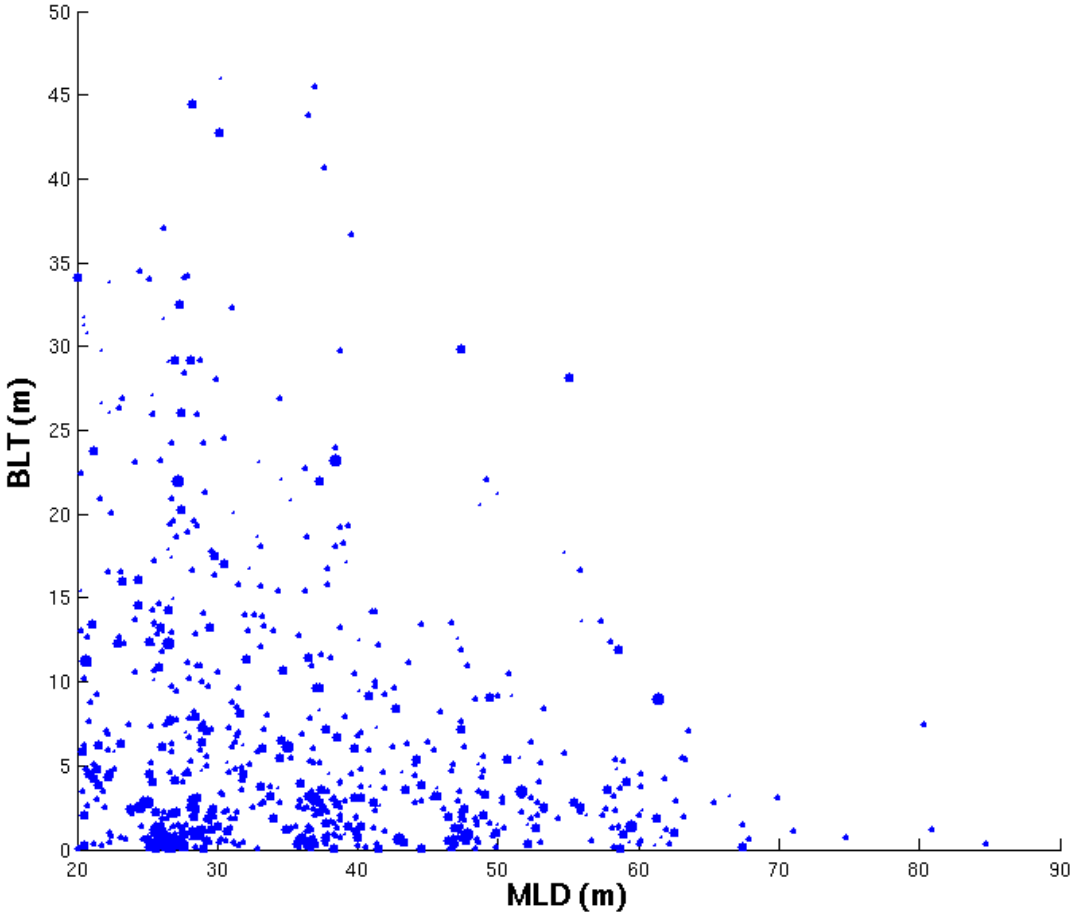

Fig. 30. Scatter plot between MLD (X-axis) and BLT (Y-axis). The size of each dot is proportional to the wind speed at that location.

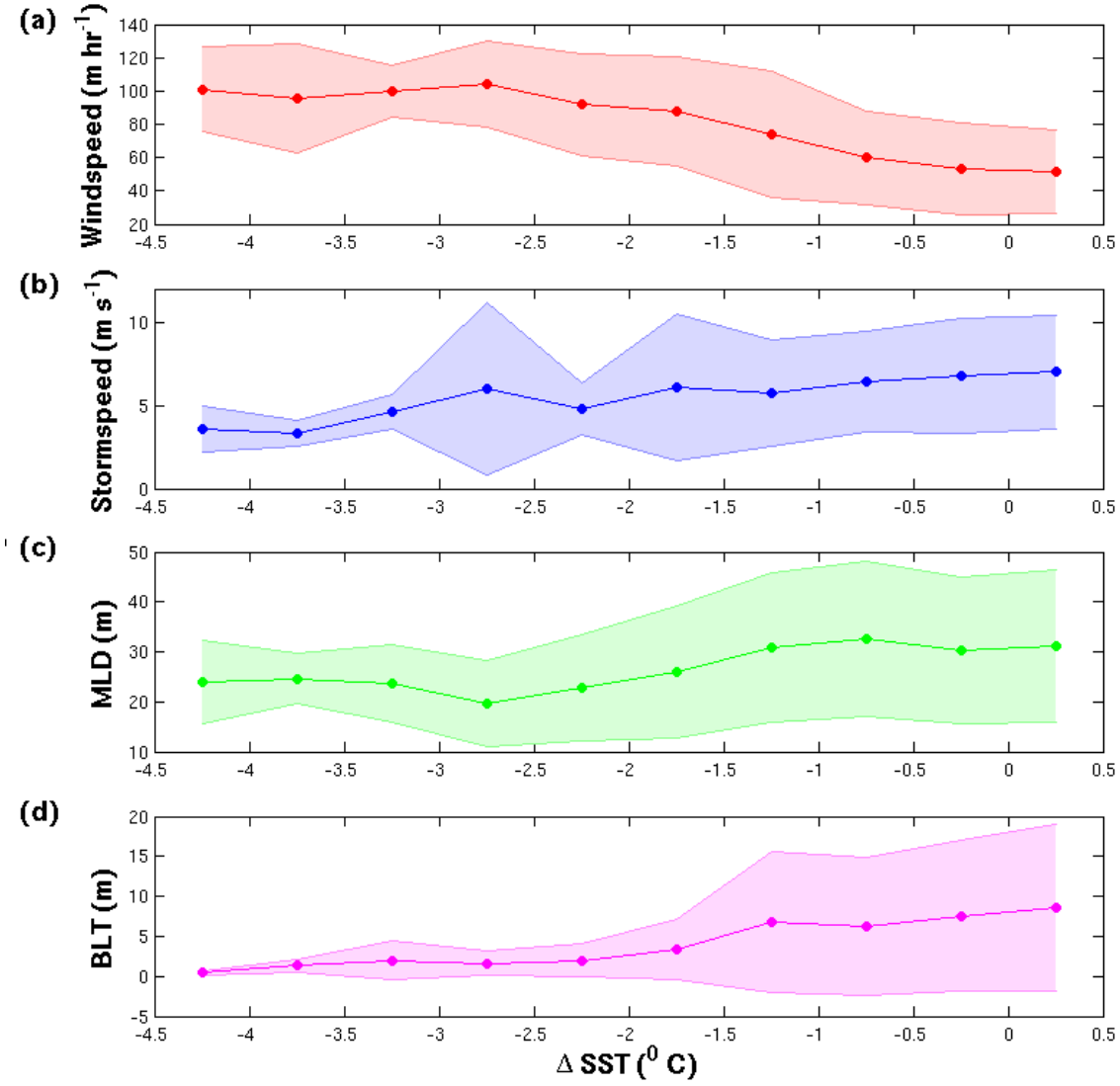

Fig. 31. Average value for each range of ΔSST is shown for (a) Wind speed (b) Storm-speed (c) MLD (d) BLT.

is the change in SST, dh is the depth of vertical mixing, dW is the width of the wake and dS is the length of the track. We use the same formulation to compute the heat anomalies induced per unit area at each location as

$$Q = \rho C_p \Delta T dh$$

We assume that the density and specific heat capacity of sea water are 1020 kg m^{-3} and 3900 J kg^{-1} K^{-1} respectively. Sriver and Huber (2007) assume the mixing depth dh to be 50 m, which clearly is error-prone as they themselves have acknowledged. We take dh to be the ILD after storm-induced mixing as this is approximately the depth until which the temperature anomalies are present. We calculate Q along the hurricane tracks and contrast for situation with and without BLs. The mean Q for situations with a BL is -5.0689 $\times$ 10^7 Watts which is about 80 % of the mean Q for situations without a BL. A Student's t test shows that this difference is statistically significant at 95 % confidence level.

F. Case Studies

The effect of BLs on the surface ocean response to TCs will now be studied by considering four particular hurricanes.

1. Hurricane Philippe

Hurricane Philippe which formed to the east of the islands of Lesser Antilles initially, lasted between 17^{th} and 23^{rd} September 2005. This was the 16^{th} named storm of that season, which was the most active hurricane season in recorded history. It reached an intensity of category 1 on the Saffir-Simpson scale with a maximum wind speed of about 130 km hr^{-1}. The prevailing hydrographic conditions with the path of Hurricane Philippe overlaid is shown in Fig. 32. Philippe initially formed as a TC

over a region with weak BLs of about 5 m - 8 m. It gradually entered a region of thick BLs of up to 20 m as it gained hurricane status and finally left that region. A scatter plot between along track SST change at each location and the corresponding BLT is shown in Fig. 33. It is seen that on an average, when the BL is thick, the SST cooling is weak. For situations when the BLT is strong, the maximum cooling is less than 1^0 C. But when the BL is weak, the maximum cooling is twice as high.

2. Hurricane Wilma

Hurricane Wilma was the most intense hurricane ever recorded in Atlantic hurricane history. It lasted between 15^{th} and 25^{th} October, 2005 and reached an intensity of category 5 on the Saffir-Simpson scale. Maximum wind speed attained was about 296 km hr^{-1}. It caused extensive damage in the Yucatan peninsula of Mexico, Cuba and Florida, resulting in many deaths and economic losses of over $ 29.1 billion. Wilma initially developed as a tropical storm to the southeast of Jamaica and underwent very rapid intensification in the open Caribbean waters. From a tropical storm, it intensified to category 5 in about 30 hrs. The prevailing BL conditions on October 15^{th} with the path of hurricane Wilma overlaid is shown in Fig. 34. Wilma intensified over an oceanic region with a BL whose maximum thickness was about 25 m.

The scatter plot between Δ SST and prevailing BLT (Fig. 35) shows that when Wilma passed over regions of strong BLs, the SST cooling induced by it was lower than when it was over regions without a BL. The average reduction in this case is about 40 %.

3. Hurricane Omar

Hurricane Omar was an unusual hurricane which took a southwest - northeast path and lasted between 13^{th} and 18^{th} October, 2008. It reached a category 4 on the Saffir-

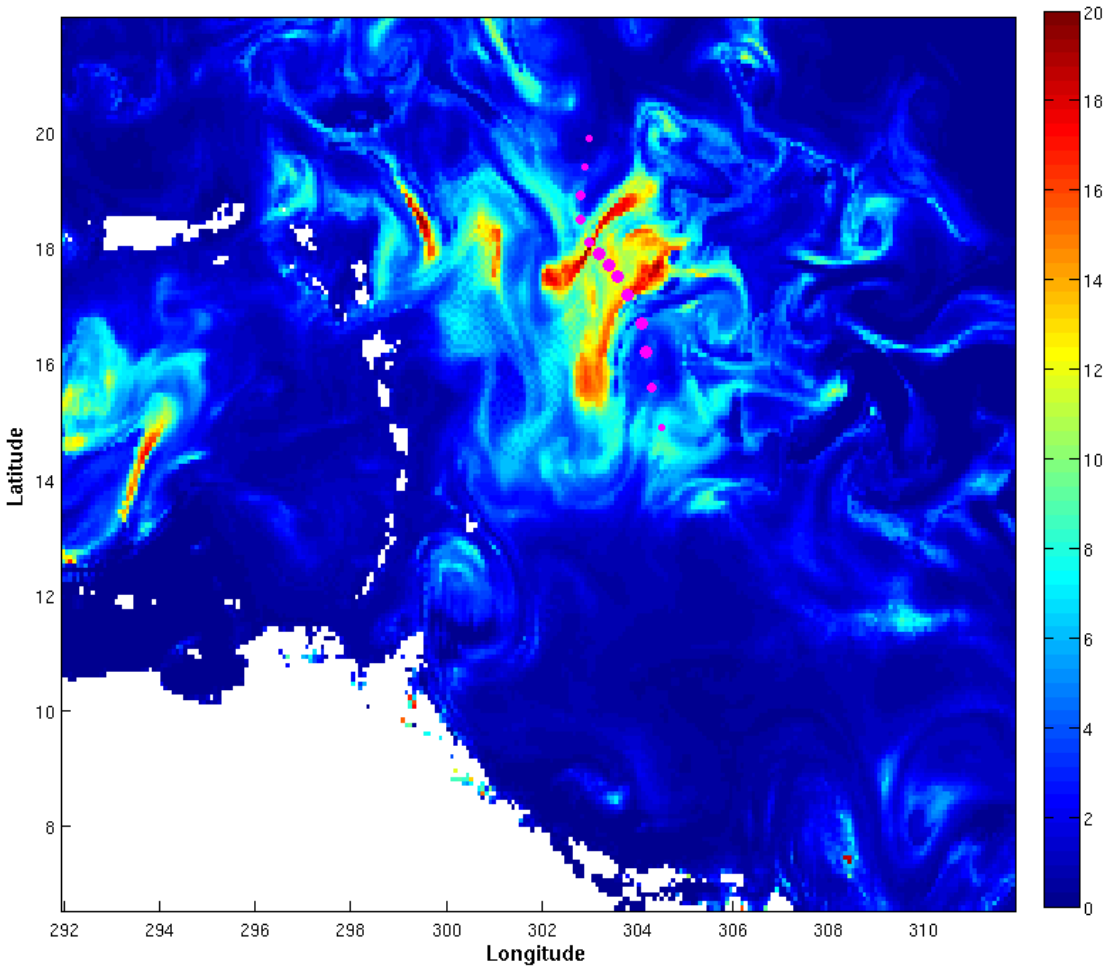

Fig. 32. Prevailing BL conditions on 17^{th} September 2005 with the path of Hurricane Philippe overlaid. The size of the dots is proportional to the wind speed.

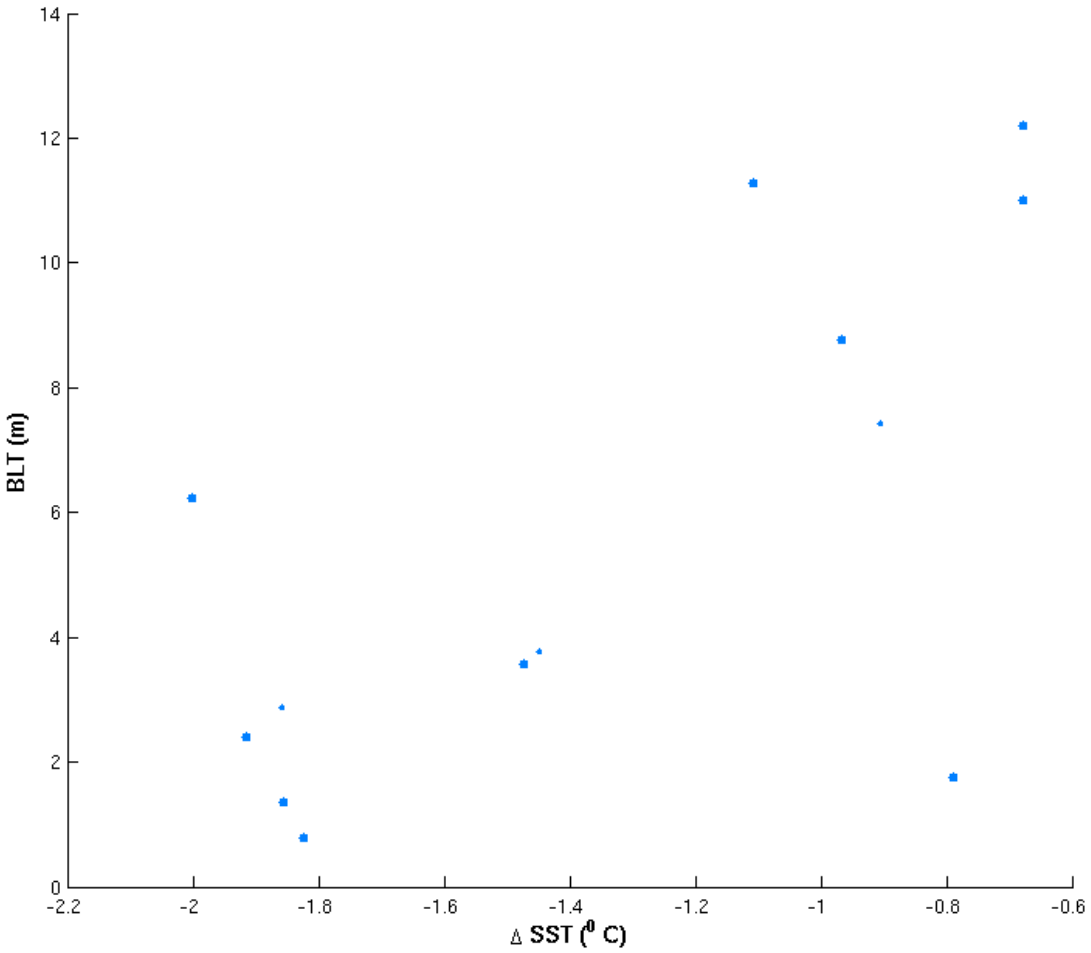

Fig. 33. Scatter plot between along track ΔSST (X-axis) and BLT (Y-axis) for Hurricane Philippe.

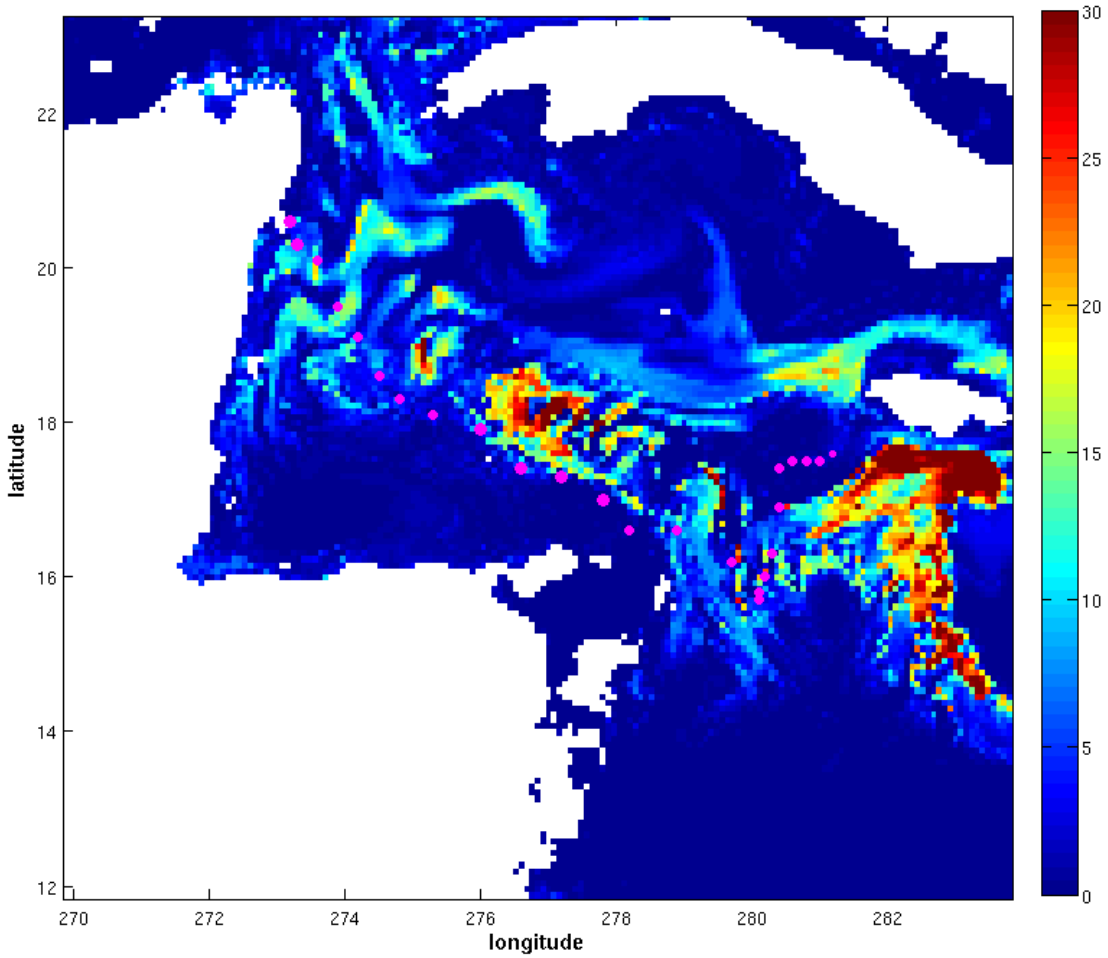

Fig. 34. Prevailing BL conditions on 15^{th} October 2005 with the path of Hurricane Wilma overlaid. The size of the dots is proportional to the wind speed.

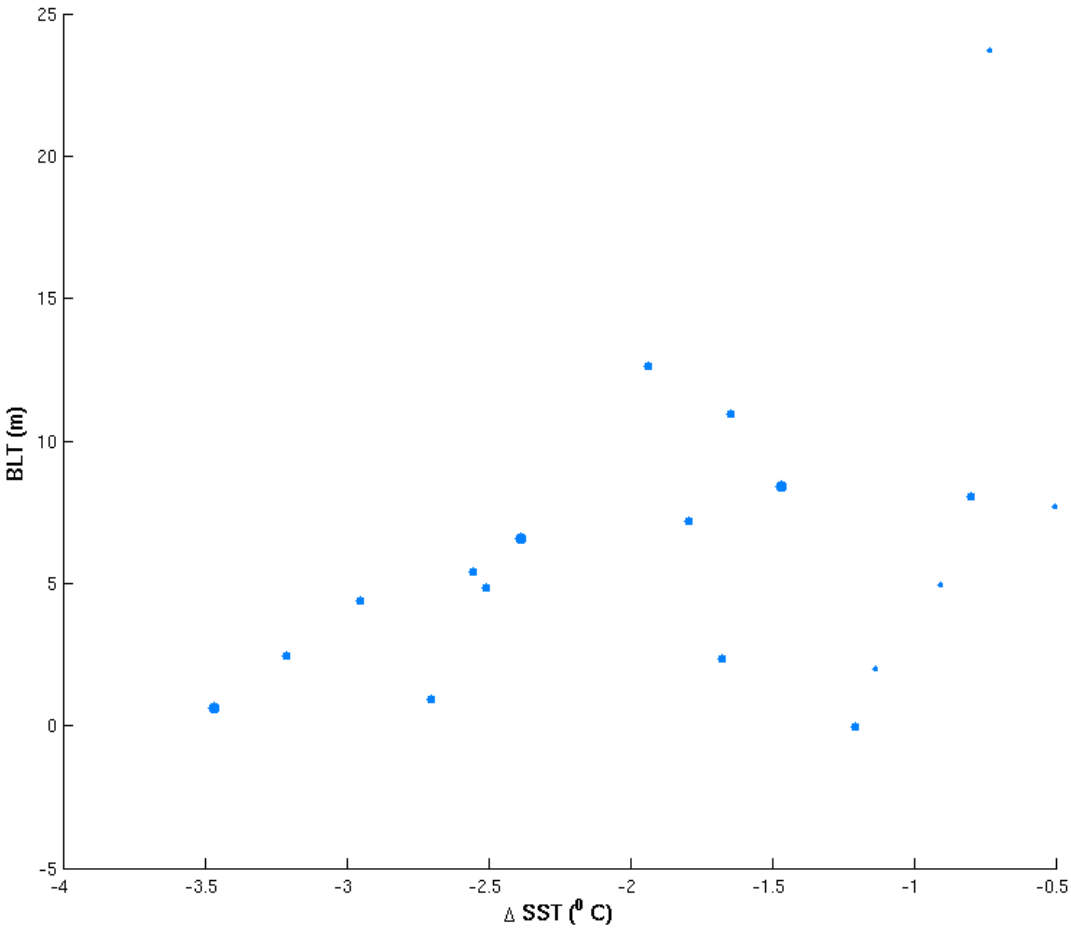

Fig. 35. Scatter plot between along track ΔSST (X-axis) and BLT (Y-axis) for Hurricane Wilma.

Simpson scale with maximum wind speed exceeding 215 km hr^{-1}. It caused extensive damage and impacted the ABC islands, Antigua and Barbuda, Leeward Islands, Puerto Rico and the United States Virgin Islands with estimated total economic loss being around $ 79 million. This was also one of the most rapidly intensifying hurricanes. It intensified from category 1 to category 4 between 15^{th} and 16^{th} October, 2008 as the storm neared Puerto Rico. However, as it left the Caribbean Sea waters and entered Atlantic waters, it rapidly weakened. The difference in SST between 18^{th} and 13^{th} October 2008 with the track of Hurricane Omar overlaid, is shown in Fig. 36 while Fig. 37 shows the prevailing BL conditions on October 13^{th}. Initially, Omar forms over a region without significant BLs and the SST cooling induced is about 2^0 C. Gradually, Omar enters a region with very thick BLs of upto 30 m and the SST cooling induced by Omar in this region is very low. As it exits this region, we note that Omar again induces significant SST cooling of upto 2^0C. When we look at the figures for SST change and the prevailing BL conditions, it gives us the general idea that broadly, there is a region with thick BLs and weak SST cooling with regions of weak BL and significant SST cooling on either sides of it. The same idea is further accentuated in the scatter plot between Δ SST and BLT in Fig. 38. We observe that for situations with thick BLs, the mean SST cooling is lower than that for situations with weak BLs.

The Argo floats are Lagrangian drifters deployed around the world ocean to measure temperature and salinity up to a depth of 2000 m. There are 3,239 Argo floats profiling the global oceans currently. These floats sink to a depth of 2000 m and drift for about 10 days and then they surface. As they rise, they measure the temperature and conductivity and once they reach the surface they transmit the data to a satellite. Using conductivity, the salinity is estimated and ultimately density. Because, typically the maximum speed of ocean currents at a depth of 2000

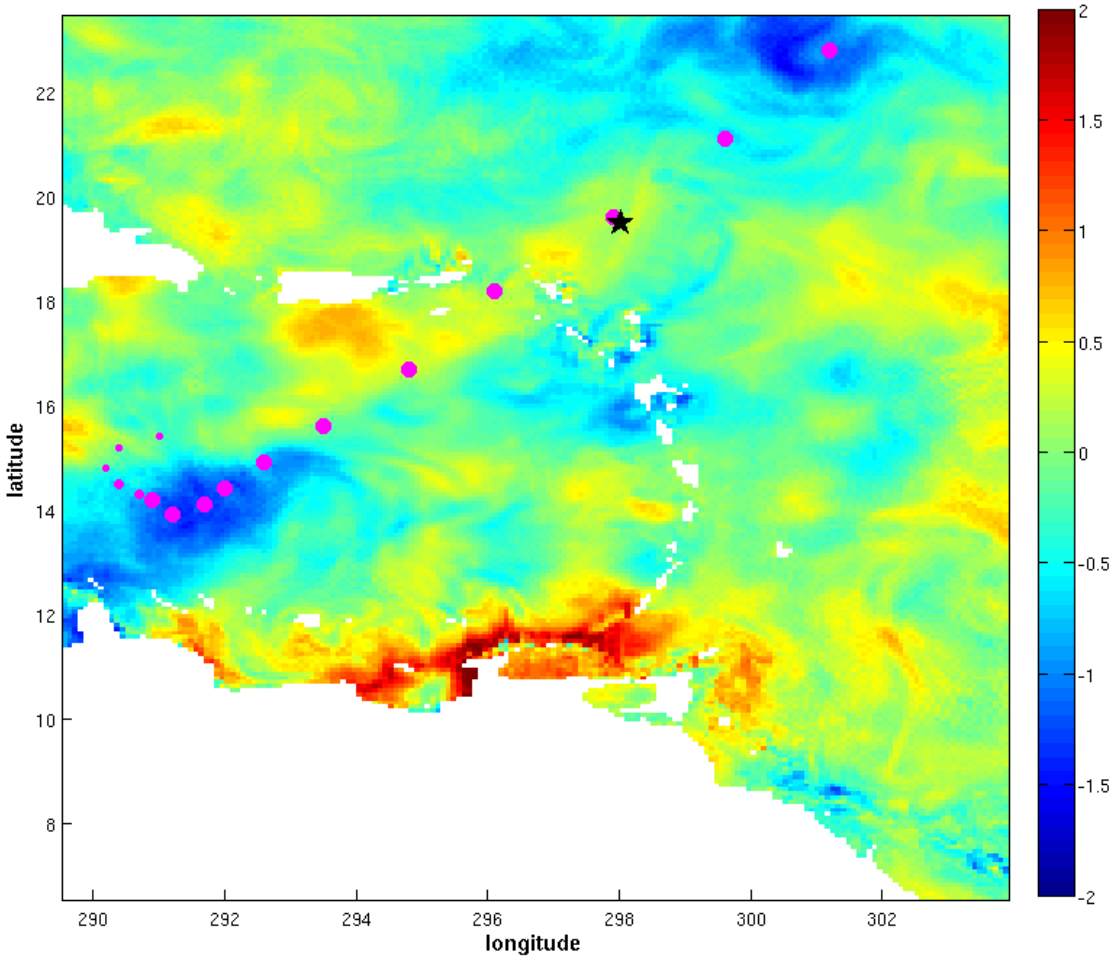

Fig. 36. SST difference between 18^{th} and 13^{th} October 2008 with the path of Hurricane Omar overlaid. The size of the dots is proportional to the wind speed. The black star indicates the location of an Argo float.

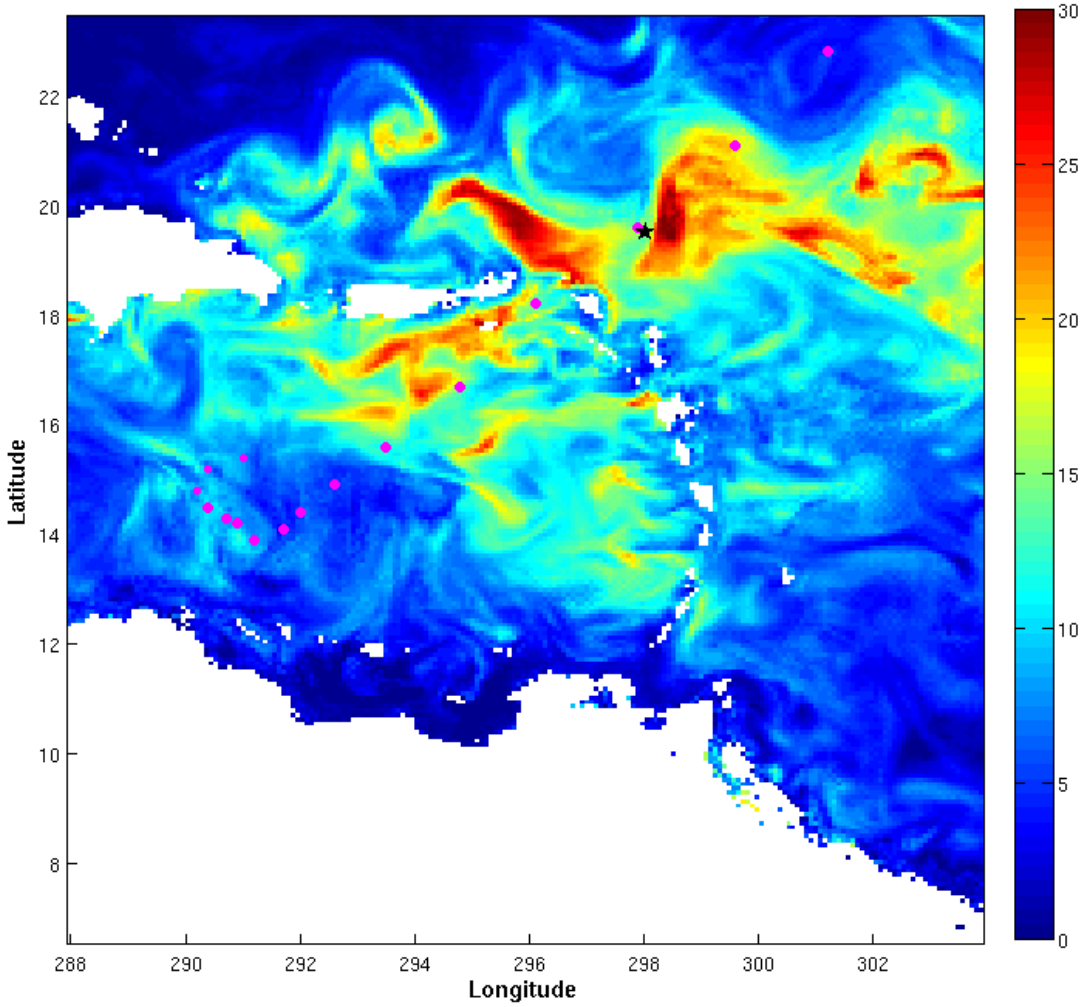

Fig. 37. Prevailing BL conditions on 13^{th} October 2008 with the path of Hurricane Omar overlaid. The size of the dots is proportional to the wind speed. The black star indicates the location of an Argo float.

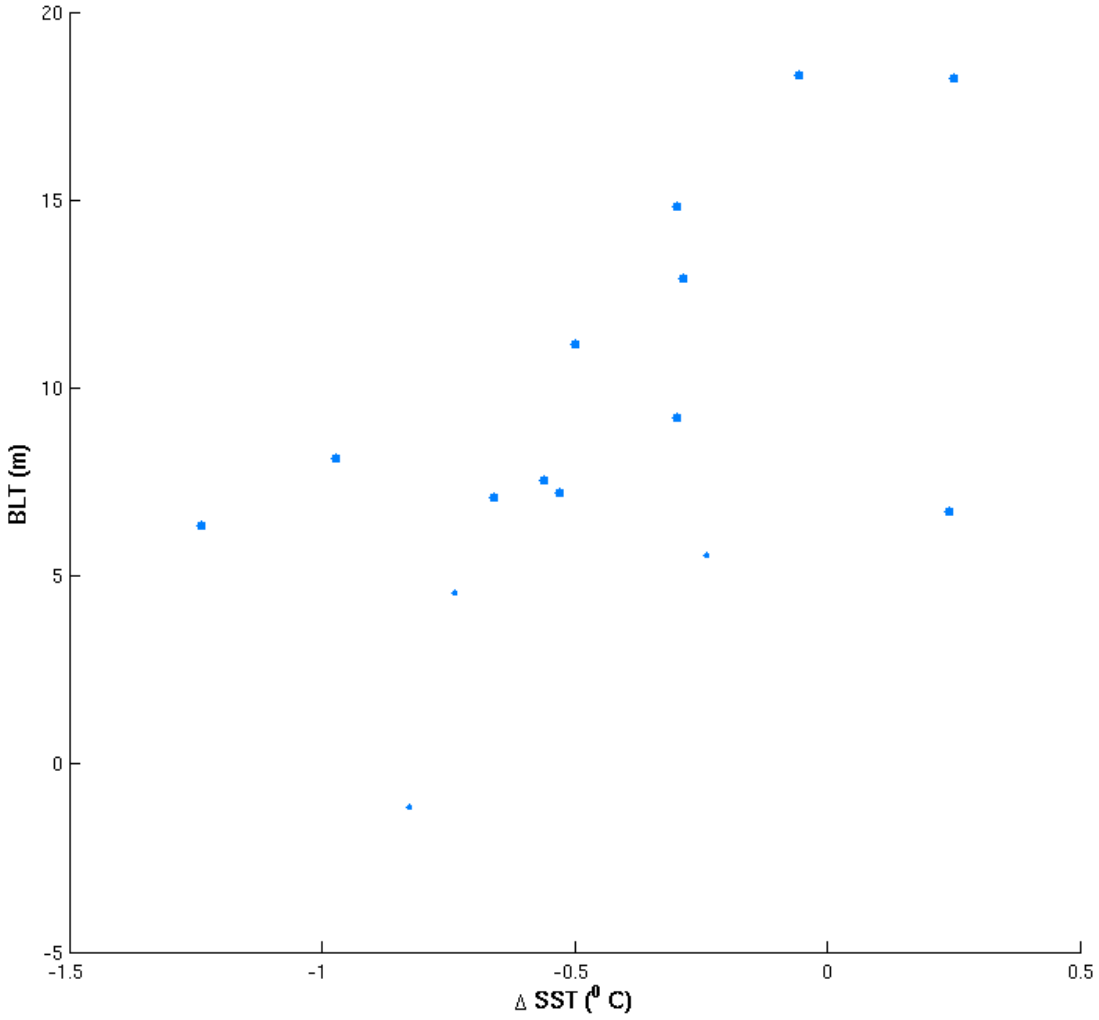

Fig. 38. Scatter plot between along track ΔSST (X-axis) and BLT (Y-axis) for Hurricane Omar.

m is about 10 cm s^{-1}, the maximum distance they can drift is less than a degree of latitude or longitude, making the points of successive measurements quite close to each other. An Argo float was located, at about 61.9 ^{0}W and 19.5 ^{0}N (black star in Fig. 37). Omars closest point of approach to this float was 62.1^{0}W and 19.6^{0}N, which is about 22 km to the west of the float. The float was able to measure the sub-surface temperature and salinity on 16th October 2008, the same day as when Omar passed over it. Hence it provides us with real time information about the prevailing sub-surface conditions. Fig. 39 shows the vertical profiles of the sub-surface salinity and temperature, along with the MLD and the ILD, recorded by the float on 16th October 2008. There was a large sub-surface salinity maximum centered at a depth of about 20m. The salinity increases from a value of about 34.5 g kg^{-1} at the surface to about 38.8 g kg^{-1} at a depth of about 20 m. Due to this salinity effect, the MLD was as shallow as 10 m, resulting in a very thick BL of about 35 m. Within the BL there was a substantial temperature inversion of almost one degree in magnitude. Previously (Fig. 36), it was shown that the SST cooling was reduced when Omar went over a region with a BL when compared to a region without. Thus it appears that TC-induced mixing caused warmer pycnocline water to enter the mixed layer, causing a reduced SST cooling or even a slight SST warming. This alleviated SST cooling might act as a positive feedback for the TC intensification.

4. Hurricane Bill

Hurricane Bill was a large-sized hurricane which lasted between 15^{th} and 24^{th} August, 2009. Areas affected by Bill were the Leeward Islands, Greater Antilles, Bahamas, Bermuda and the east coast of the US. Atlantic Canada and the United Kingdom were also affected after reaching extra-tropical status. Bill reached a category 4 strength on the Saffir-Simpson scale with maximum wind speeds of up to 215 km hr^{-1}. The total

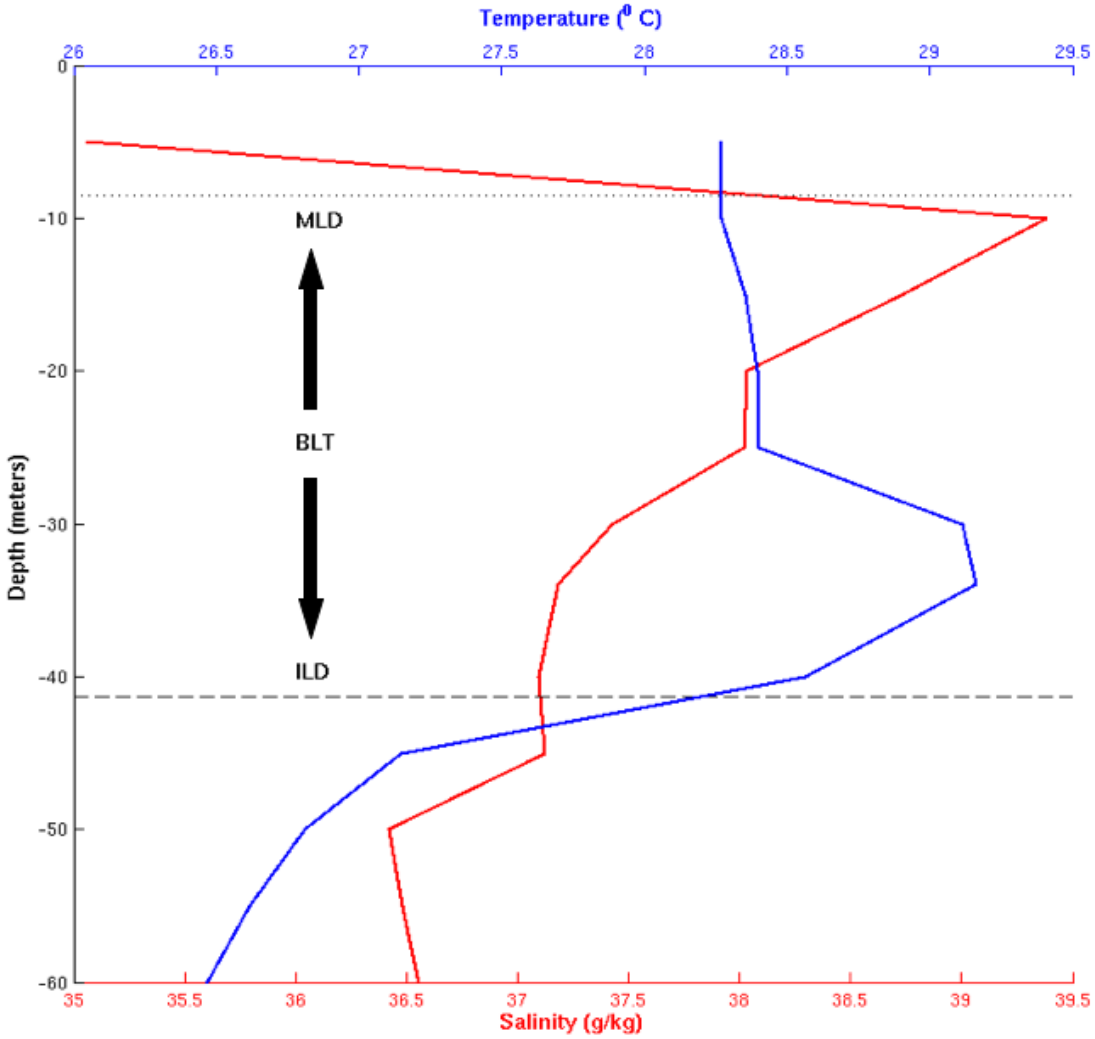

Fig. 39. Prevailing sub-surface hydrographic conditions from an Argo float at 19.6 ^{0}N, 62.1 ^{0}W on 16th October 2008: Salinity (red), Temperature (blue), MLD (black, dotted), ILD (black, dashed).

economic losses were estimated as $ 46.2 million. For our present analysis, we consider the path between 18^{th} and 22^{nd} August when Bill intensified from a tropical storm to a major hurricane and back to hurricane status in the Atlantic to the east of the Caribbean sea. Fig. 40 shows the path of Hurricane Bill overlaid on the prevailing BL conditions on 17^{th} August before Bill approached the region. The white star indicates the location of an Argo float (AOML float number : 4900360).

Bill intensified rapidly from category 1 to category 4 between 17^{th} and 19^{th} August, 2009 with wind speed increasing from 110 km hr^{-1} to 215 km hr^{-1}. From Fig. 40, we can see that Bill gradually enters a region of thick BLs of up to 30 m thickness during this period. We also see from the figure that there was an Argo float close to the path of the hurricane, located at 61.478^0W and 23.566^0N. The closest approach of the hurricane to the location of the float was at 62.4^0W and 23.1^0N. At this point, the float was located approximately at a distance of 103 km to the right of the storm track. Despite the distance, as Bill was a relatively large sized hurricane, the float was able to capture its passage reasonably well. Another important reason for this could be that the float was located to the right of the storm track. In the northern hemisphere, the surface ocean response to TCs is more pronounced to the right of the storm track when compared to the left side. This is because on the right side, the wind vector rotates clockwise and is in phase with Ekman currents and the resultant resonant currents produce a much stronger response when compared to the left of the storm track where the wind opposes the inertial currents generated. The changes in the subsurface salinity and temperature are shown in Fig. 41. At the location of the float, the hurricane had reached the status of a major hurricane and the intense surface winds with speed exceeding 200 km hr^{-1} and cause tremendous upwelling. As a consequence, the surface salinity increases (Fig. 41a) by about 0.5 g kg^{-1} and the surface temperature decreases by 2^0 (Fig. 41b).

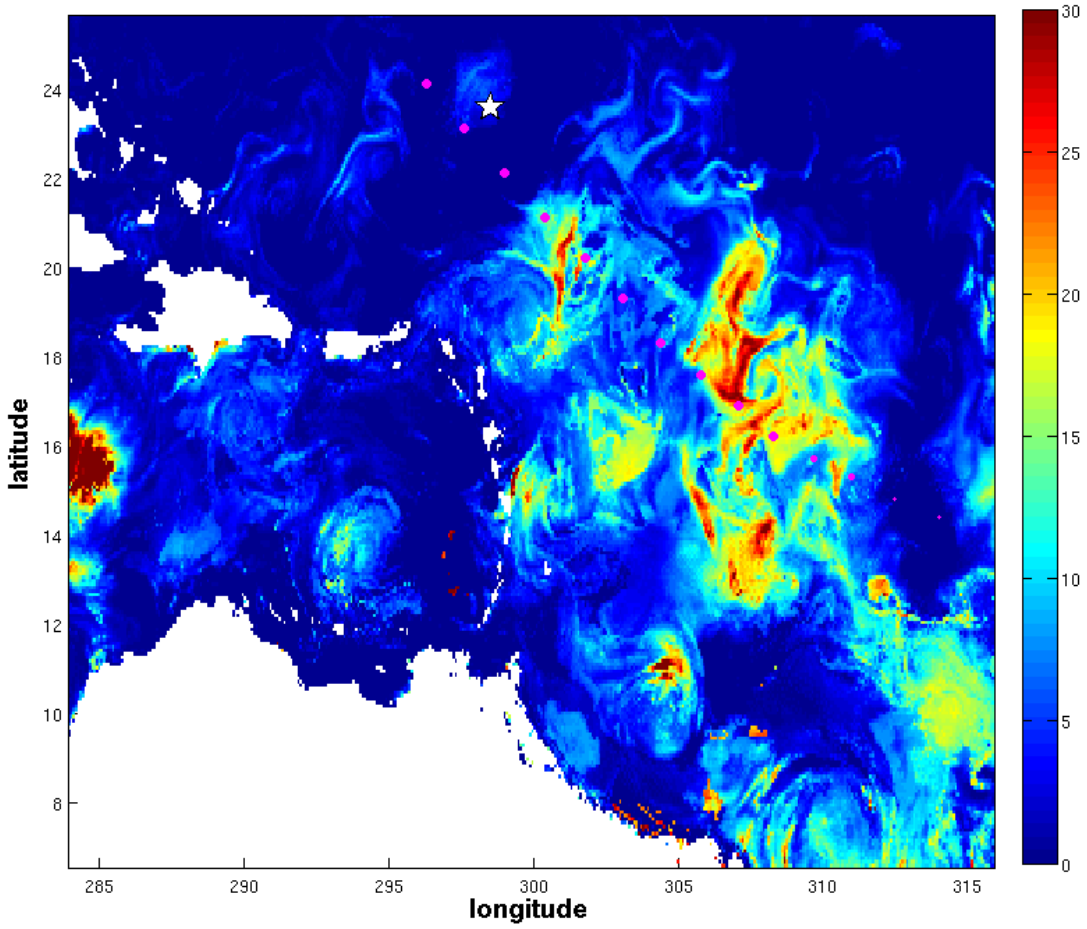

Fig. 40. Prevailing BL conditions on 17^{th} August 2009 with the path of Hurricane Bill overlaid. The size of the dots is proportional to the wind speed. The white star indicates the location of an Argo float.

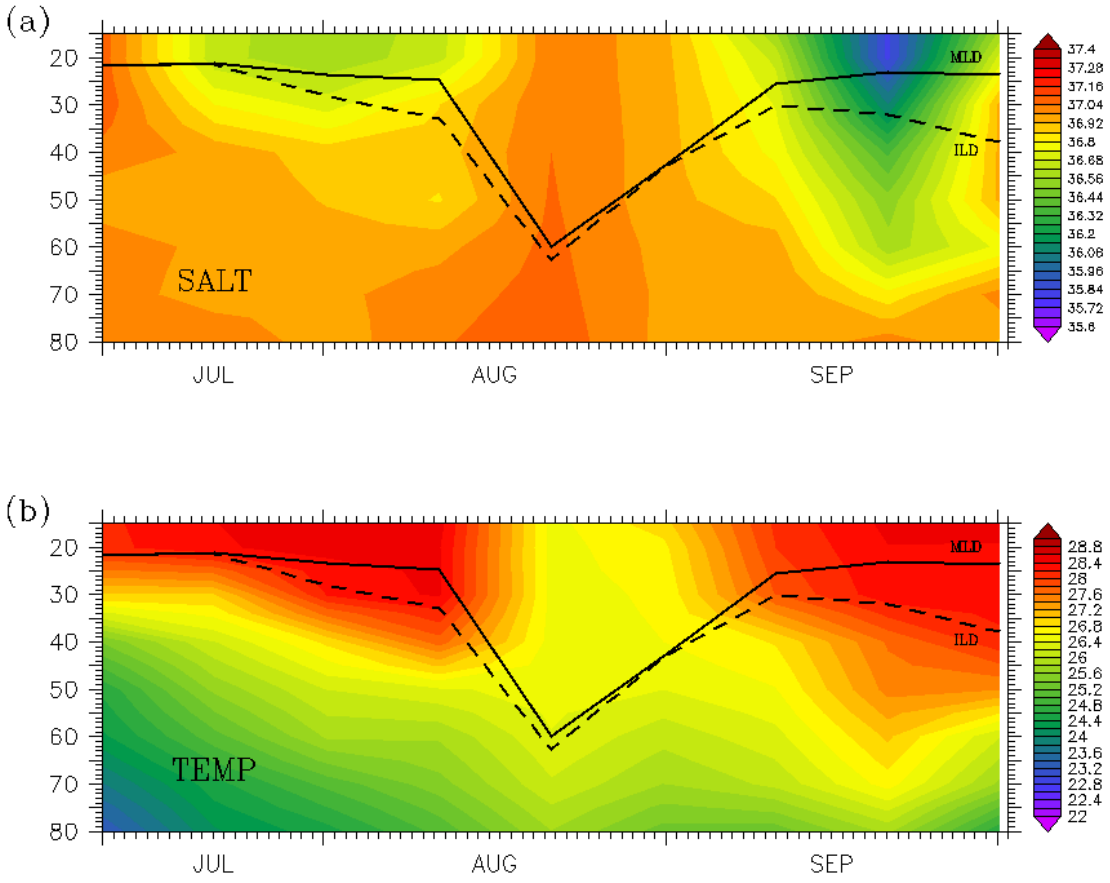

Fig. 41. Passage of Hurricane Bill as captured by an Argo float (AOML float number : 4900360) (a) Salinity changes in the sub-surface (b) Temperature changes in the sub-surface. The solid line indicates MLD and the dashed line indicates ILD.

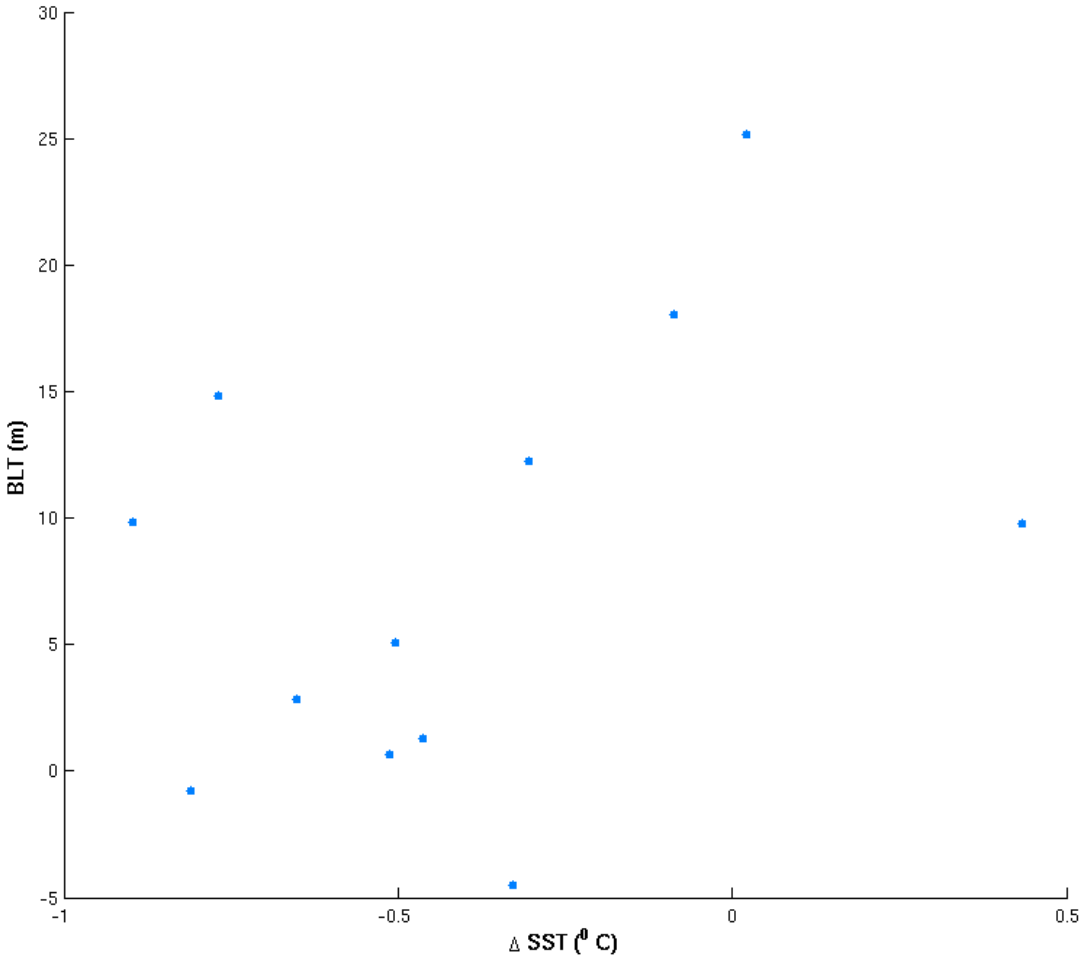

Fig. 42. Scatter plot between along track ΔSST (X-axis) and BLT (Y-axis) for Hurricane Bill.

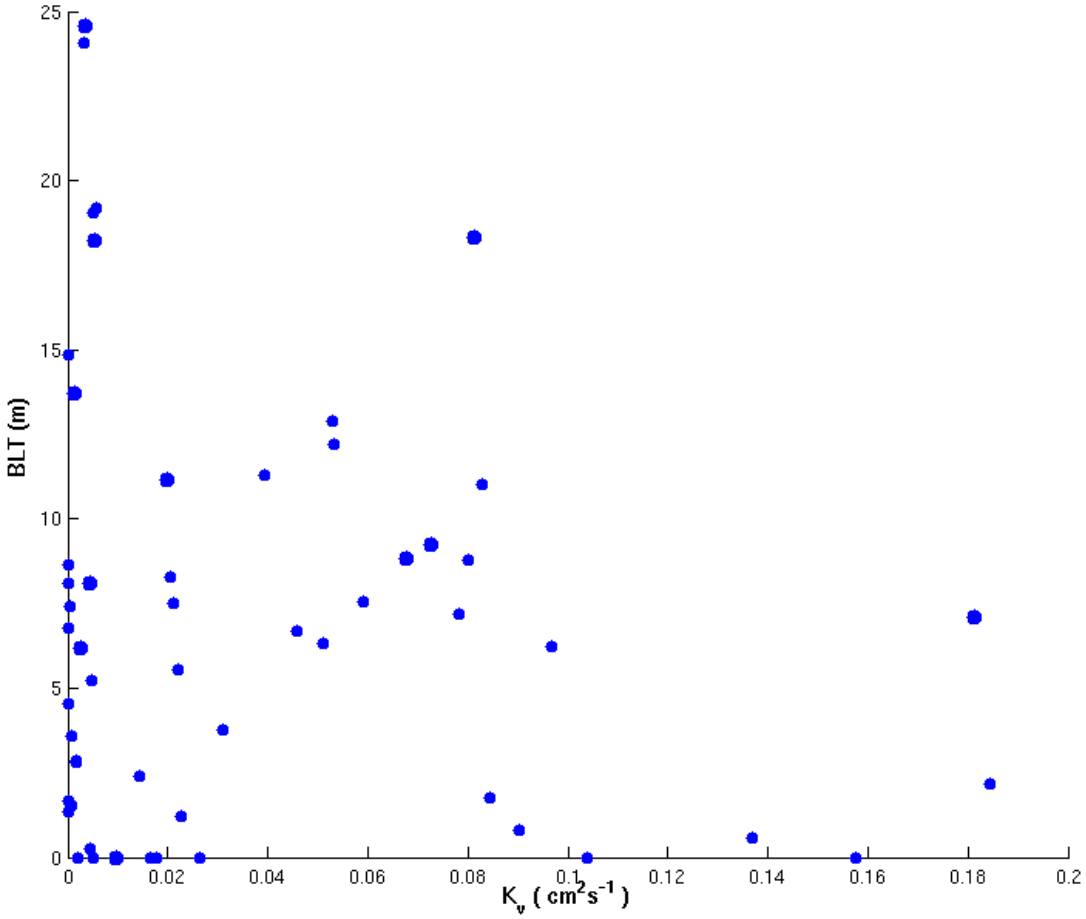

Fig. 43. Scatter plot between along track K_v (X-axis) and BLT (Y-axis) for Hurricanes Philippe, Omar and Bill. The size of the dots is proportional to the wind speed.

The along track changes for Hurricane Bill is shown in Fig. 42. As before, on an average, for situations with strong BLs the magnitude of SST cooling is lower than that for situations with weak BLs.

G. TC Induced Vertical Mixing

The TC induced vertical mixing is estimated by Sriver and Huber (2007) as $K_v = \frac{L^2}{\tau}$, as was noted before. We now extend it and express the vertical mixing coefficient as a function of the initial and final MLDs . Using the first order Taylor series approximation, the temperature at a depth z below the mixed layer can be expressed in the following way.

$$T(z) = T - \frac{\partial T}{\partial z} z$$

Here T is the mixed layer temperature and $\frac{\partial T}{\partial z}$ is the rate of decrease of temperature below the mixed layer. If the initial MLD and mixed layer temperature are h and T respectively, the final MLD and mixed layer temperature are $h + h'$ and T' respectively and if the SST change at the surface is assumed to occur primarily due to mixing of the surface ocean to a depth of $h + h'$, then the final mixed layer temperature T' and consequently the vertical mixing coefficient K_v interms of h and h' can be expressed as follows.

$$T' \times (h + h') = \int_0^{h+h'} T(z)dz = \int_0^h T dz + \int_h^{h+h'} (T - \frac{\partial T}{\partial z} z)dz$$

$$K_v = \frac{L^2}{\tau} = \frac{(\frac{\Delta T}{\frac{\partial T}{\partial z}})^2}{\tau} = \frac{(\frac{(h+h')^2 - h^2}{2(h+h')})^2}{\tau}$$

Having thus expressed the vertical mixing coefficient, we compute the value of K_v for points along the tracks of Hurricanes Philippe, Omar and Bill. Fig. 43 shows

the scatter between K_v and the pre-existing BLT. It is clear that in the presence of strong BLs, the vertical mixing coefficients are lower than in situations with weak BLs due to the enhanced haline stratification within the isothermal layer. The magnitude of K_v ranges between 0 and 0.2 $cm^2\ s^{-1}$, which is within the range obtained by Sriver and Huber (2007) from their analysis for Atlantic hurricanes. On an average, the mixing coefficient is reduced by about 25 %.

H. Summary

The effect of BLs on the surface ocean response to TCs was studied in this Cshapter using various satellite and in situ data sets. Also used were several re-analysis data sets. Along track SST changes were computed for all Atlantic hurricanes for the period 1998-2007 using TRMM daily SST data and hurricane track information from HRD (AOML - NOAA). The pre-existing hydrographic conditions were obtained from SODA re-analysis data at 5-day mean. It is seen that on an average the SST cooling induced by TCs is directly proportional to the wind speed and inversely proportional to both the stormspeed and the MLD. This is consistent with the hypothesis of Price (1981). Comparing the SST change between situations with and without BLs shows that in the presence of BLs, the mean SST cooling is reduced by about 48 % when compared to situations without BLs. Performing a t-test confirms that this difference is statistically significant. Totally we have used 152 storms and TCs, which includes more than 1400 points for our computation out of which approximately 300 were with a BL, which is about 22 % of the total number of points. It is also seen that regions of thick BL formation are not necessarily regions of thick mixed layers.

We next conducted case-studies for four Atlantic Hurricanes Philippe (2005), Wilma (2005), Omar (2008) and Bill (2009). While Omar, a category 4 hurricane

and Wilma, a category 5 hurricane intensified over the Caribbean waters, Philippe and Bill, which reached intensities of category 1 and 4 respectively, intensified over the Atlantic waters to the east of the Leeward and Lesser Antilles Islands. We used high resolution re-analysis daily data and hurricane track data to compute track SST changes and it is seen that in the presence of BLs the SST cooling is significantly alleviated. Argo float data was used to examine the sub-surface hydrographic conditions at a location close to the track of Hurricane Omar. Sub-surface temperature inversions with a magnitude as high as 1^0 existed and we speculate that under the influence of these inversions, SST cooling due to TC-induced mixing could be alleviated or there could even be a slight warming. This in turn could act as a positive feedback for the TC intensification. We were able to capture the passage of Bill with the aid of an Argo float located very close to its path. The magnitude of surface cooling was as high as 2^0 C and there was also an increase of surface salinity by about 0.5 g kg^{-1} due to the strong upwelling and entrainment caused by Bill.

Finally, we extended the formulation of vertical mixing coefficients due to TC induced mixing, as given by Sriver and Huber (2007) , by re-writing the mixing coefficient as a function of the initial and final MLDs and used this formulation to calculate the vertical mixing coefficients induced by Hurricanes Philippe, Wilma, Omar and Bill. The mixing coefficient values were consistent with the values obtained by Sriver and Huber (2007) for Atlantic hurricanes. In the presence of strong BLs, the vertical mixing coefficients are reduced by about 25 % on an average.

Several previous studies point to the role played by SST change in the high-wind speed eye-wall regime of the TC on the air-sea heat flux exchange and eventually on the TC intensification. Our current study, using an array of observational/re-analysis data sets, including TRMM, Argo, SODA and HYCOM reanalysis products, suggests that the role played by BLs may not be negligible in TC forecast studies.

CHAPTER V

EFFECT OF BARRIER LAYERS ON THE SURFACE OCEAN RESPONSE TO TROPICAL CYCLONES. PART 2: STUDY USING A COUPLED REGIONAL CLIMATE MODEL

In the previous chapter, we studied the modulation of the surface ocean response to TC induced mixing using a variety of observational and in situ data sets. We now continue the study only this time within the framework of a coupled model. The observational/reanalysis study from the previous chapter suggests that BLs may play a role in the SST response to TCs and that they might even have an impact on the intensification of TCs. Furthermore, TCs may also in turn influence the BLs through a feedback loop. To the best of our knowledge, the role of BLs in the air-sea interaction associated with TCs has not been fully investigated using a comprehensive modeling approach, i.e., a coupled general circulation model that includes realistic representations of the mutual feedbacks between TCs and the ocean. In the present study, we investigate how BLs modulate the upper ocean SST response to TCs by examining the output from a high-resolution Coupled Regional Climate Model.

A. Model Description

The model output used in this study is from a high-resolution Coupled Regional Climate Model (CRCM). The oceanic component of the model is ROMS 3.3 (Regional Ocean Modeling System developed by Rutgers University and the University of California at Los Angeles) and the atmospheric component is WRF-ARW 3.1.1 (Advanced Weather Research & Forecasting model developed by NCAR). ROMS is configured at a horizontal resolution of 9 km and 30 vertical levels. WRF is configured at a horizontal resolution of 27 km and 28 vertical levels. Both models have

been configured for the Atlantic domain with the domain for WRF being 110^0W to 27^0E and 46^0S to 61^0N. The ROMS domain is slightly smaller than the WRF domain. The initial and boundary conditions for WRF are taken from the climatology of NCEP-NCAR reanalysis (Kalnay et al., 1996). The lateral boundary conditions are updated every 6 hours based upon linear interpolation from the monthly mean climatology of NCEP-NCAR reanalysis, including winds, temperature and moisture on pressure levels. The initial and lateral boundary conditions for ROMS are derived from the monthly mean climatology of Simple Ocean Data Assimilation (Carton et al., 2000b,a). The model time steps used in the coupled simulation are 90 seconds for WRF and 10 minutes for ROMS. The coupled model is integrated by exchanging surface heat, momentum fluxes and SST between WRF and ROMS at every 6 hours of model simulations, allowing the model to resolve the diurnal cycle. The physics parameterizations used for WRF simulation are WSM3-class simple ice scheme for microphysics, Rapid Radiative Transfer Model (RRTM) for long wave parameterization, Goddard short wave radiation scheme, and YSM planetary boundary layer scheme, while we used the Mellor/Yamada level-2.5 closure vertical mixing scheme in ROMS. The model is able to simulate the mean climate of the tropical Atlantic fairly well over the two-year period. It also demonstrates the ability to simulate TC-like vortices and BLs. The model is initialized on May 1^{st} each time with slightly different initial condition and run through the hurricane season. Data from five model simulated hurricane seasons is used for our analysis, which includes over 150 tropical storms and cyclones. We follow the criterion given by Camargo and Zebiak (2002) for tracking Tropical Storms/Cyclones in our model simulations.

B. Results

Fig. 44 shows the model simulated TC tracks. Majority of the simulated TCs reach either tropical storm (17 m s^{-1} < wind speed $\leq$ 32 m s^{-1}) or Category 1 (33 m s^{-1} < wind speed $\leq$ 42 m s^{-1}) status on the Saffir-Simpson scale with a very few reaching the status of Category 2 (43 m s^{-1} < wind speed $\leq$ 49 m s^{-1}) . When compared to observations (Fig. 24), the number of tropical storms and TCs simulated in the model is higher. On an average nearly 32 Tropical Storms and TCs are simulated per season in the model, which is nearly twice as many in observations.

The model simulates both the magnitude and extent of BLs for the hurricane season reasonably well. Figs. 45a and 45b show the mean BLT in the northern tropical Atlantic for the summer (May - July) and fall (Aug - Oct) seasons respectively from the observational climatology of Mignot et al. (2007) while Figs. 45c and 45d show the same from model simulations. The model particularly simulates the summer BLT well. May-June is the period of maximum Amazon river discharge and consistent with this we find BLs extending northwestwards from the mouth of the river towards the Caribbean. The maximum BLT being about 25 m and occurs near the islands of lesser Antilles. The model also simulates the BLs to the east of 50^0W, which result partly from the intense precipitation of the ITCZ and also the transport of Amazon water by the seasonal NECC. However, when it comes to the late summer and fall BLs, the model simulates well the magnitude but under-estimates the extent. The northernmost extent of observed BLs is about 25^0N while most of the model simulated BLs are confined to the south of the Caribbean Islands. However, the model is able to capture the BL to the east of 50^0W and centered at 25^0W and 8^0N.

The TCs induce a vigorous mixing in the upper ocean causing cooler sub-surface water to enter the mixed layer, resulting in SST cooling. However, in situations when

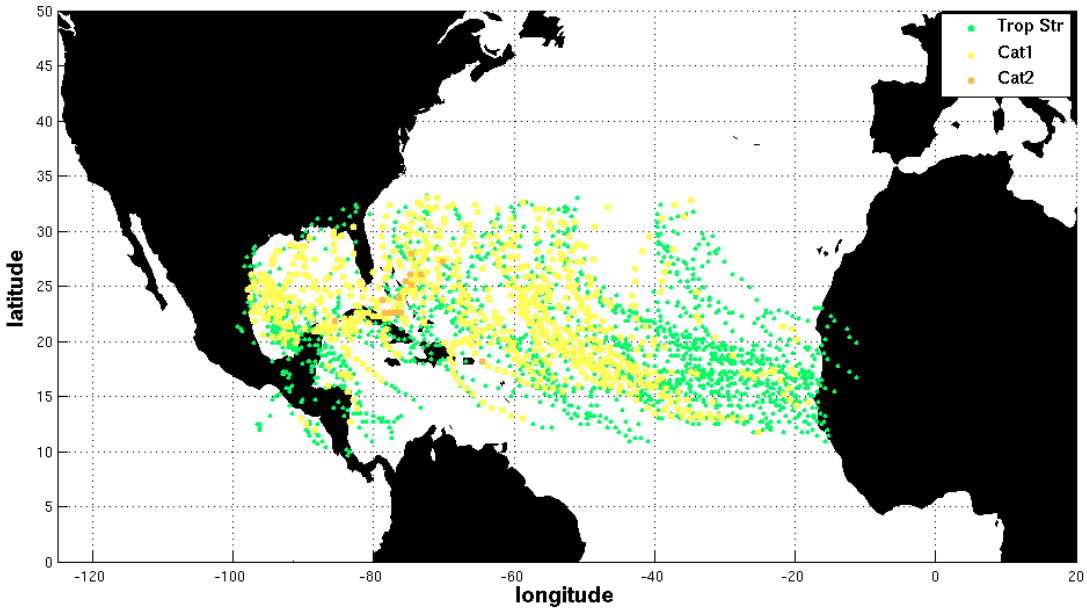

Fig. 44. Illustration of the model simulated TC tracks. The storms have been categorically differentiated according to the Saffir-Simpson scale.

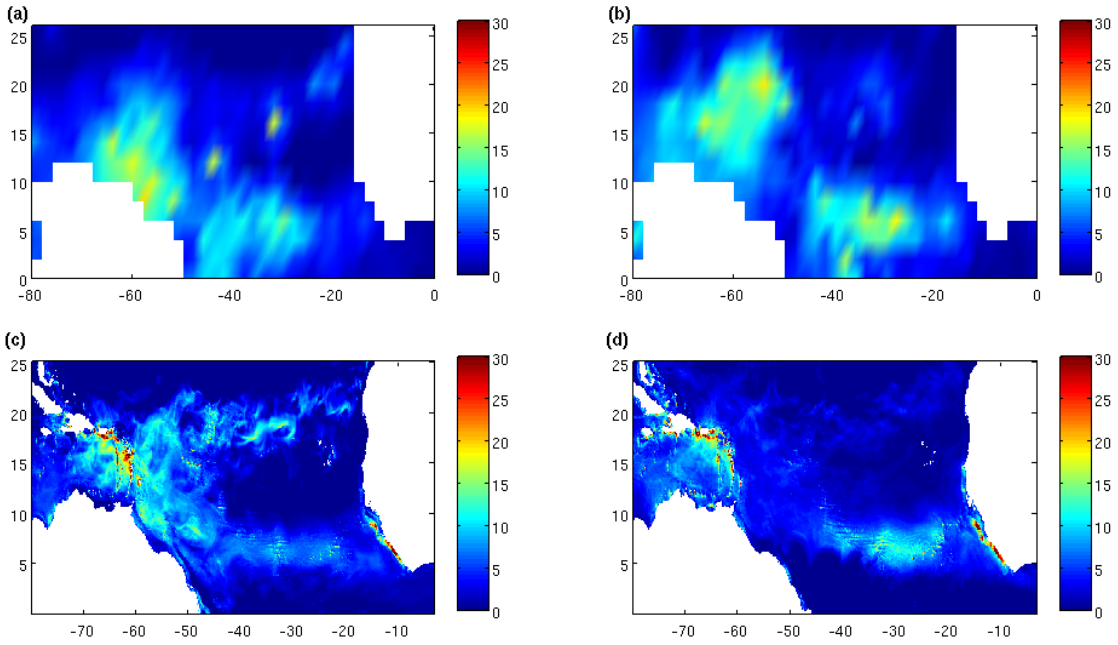

Fig. 45. The observed mean BLT (m) in the tropical Atlantic for the hurricane season (a) May - July (b) Aug - Oct. The model simulated mean BLT (m) in the tropical Atlantic for the hurricane season (c) May - July (d) Aug - Oct.

the TC passes over a BL with an associated temperature inversion, vertical mixing can cause warmer sub-surface water to enter the mixed layer causing a slight SST warming. Fig. 46 is an illustration of this phenomenon. In Fig. 46a, the location of the storm is indicated at about 92.2^0W and 21.1^0N in the Gulf of Mexico (black star), overlaid on the prevailing BLT. The maximum wind speed of the storm at that location is about 29.28 ms^{-1}. The sub-surface temperature profiles at the same location before (red) and after (blue) the passage of the storm are shown in Fig. 46b. Initially, there was a sub-surface temperature inversion of about 0.1 ^{0}C in magnitude. An examination of profiles before and after mixing shows that due to the prevailing sub-surface warming, mixing leads to a SST increase albeit small in magnitude. This in turn could lead to a higher flux of heat from the ocean into the atmosphere causing an intensification of the TC.

To consider further the impact of BLs on the surface ocean response to TCs, we perform a composite analysis. Subsurface temperature change is computed along the path of various storms, at each point in a reference frame oriented perpendicular to the direction of the storm. The width of the wake considered is 100 km or 50 km on either side of the center of the storm, which is the typical assumption. The mixing depth of TCs in the Atlantic is about 100-200 m. As we are unable to simulate TCs with a strength of major hurricanes in our model, we consider a depth of about 125 m. Fig. 47a shows the composite for tropical storms. There is a conspicuous rightward bias in surface cooling. The cooling to the right of the storm is about 0.3^0 higher than on the left side. This asymmetry in cooling can be attributed to two factors, the asymmetry in the forcing and non-linear advection (Greatbatch, 1983; Zedler, 2009). The effect of asymmetry in forcing is that to the right of the storm, the wind vectors rotate clock-wise and resonate with the inertial currents and thus enhance the turbulent mixing due to the breaking of inertial waves (Price, 1981).

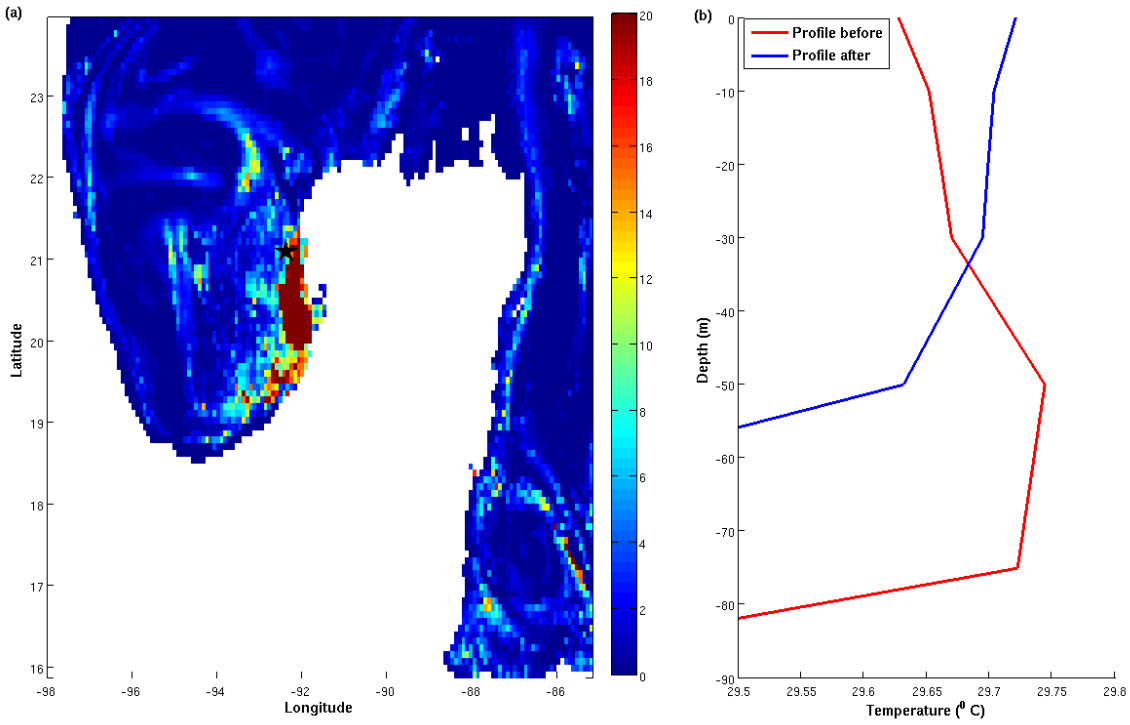

Fig. 46. (a) The prevailing BL conditions with the location of the tropical storm indicated (black star) at 92.2^{0}W and 21.1^{0}N (b) The sub-surface temperature profiles at that location before (red) and after (blue) the passage of the TC.

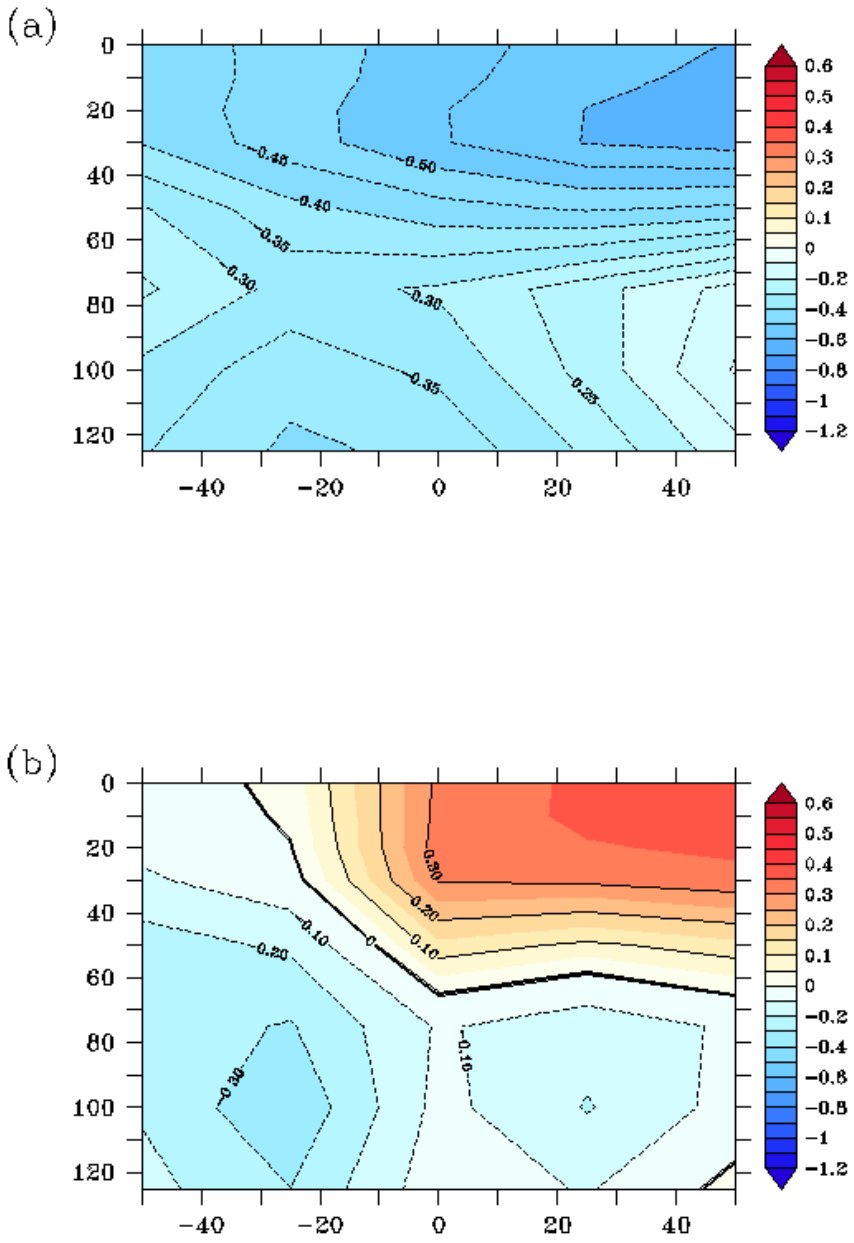

Fig. 47. (a) A composite of sub-surface temperature change due to mixing by tropical storms. (b) Difference in composites for situations with and without BLs. Depth (m) on Y-axis and width (km) on X-axis.

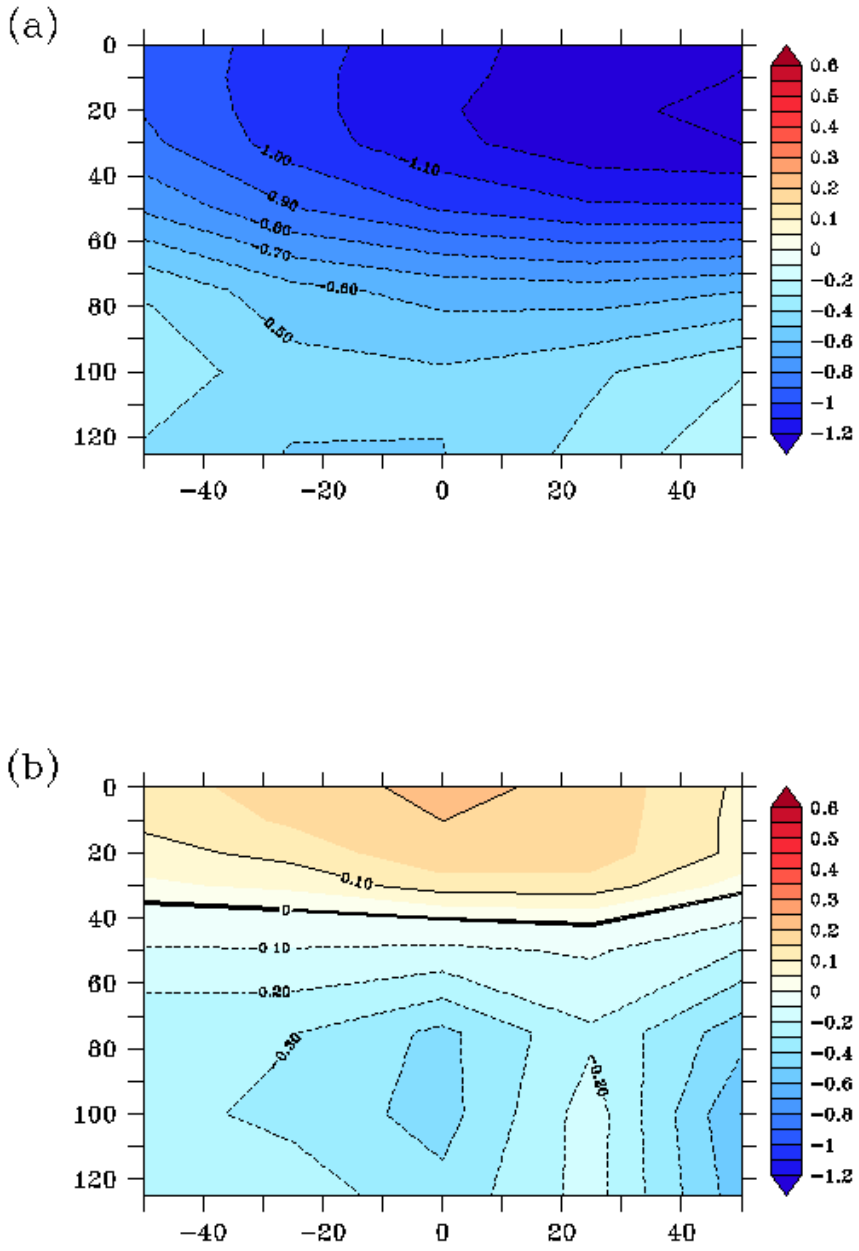

Fig. 48. (a) A composite of sub-surface temperature change due to mixing by Category 1 TCs. (b) Difference in composites for situations with and without BLs. Depth (m) on Y-axis and width (km) on X-axis.

Next we decompose the members of the composite into members with and without BLs and take the difference between their means. Fig. 47b shows this difference and it can readily be seen that BLs reduce the cooling of the mixed layer and significantly reduce the rightward bias. To the right of the storm, there is a relative warming of about 0.3-0.4^{0}C, which is quite substantial when compared to the mean surface cooling. The composite for Category 1 hurricanes is shown in Fig. 48a. Again, there is a notable rightward bias in surface cooling and the maximum surface cooling to the right of the storm center is about 1.3^{0}C, which is considerably higher than for tropical storms (Fig. 47a). When we consider the difference between the composites with and without BLs (Fig. 48b), we find that BLs reduce the cooling of the mixed layer by about 0.3^0, which is nearly 25 % of the mean surface cooling. However, there is no pronounced rightward bias as in the case of tropical storms (Fig. 47b). This is because the winds are strong enough to break through the stratification barrier and mix cooler sub-surface water into the mixed layer. Hence, the BLs significantly reduce the cooling of the surface mixed layer caused by Category 1 TCs but uniformly on either side of the storm center.

Let us now consider the impact of the three most important factors (Price, 1981), namely the windspeed, stormspeed and the MLD on the SST response to storm induced mixing in the model simulations, as we had done previously using observational data sets. The scatter plot between along track ΔSST and windspeed is shown in Fig. 49. At low windspeeds the magnitude of maximum SST cooling is smaller than that at higher windspeeds. This implies that when the windspeed is low, irrespective of other factors, the SST cooling is weak. As we move to higher windspeeds, a range of SST cooling is possible, depending on other factors.

Figs. 50 and 51 show the along track ΔSST plotted against stormspeed and MLD respectively. The scatter plot between ΔSST and stormspeed suggests that when the

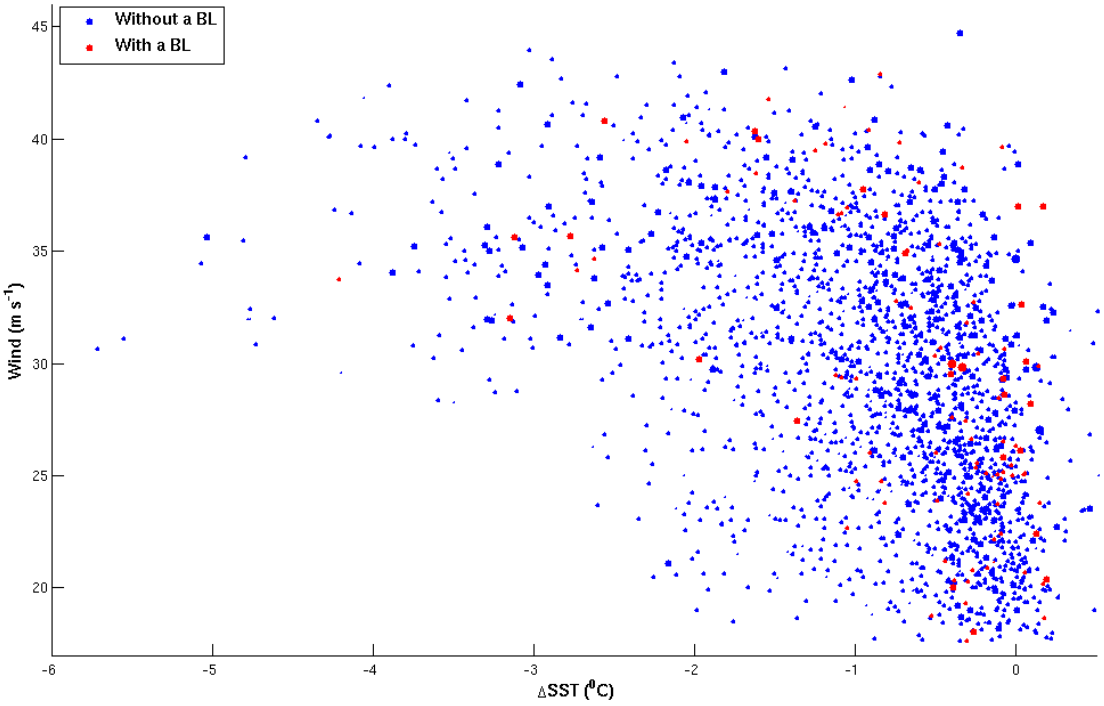

Fig. 49. Scatter plot between ΔSST (X-axis) and wind speed (Y-axis). The size of each dot is proportional to the initial MLD at that location.

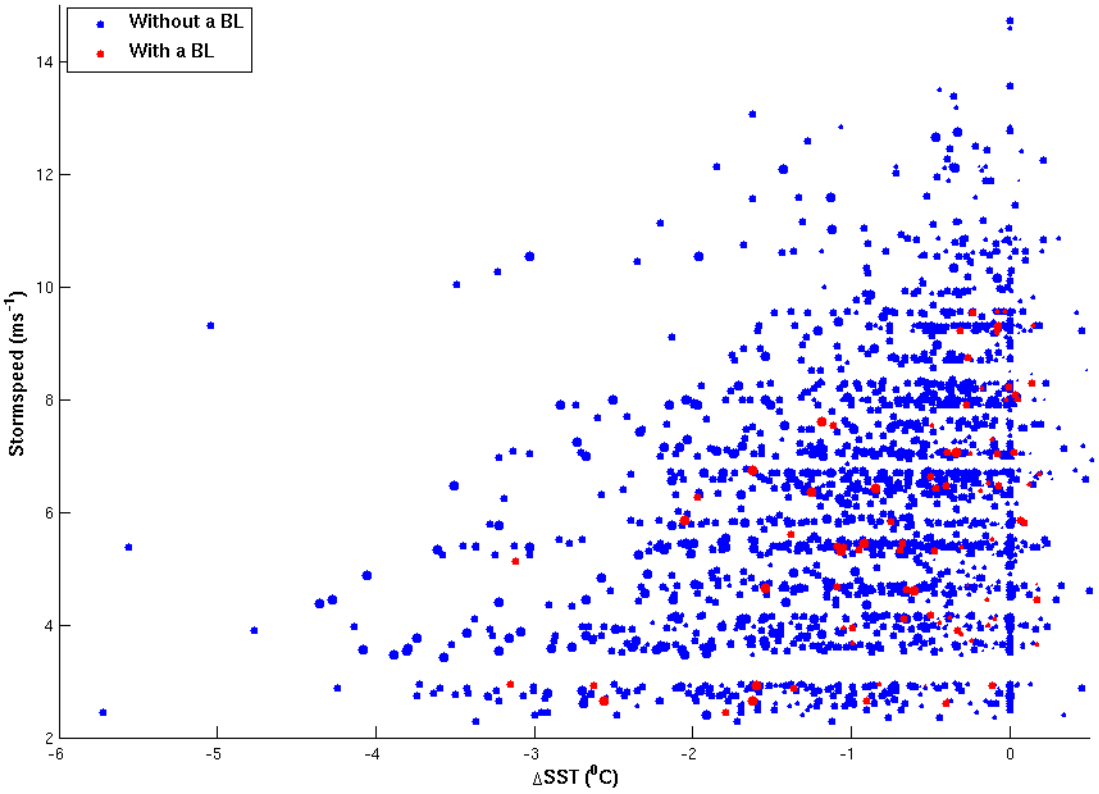

Fig. 50. Scatter plot between ΔSST (X-axis) and storm speed (Y-axis). The size of each dot is proportional to the initial MLD at that location.

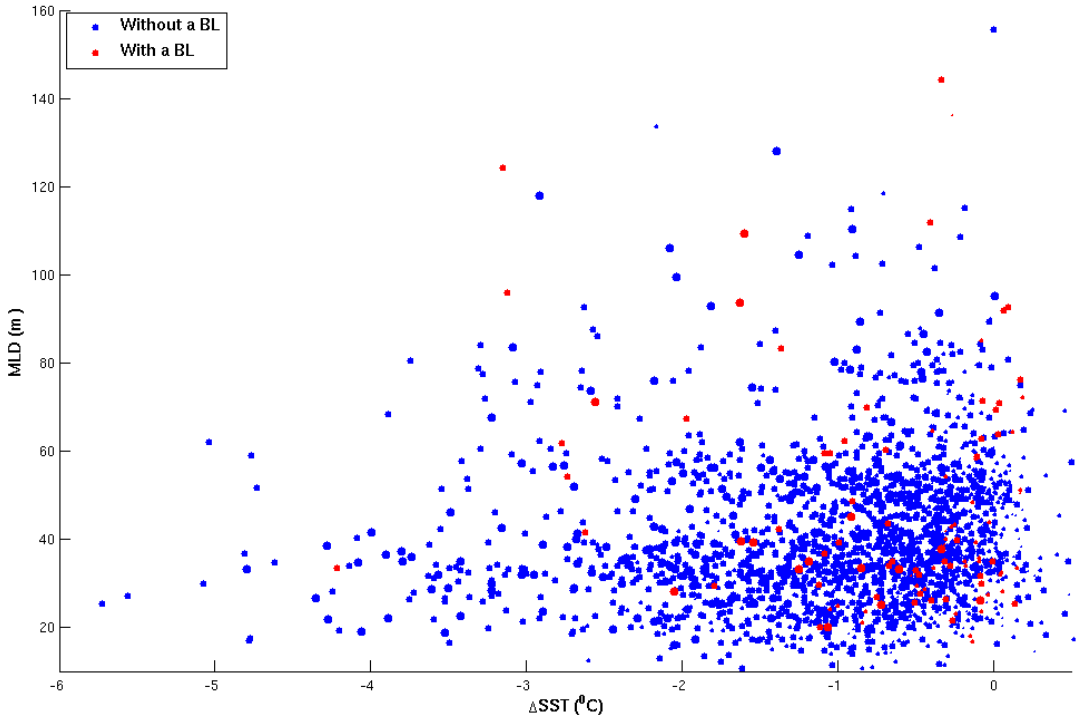

Fig. 51. Scatter plot between ΔSST (X-axis) and MLD (Y-axis). The size of each dot is proportional to the wind speed at that location.

storm translational speed is high, the magnitude of SST cooling on an average is weak. But as we go to the regime of low storm speeds, the magnitude of cooling on an average is stronger. This is because when the stormspeed is high, the storm does not spend sufficient time at a place to cause cooling by upwelling, vertical mixing or through the flux of latent and sensible heat. On the other hand, the scatter plot between ΔSST and MLD indicates that when the MLD is very thick, the SST cooling induced on an average is low. But as the MLD gets shallower, a range of SST cooling is possible depending on other factors and the magnitude of maximum SST cooling increases. This is simply because the shallower the MLD, the easier it is for the storm to break through the stratification and mix cooler thermocline water into the mixed layer

Also, from the three plots, we find that in the presence of a BL, the SST cooling is alleviated when compared to situations without a BL. Fig. 52 further accentuates this finding. Figs. 52a and 52b compare the probability distribution function (PDF) of SST change when the tropical storm passes over an oceanic region with a BL to that without a BL. The difference between the two PDFs is shown in Fig. 52 (c). Clearly, ΔSST is reduced when a BL is present. The mean ΔSST with a BL present is only about 65.5 % of the mean ΔSST without a BL. This difference satisfies the t-test for difference of means at 95% confidence level and therefore is statistically significant. Also, the along track latent and sensible heat flux exchange is computed and contrasted for situations with and without a BL. It is found that in the presence of BLs, the latent and sensible heat input into the atmosphere from the ocean, which is the main driver for the TC, increases by about 16.4 %. This value is statistically significant at 95% confidence level. The PDF in Fig. 53 illustrates this point further. The PDF of heat flux for situations with and without a BL are shown in Figs. 53a and 53b respectively while the difference between them is shown in Fig. 53c. It can

be seen that the PDF for situations with a BL is relatively skewed to the right.

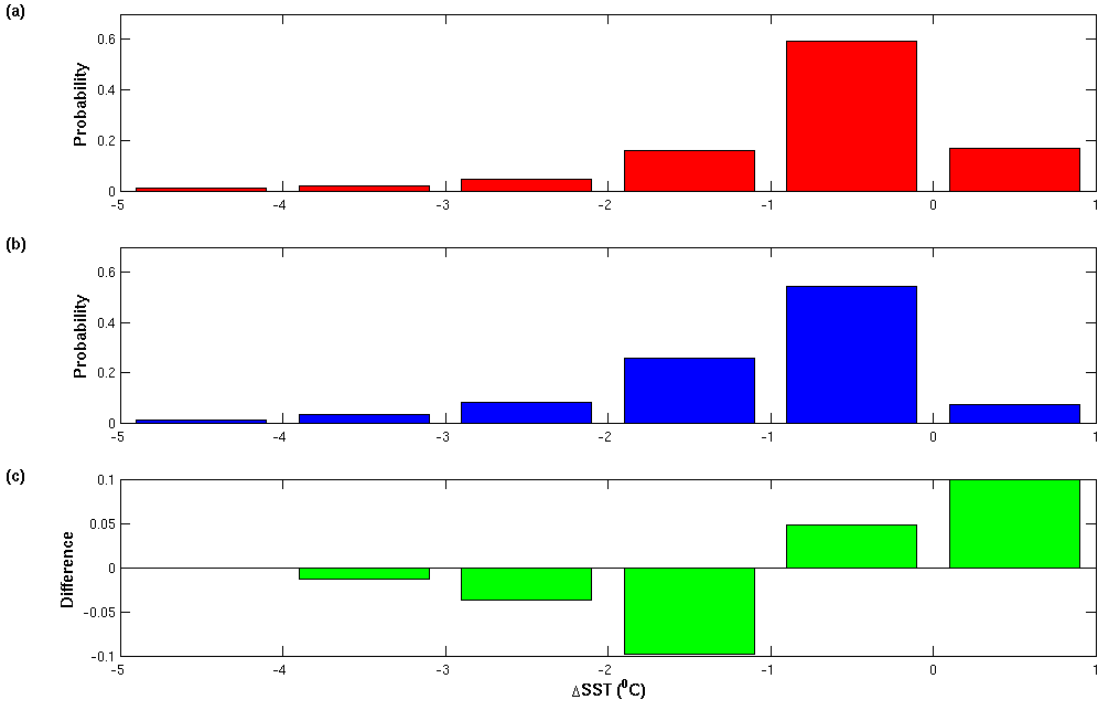

Fig. 52. PDF of ΔSST (a) Situations with a BL (b) Situations without a BL (c) Difference between the two.

TCs cause tremendous vertical mixing in the upper ocean. During this process, sub-surface denser water is mixed with lighter surface water resulting in an increase of the surface ocean potential energy. Sengupta et al. (2008) estimated the changes in the upper ocean potential energy for TCs in the Indian Ocean and estimated a value of about 10^4 J m^{-1}. However, they assume a uniform salinity in the sub-surface which, as acknowledged by them, would lead to an under-estimation. Potential energy change is computed along the tracks of various Tropical Storms and TCs using the following formulation.

$$\Delta \mathrm{PE} \quad = \quad \int_0^h \rho_f(z)(h - z)\, g\, dz - \int_0^h \rho_i(z)(h - z)\, g\, dz$$

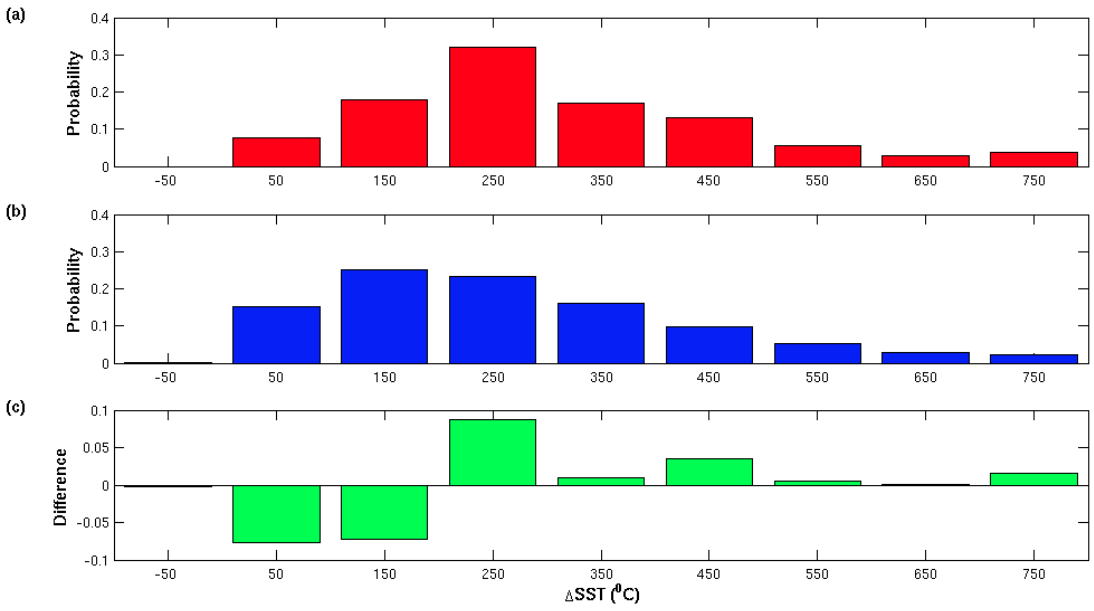

Fig. 53. PDF of enthalpy fluxes at air-sea interface (a) Situations with a BL (b) Situations without a BL (c) Difference between the two.

Here, ΔPE is the change in potential energy, $\rho_f(z)$ is the final density profile, $\rho_i(z)$ is the initial density and h is the reference depth (100 m). The mean change in the upper ocean ΔPE is found to be about 1.5×10^4 J m^{-2}. The scatter plot between ΔPE and windspeed is shown in Fig. 54. As expected, it is seen that at higher windspeeds, the ΔPE is considerably higher than at lower windspeeds. Also, in the presence of a BL, the mean ΔPE is reduced by about 24 % and a t-test confirms the statistical significance of this result.

As noted earlier, TCs cause intense stirring in the upper ocean resulting in cooling in the surface ocean and warming in the sub-surface. The enthalpy fluxes at the air-sea interface restore the cooling in the surface but the warm anomalies in the sub-surface remain. During this process, net column integrated heating occurs and for steady-state maintenance there has to be a poleward heat transport (Emanuel, 2001). The formulation described in Chapter IV is used to calculate the integrated heat anomalies along the TC tracks in the model simulations. The annual mean integrated heat transport is estimated to be 0.02 PW.

C. Summary

The interaction between TCs and the upper ocean involves complex air-sea feedback processes. Previous studies have shown in the past that atmosphere-ocean coupling significantly impacts the simulated TC intensity (Knutson et al., 2001; Bao et al., 2000). The goal of the present study is to investigate how BLs may modulate the air-sea coupling associated with TCs. To that end, we have analyzed output from a high-resolution CRCM (ROMS-WRF). To the best of our knowledge, our study is unique in using a coupled model of this complexity to investigate the SST response to TCs in the context of BLs. Our results indicate that the BL effect can lead to

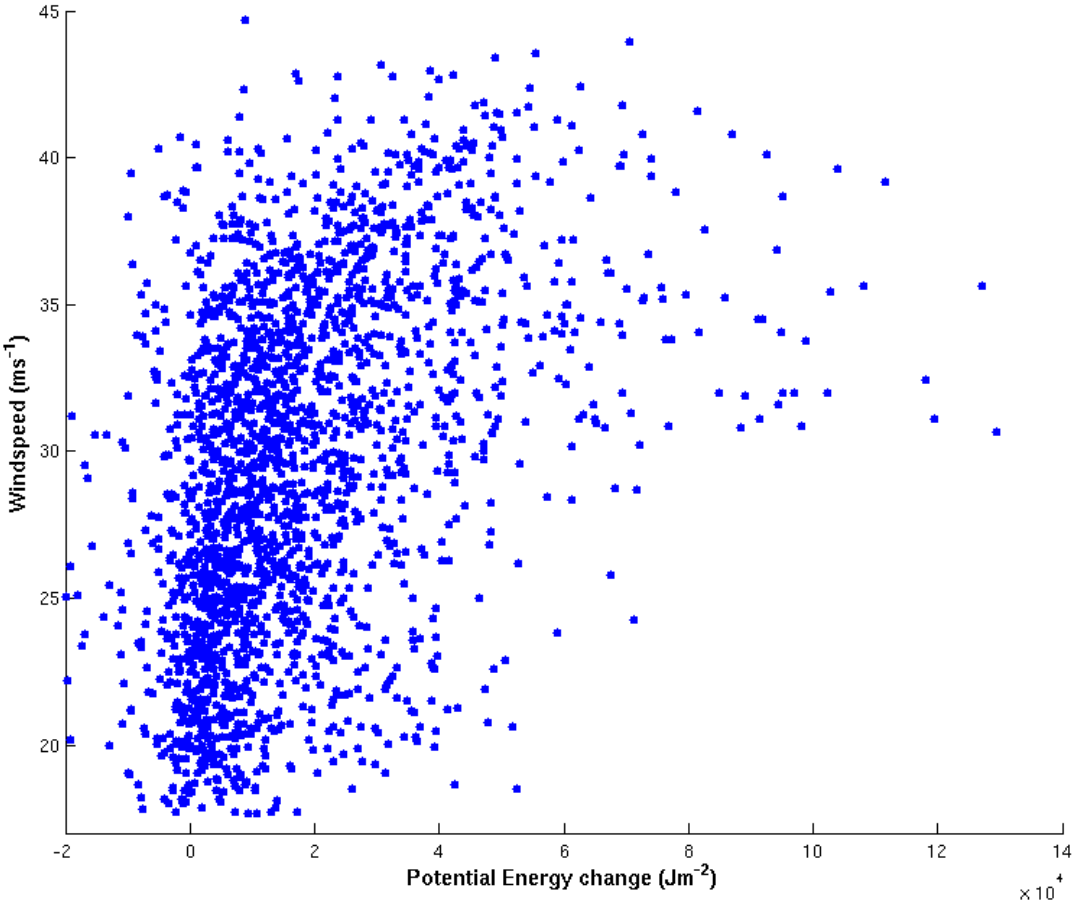

Fig. 54. Scatter plot between ΔPE (X-axis) and wind speed (Y-axis).

statistically significant weakened surface cooling in the wake of TCs. In case of a temperature inversion associated with a BL, TC induced mixing can even lead to a slight SST warming. A composite analysis confirms the pronounced rightward bias in the surface ocean cooling. In the case of Tropical Storms, BLs considerably reduce the rightward bias but in the case of Category 1 TCs, the reduction in the bias is less pronounced. The PDF of the simulated change in SST associated with the passage of a TC indicates that the reduced thermal stratification associated with BLs considerably attenuates the surface cooling, reducing the amplitude of the cooling by nearly 35 %. It is also seen that, in the presence of a BL, the latent and sensible fluxes of heat from the ocean into the atmosphere increase by about 16 %. The intense vertical mixing caused by TCs result in a mean increase in the upper ocean potential energy by about $1.5\times10^4 \mathrm{J}m^{-2}$ and in the presence of BLs, this value reduces this by about 25 %. Finally, the heat anomalies caused by TC induced mixing could result in a poleward heat transport of about 0.02 PW. In the light of previous studies which show the significance of heat fluxes at the air-sea interface for the formation and invigoration of TCs, the above results assume significance for TC forecast studies.

CHAPTER VI

CONCLUSIONS AND DISCUSSION

This dissertation research revolves around a phenomenon in the upper ocean where salinity plays a dominant role in the determination of density. In the upper ocean, when discrepancies arise between the uniform density MLD and the uniform temperature ILD, the difference between the base of the ILD and the base of the MLD is defined as the BL as it acts as a 'barrier' to entrainment cooling and turbulent mixing (Godfrey and Lindstrom, 1989; Lukas and Lindstrom, 1991). For this dissertation research, we have focused on the BLs occurring in the northwestern tropical Atlantic, which are considered as one of the most prominent features of the global tropics (Mignot et al., 2007).

After a brief review of the formation mechanism of BLs in the three tropical oceanic regions (Sprintall and Tomczak, 1992), we examined the BL simulations from both, the uncoupled and coupled versions of the state-of-the-art OGCM POP. In the coupled mode, the model was part of the NCAR climate model CCSM 3.0. Even though the model, in either versions, was unable to reproduce the observed BLs in any of the three tropical oceanic regions, the uncoupled version of the model fared a lot better than the coupled version. This led us naturally to consider the causes of the biases in the coupled model simulations.

Most coupled models that exist today fail to accurately simulate the mean climate of the tropical Atlantic. These models have well-known biases in SST and precipitation. However, these models also have biases in the upper ocean salinity stratification. The upper ocean salinity budget of the northwestern tropical Atlantic is dominated by the Amazon and Orinoco river systems which together contribute to nearly 20 % of the total global freshwater discharge into the oceans. This sparked the hypothe-

sis by Breugem et al. (2008) that errors in precipitation and discharge of the river systems translate into errors in surface salinity stratification and consequently BLs, which then might feedback positively to the climate of the coupled system through the BL-SST-ITCZ mechanism. We tested the above hypothesis within the framework of a state-of-the-art CGCM, CCSM 3.0 of NCAR. We performed a set of numerical experiments by artificially adding precipitation anomalies to study the sensitivity of BL formation in the northwestern tropical Atlantic to these anomalies.

The upper ocean salinity stratification in the northwestern tropical Atlantic is primarily controlled by two mechanisms. While the surface salinity is controlled by the advection of low salinity anomalies from the river mouths by the strong NBC and the Guyana current systems towards the Caribbean sea (Hellweger and Gordon, 2002), the sub-surface salinity is primarily controlled by the remote mechanism of subduction. High salinity waters form in the centers of the sub-tropical gyre systems partly in response to evaporation, subduct and flow at a depth in the sub-surface towards the Caribbean. We notice that the model has a high salinity bias near the river mouth and a low salinity bias in the subduction region. Proceeding thus, we design a set of mechanistic forcing experiments to test the sensitivity of the BL formation in the northwestern tropical Atlantic to these two factors. An ensemble is performed with each forcing in order to reduce the effects of the internal variability of the system.

In the first experiment, we add a positive precipitation anomaly over the Amazon region to emulate increased river discharge. The magnitude of the anomaly relates to the magnitude of the precipitation bias over that region. In response to the forcing, the SSS decreases extending from the mouth of the Amazon rRver into the Caribbean. Also there is a reduction of MLD and an increase of BLT in the Caribbean by about 10m. Even though there is a slight increase of SST in the region of BL increase, the

SST change does not satisfy the t-test for statistical significance.

In the next experiment, in addition to the positive precipitation anomaly over the Amazon region we also add a negative precipitation anomaly over the northern sub-tropical salinity maxima region in order to increase the salinity of the subducted waters. It is seen that high salinity anomalies subduct and flow southwestward at depth towards the Caribbean. The low salinity anomalies at the surface and the high salinity anomalies in the sub-surface enhance the stratification in the Caribbean and cause a reduction of MLD, with a coincident increase in BLT, by about 15-20 m. We next perform another experiment to test the sensitivity of the BL magnitude to the forcing employed, by doubling the forcing of the previous experiment. As a response to this forcing the increase in BLs (20-25 m) is higher than in the previous experiment. The three sets of experiments conducted suggest that the improvement in BLs of the northwestern tropical Atlantic is more sensitive to changes in sub-surface salinity when compared to the surface salinity in this model. This is because the magnitude of the model bias in the sub-surface is higher than in the surface. However, even in these two sets of experiments, the change in SST in the region of BL increase is not statistically significant.

In the third experiment, we have an equatorial SST cooling and a decrease in precipitation, which coincides with the region of positive precipitation bias and is statistically significant. The precipitation bias is improved by about 15-20 %. An examination of surface wind circulation changes and changes in the oceanic vertical velocity shows that there is an enhanced divergence of winds near the equator which increases the equatorial upwelling and results in SST cooling. We speculate that this SST cooling is responsible for the negative precipitation anomalies. It is not entirely clear how these changes in atmospheric circulation are brought about. We speculate that changes in convection over continental South America cause them.

One of the most interesting aspects of BL formation in the Caribbean is the formation of temperature inversions during boreal winter (de Boyer Montégut et al., 2007). The model is unable to simulate the formation of these inversions in its control simulation. In our experiments, we find that improvement in temperature inversion formation goes hand in hand with the improvement in BL simulation. In the third experiment, when the forcing used is strong, the magnitude of inversions was as high as 0.2^0C. Our experiments thus suggest that improvement in upper ocean salinity stratification in coupled models may help in the improvement of temperature inversion formation in coupled models.

A heat budget analysis performed for the region of BL increase shows that the primary balance is between changes in advective heat flux and net surface heat flux. Further examination reveals that latent and sensible heat flux changes occur which tend to cool the surface. In the second and third experiments, where we added a negative precipitation anomaly in the subduction region, there is considerable cooling to the north and northeast of the region of BL increase due to enhanced evaporation. This cooling reinforces the prevailing northeasterly trade winds and causes the heat loss in the region of improved BL simulation.

There are however, certain caveats in our study. In reality, the Amazon plume is not just associated with a low salinity but is also very high in suspended sediments (Hu et al., 2004). These suspended particles absorb the incident shortwave radiation very quickly and arrest its penetration. This factor, along with the increased stratification, consequently causes the river plume to have considerably high SSTs than the surrounding ocean region by atleast 2-3^0C. But in our experiments. we artificially reduce the salinity near the Amazon mouth and such effects are not taken into consideration. It might be useful to perform numerical experiments using the coupled model by actually varying the river-discharge. Also, to enhance the salinity

in the sub-tropical salinity maxima region we add a negative precipitation (positive evaporation) anomaly, that causes significant cooling to the north of the region of BL increase, which then reinforces the prevailing northeasterly trades. This acts as a damping mechanism for SST warming in the region of BL increase. It might be worthwhile to devise other means of improving BL simulation in the coupled model, like actually changing the river discharge, to avoid such an atmospheric response.

Having thus studied the formation mechanism of BLs, we next investigated its effect on the surface ocean response to TCs. In the tropical Atlantic, most of the TC intensification occurs in the Atlantic warmpool, facilitated by the high nature of SSTs found in this region. Historical hurricane track analysis in the tropical Atlantic (Ffield, 2007) has revealed that 68% of category 4 and 5 hurricanes have passed over the region of the Amazon plume which have high SSTs and BLs. More recently McPhaden et al. (2009) show using a variety of in situ data sets that TC Nargis, which formed over the Bay of Bengal in 2008 and caused large-scale destruction, intensified over a region with a BL and high SSTs. Several numerical studies have shown that the SST cooling at the surface could act as a negative feedback factor on TC intensity (Schade and Emanuel, 1999).

Track data from all the hurricane tracks in the tropical Atlantic for the period 1998-2007 is used and SST changes induced by these TCs is calculated using TRMM satellite daily SST. Then we consider the influence of the three most important factors for the surface ocean response to TCs, wind speed, storm speed and the MLD. It is found that, on an average, most cooling occurs in situations with a high wind speed, low storm speed and shallow MLD, consistent with the hypothesis of Price (1981). Next, we considered the SST change along the tracks and contrasted for situations with and without BLs. It is found that BLs reduce the SST cooling by nearly 48%. High resolution Hycom assimilation data was used to examine the modulation

of surface SST change by BLs for four Atlantic hurricanes, Philippe (2005), Wilma (2005), Omar (2008) and Bill (2009). Data from a couple of Argo floats was also used to examine the sub-surface hydrographic conditions for hurricanes Omar and Bill. When hurricanes pass over regions with thick BLs and with or without associated temperature inversions, the cooling induced at the surface may be alleviated or could even be weakly positive depending on the strength of the inversion, which consequently may act as a positive feedback for hurricane intensification.

We have also analyzed output from a high-resolution CRCM. To the best of our knowledge, our study is unique in using a coupled model of this complexity to investigate the SST response to TCs in the context of BLs. Our results indicate that the BL effect can lead to statistically significant weakened surface cooling in the wake of TCs. Moreover, in locations where the BL is associated with a temperature inversion, TC-induced mixing can result in weak surface warming. BLs considerably reduce the rightward bias in surface cooling for Tropical Storms, but the effect is less conspicuous for TCs. The PDF of the simulated change in SST associated with the passage of a TC indicates that the reduced thermal stratification associated with BLs considerably attenuates the surface cooling, reducing the amplitude of the cooling by nearly 35%. It is also seen that in the presence of BLs, the latent and sensible heat flux into the atmosphere increases by more than 16 % and reduce the increase in upper ocean potential energy due to TC induced mixing by nearly 25 %. These results further support our conclusions from the observational data analysis described earlier.

It has been suggested that, in the extratropics, in the presence of huge sub-surface temperature inversions, mixing due to polar lows can lead to an SST warming, which in turn can help in their intensification (Saetra et al., 2008). In the tropics, even though the maximum magnitude of temperature inversions is about one degree, it has

a similar effect on enthalpy flux transfer during a TC event. Apart from the western tropical Atlantic, persistent BLs also occur in the Western Pacific warmpool and the Bay of Bengal in the Northern Indian ocean (Sprintall and Tomczak, 1992), which are all TC formation regions. Previous studies have suggested that the knowledge of upper ocean thermal structure may help in the intensity forecasting of TCs (Goni and Trinanes, 2003). Our present study indicates that in the regions of BL formation, where salinity dominates the upper ocean density structure, the sub-surface haline structure may also play an important role in determining the SST response to TCs. Thus, our study suggests that prior knowledge of the prevailing BL conditions may help improve forecasts of TC intensity in these regions.

The variability of discharge from the Amazon and Orinoco river systems seems to be intimately related to major climatic phenomena like ENSO and the NAO at inter-annual and decadal timescales (Labat et al., 2005). Also we had seen earlier that one of the main reasons for BL formation in the western tropical Atlantic is the discharge due to these river systems. Fig. 55a shows the time-series correlation between the Nino 3.4 SST index and the SST anomaly averaged over the region between 70^0W to 50^0W and between 10^0N and 20^0N, which is part of the main development region for hurricanes. A 50-year monthly mean SODA time-series is used for this analysis. The indices are correlated at 0.47 with the Nino index leading the other by 5 months. The time-series correlation between BLT and SST anomalies is shown in Fig. 55b. A correlation coefficient higher than 0.1 is statistically significant. Regions of significant correlation exist indicating the considerable influence of the BL on the SST in this region, albeit not to the first order. It is well accepted that the Atlantic hurricane activity is related to the ENSO through factors like vertical wind-shear (Bove et al., 1998). However, the role of inter-annual variability of the surface ocean stratification in the western tropical Atlantic on that of the Atlantic hurricane activity has not been

explored to our knowledge. Vizy and Cook (2010) recently studied this problem using a regional atmospheric model and show the significance of the Amazon/Orinoco warm plume SSTs on the Atlantic climate system and hurricane activity. However, their model does not include complex coupled feedback mechanisms which are fundamental to the nature of this problem. Our study seems to suggest that BLs may play a role in the TC events through the modulation of SST response and consequently the air-sea flux transfer. Exploring potential relationships between the inter-annual variability of BL formation in the western tropical Atlantic and climatic phenomena like ENSO, NAO etc., might shed more light on this hitherto unknown aspect of Atlantic hurricane activity.

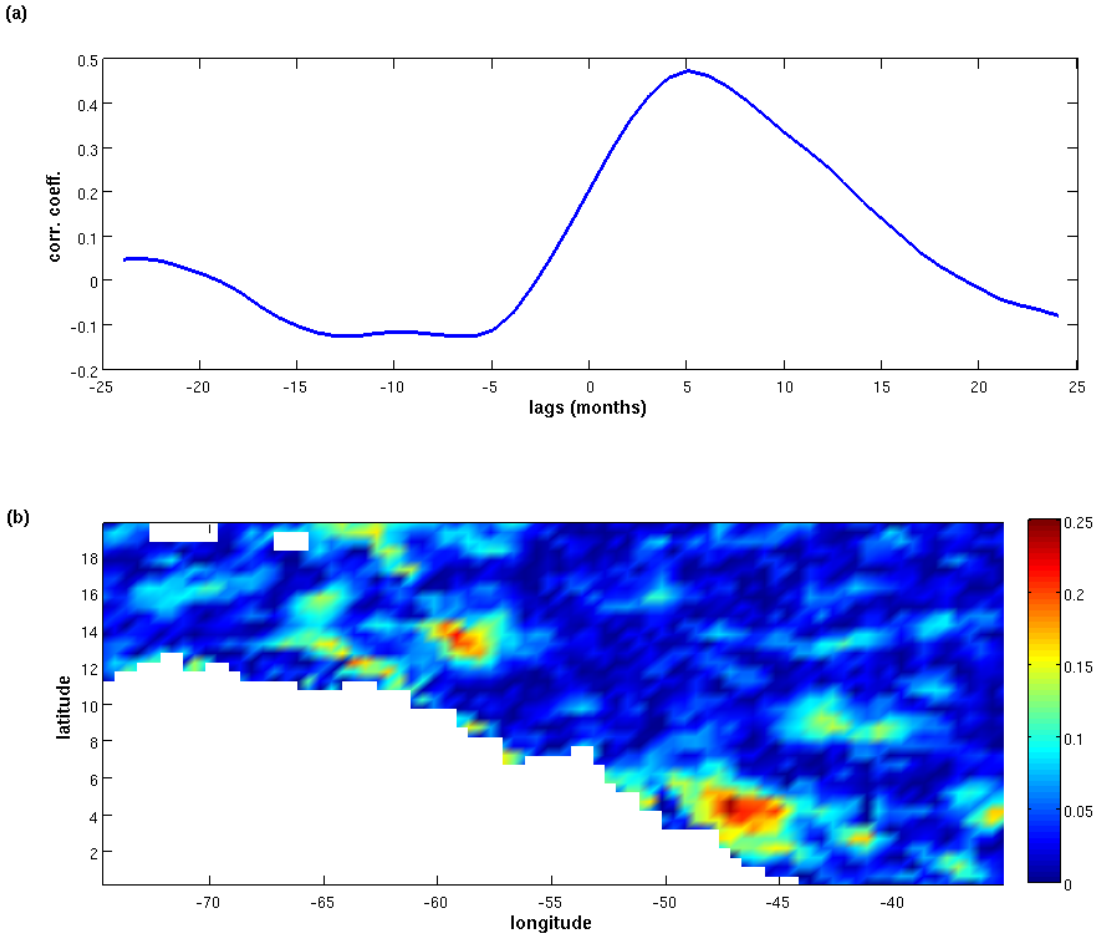

Fig. 55. (a) A time-series correlation between the Nino 3.4 index and the SST averaged over the region between 70^0W to 50^0W and 10^0N to 20^0N. Positive lag values indicate Nino index leads. (b) Time-series correlation between BLT and SST anomaly for the north-western tropical Atlantic. Values higher than 0.1 are statistically significant.

REFERENCES

Bao, J., J. Wilczak, J. Choi, and L. Kantha, 2000: Numerical simulations of air-sea interaction under high wind conditions using a coupled model: A study of hurricane development. *Monthly Weather Review*, **128**, 2190–2210.

Baumgartner, A., E. Reichel, and R. Lee, 1975: *The World Water Balance: Mean Annual Global, Continental and Maritime Precipitation, Evaporation and Run-off.* Elsevier, Amsterdam.

Bender, M. and I. Ginis, 2000: Real-case simulations of hurricane-ocean interaction using a high-resolution coupled model: Effects on hurricane intensity. *Monthly Weather Review*, **128**, 917–946.

Blanke, B., M. Arhan, A. Lazar, and G. Prévost, 2002: A Lagrangian numerical investigation of the origins and fates of the salinity maximum water in the Atlantic. *Journal of Geophysical Research*, **107**, 1–15.

Bove, M., J. O'Brien, J. Eisner, C. Landsea, X. Niu, et al., 1998: Effect of El Niño on US landfalling hurricanes, revisited. *Bulletin of the American Meteorological Society*, **79**, 2477–2482.

Breugem, W., P. Chang, C. Jang, J. Mignot, and W. Hazeleger, 2008: Barrier layers and tropical Atlantic SST biases in coupled GCMs. *Tellus A*, **60**, 885–897.

Camargo, S. and S. Zebiak, 2002: Improving the detection and tracking of tropical cyclones in atmospheric general circulation models. *Weather and Forecasting*, **17**, 1152–1162.

Carton, J., G. Chepurin, and X. Cao, 2000a: A simple ocean data assimilation analysis of the global upper ocean 1950-1995 Part 2: Results. *Journal of Physical Oceanography*, **30**, 311–326.

Carton, J., G. Chepurin, X. Cao, and B. Giese, 2000b: A simple ocean data assimilation analysis of the global upper ocean 1950-1995, Part 1: Methodology. *Journal of Physical Oceanography*, **30**, 294–309.

Carton, J. and Z. Zhou, 1997: Annual cycle of sea surface temperature in the tropical Atlantic Ocean. *Journal of Geophysical Research*, **102**, 27813–27824.

Chan, J., Y. Duan, and L. Shay, 2001: Tropical cyclone intensity change from a simple ocean-atmosphere coupled model. *Journal of the Atmospheric Sciences*, **58**, 154–172.

Chang, P., Y. Fang, R. Saravanan, L. Ji, and H. Seidel, 2006: The cause of the fragile relationship between the Pacific El Niño and the Atlantic Niño. *Nature*, **443**, 324–328.

Cione, J. and E. Uhlhorn, 2003: Sea surface temperature variability in hurricanes: Implications with respect to intensity change. *Monthly Weather Review*, **131**, 1783–1796.

Collins, W., M. Blackmon, G. Bonan, J. Hack, T. Henderson, et al., 2006: The community climate system model version 3 (CCSM3). *Journal of Climate*, **19**, 2122–2143.

de Boyer Montégut, C., J. Mignot, A. Lazar, and S. Cravatte, 2007: Control of salinity on the mixed layer depth in the world ocean: 1. General description. *Journal of Geophysical Research*, **112**, C06011, doi:10.1029/2006JC003953.

Defant, A., 1961: *Physical Oceanography*. Elsevier, New York.

DeMaria, M., 1996: The effect of vertical shear on tropical cyclone intensity change. *Journal of the Atmospheric Sciences*, **53**, 2076–2087.

Denman, K., 1973: A time-dependent model of the upper ocean. *Journal of Physical Oceanography*, **3**, 173–184.

DeWitt, D., 2005: Diagnosis of the tropical Atlantic near-equatorial SST bias in a directly coupled atmosphere-ocean general circulation model. *Geophysical Research Letters*, **32**, L01703.

Dorman, C. and R. Bourke, 1981: Precipitation over the Atlantic Ocean, 30 S to 70 N. *Monthly Weather Review*, **109**, 554–563.

Emanuel, K., 1986: An air-sea interaction theory for tropical cyclones. Part I: Steady-state maintenance. *Journal of the Atmospheric Sciences*, **43**, 585–604.

Emanuel, K., 2001: Contribution of tropical cyclones to meridional heat transport by the oceans. *Journal of Geophysical Research*, **106**, 14771–14781.

Emanuel, K., 2003: Tropical cyclones. *Annual Review of Earth and Planetary Sciences*, **31**, 75–104.

Emanuel, K., 2005: Increasing destructiveness of tropical cyclones over the past 30 years. *Nature*, **436**, 686–688.

Fedorov, A., C. Brierley, and K. Emanuel, 2010: Tropical cyclones and permanent El Niño in the early Pliocene epoch. *Nature*, **463**, 1066–1070.

Ffield, A., 2007: Amazon and Orinoco River plumes and NBC rings: Bystanders or participants in hurricane events? *Journal of Climate*, **20**, 316–333.

Foltz, G. and M. McPhaden, 2009: Impact of barrier layer thickness on SST in the central tropical North Atlantic. *Journal of Climate*, **22**, 285–299.

Gallacher, P., R. Rotunno, and K. Emanuel, 1989: Tropical cyclogenesis in a coupled ocean–atmosphere model. *18th Conf. on Hurricanes and Tropical Meteorology*, May 16–19, San Diego, CA, Amer. Meteor. Soc, 121–122.

Gent, P. and J. Mcwilliams, 1990: Isopycnal mixing in ocean circulation models. *Journal of Physical Oceanography*, **20**, 150–155.

Godfrey, J. and E. Lindstrom, 1989: The heat budget of the equatorial western Pacific surface mixed layer. *Journal of Geophysical Research*, **94**, 8007–8017.

Goni, G. and J. Trinanes, 2003: Ocean thermal structure monitoring could aid in the intensity forecast of tropical cyclones. *Eos Trans. AGU*, **84**, 573–580.

Greatbatch, R., 1983: On the response of the ocean to a moving storm: The nonlinear dynamics. *Journal of Physical Oceanography*, **13**, 357–367.

Hazeleger, W. and R. Haarsma, 2005: Sensitivity of tropical Atlantic climate to mixing in a coupled ocean–atmosphere model. *Climate Dynamics*, **25**, 387–399.

Hellweger, F. and A. Gordon, 2002: Tracing Amazon River water into the Caribbean Sea. *Journal of Marine Research*, **60**, 537–549.

Hu, C., E. Montgomery, R. Schmitt, and F. Muller-Karger, 2004: The dispersal of the Amazon and Orinoco River water in the tropical Atlantic and Caribbean Sea: Observation from space and S-PALACE floats. *Deep Sea Research Part II: Topical Studies in Oceanography*, **51**, 1151–1171.

Huang, B., Z. Hu, and B. Jha, 2007: Evolution of model systematic errors in the Tropical Atlantic Basin from coupled climate hindcasts. *Climate Dynamics*, **28**, 661–682.

Huffman, G., R. Adler, P. Arkin, A. Chang, R. Ferraro, et al., 1997: The global precipitation climatology project (GPCP) combined precipitation dataset. *Bulletin of the American Meteorological Society*, **78**, 5–20.

Jansen, M. and R. Ferrari, 2009: Impact of the latitudinal distribution of tropical cyclones on ocean heat transport. *Geophysical Research Letters*, **36**, L06604.

Jochum, M. and P. Malanotte-Rizzoli, 2003: On the generation of North Brazil current rings. *Journal of Marine Research*, **61**, 147–173.

Kalnay, E., M. Kanamitsu, R. Kistler, W. Collins, D. Deaven, et al., 1996: The NCEP/NCAR 40-year reanalysis project. *Bulletin of the American Meteorological Society*, **77**, 437–471.

Khain, A. and I. Ginis, 1991: The mutual response of a moving tropical cyclone and the ocean. *Beitraege zur Physik der Atmosphaere*, **64**, 125–141.

Knutson, T., R. Tuleya, W. Shen, and I. Ginis, 2001: Impact of CO2-induced warming on hurricane intensities as simulated in a hurricane model with ocean coupling. *Journal of Climate*, **14**, 2458–2468.

Korty, R., K. Emanuel, and J. Scott, 2008: Tropical cyclone-induced upper-ocean mixing and climate: Application to equable climates. *Journal of Climate*, **21**, 638–654.

Kraus, E. and J. Turner, 1967: A one-dimensional model of the seasonal thermocline II. The general theory and its consequences. *Tellus*, **19**, 98–106.

Labat, D., J. Ronchail, and J. Guyot, 2005: Recent advances in wavelet analyses: Part 2–Amazon, Parana, Orinoco and Congo discharges time scale variability. *Journal of Hydrology*, **314**, 289–311.

Large, W. and G. Danabasoglu, 2006: Attribution and impacts of upper-ocean biases in CCSM3. *Journal of Climate*, **19**, 2325–2346.

Large, W., J. McWilliams, and S. Doney, 1994: Oceanic vertical mixing: A review and a model with a nonlocal boundary layer parameterization. *Reviews of Geophysics*, **32**, 363–403.

Large, W. and S. Yeager, 2004: *Diurnal to Decadal Global Forcing for Ocean and Sea-ice Models: The Data Sets and Flux Climatologies*. National Center for Atmospheric Research, Boulder.

Levitus, S., 1982: *Climatological Atlas of the World Oceans*. US Government Printing Office, Washington, DC.

Lin, I., W. Liu, C. Wu, J. Chiang, and C. Sui, 2003a: Satellite observations of modulation of surface winds by typhoon-induced upper ocean cooling. *Geophysical Research Letters*, **30**, 1131, doi:10.1029/2002GL015 674.

Lin, I., W. Liu, C. Wu, G. Wong, C. Hu, et al., 2003b: New evidence for enhanced ocean primary production triggered by tropical cyclone. *Geophysical Research Letters*, **30**, 1718, doi:10.1029/2003GL017141.

Lukas, R. and E. Lindstrom, 1991: The mixed layer of the western equatorial Pacific Ocean. *Journal of Geophysical Research*, **96**, 3343–3357.

Madin, J. and S. Connolly, 2006: Ecological consequences of major hydrodynamic disturbances on coral reefs. *Nature*, **444**, 477–480.

Maes, C., K. Ando, T. Delcroix, W. Kessler, M. McPhaden, and D. Roemmich, 2006: Observed correlation of surface salinity, temperature and barrier layer at the eastern edge of the western Pacific warm pool. *Geophysical Research Letters*, **33**, L06601, doi:10.1029/2005GL024772.

Maes, C., J. Picaut, and S. Belamari, 2002: Salinity barrier layer and onset of El Nino in a Pacific coupled model. *Geophysical Research Letters*, **29**, 2206, doi:10.1029/2002GL016029.

Masson, S. and P. Delecluse, 2001: Influence of the Amazon River runoff on the tropical Atlantic. *Physics and Chemistry of the Earth, Part B: Hydrology, Oceans and Atmosphere*, **26**, 137–142.

Masson, S., J. Luo, G. Madec, J. Vialard, F. Durand, et al., 2005: Impact of barrier layer on winter-spring variability of the southeastern Arabian Sea. *Geophysical Research Letters*, **32**, L07703, doi:10.1029/2004GL021980.

McPhaden, M., G. Foltz, T. Lee, V. Murty, M. Ravichandran, et al., 2009: Ocean-atmosphere interactions during cyclone Nargis. *Eos*, **90**, 53–60.

Mignot, J., C. de Boyer Montégut, A. Lazar, and S. Cravatte, 2007: Control of salinity on the mixed layer depth in the world ocean: 2. Tropical areas. *Journal of Geophysical Research*, **112**, C10010, doi:10.1029/2006JC003954.

Miller, J., 1976: The salinity effect in a mixed layer ocean model. *Journal of Physical Oceanography*, **6**, 29–35.

Moisan, J. and P. Niiler, 1998: The seasonal heat budget of the North Pacific: Net heat flux and heat storage rates (1950-1990). *Journal of Physical Oceanography*, **28**, 401–421.

Morey, S., M. Bourassa, D. Dukhovskoy, and J. OBrien, 2006: Modeling studies of the upper ocean response to a tropical cyclone. *Ocean Dynamics*, **56**, 594–606.

Munk, W. and C. Wunsch, 1998: Abyssal recipes II: Energetics of tidal and wind mixing. *Deep-Sea Research Part I*, **45**, 1977–2010.

Oberhuber, J., 1988: An atlas based on the COADS data set: The budgets of heat, buoyancy and turbulent kinetic energy at the surface of the global ocean, Rep. 15. Max–Planck–Institut für Meteorologie, Hamburg, Germany.

O'Brien, J., 1967: The non-linear response of a two-layer, baroclinic ocean to a stationary, axially-symmetric hurricane. Part II. Upwelling and mixing induced by momentum transfer. *Journal of Atmospheric Sciences*, **24**, 208–214.

Ohlmann, J. C., 2003: Ocean Radiant Heating in Climate Models. *Journal of Climate*, **16**, 1337–1351.

Pailler, K., B. Bourlès, and Y. Gouriou, 1999: Barrier layer in the western Tropical Atlantic Ocean. *Geophysical Research Letters*, **26**, 2069–2072.

Pasquero, C. and K. Emanuel, 2010: Tropical cyclones and transient upper-ocean warming. *Journal of Climate*, **21**, 149–162.

Price, J., 1981: Upper ocean response to a hurricane. *Journal of Physical Oceanography*, **11**, 153–175.

Richter, I. and S. Xie, 2008: On the origin of equatorial Atlantic biases in coupled general circulation models. *Climate Dynamics*, **31**, 587–598.

Saetra, O., T. Linders, and J. Debernard, 2008: Can polar lows lead to a warming of the ocean surface? *Tellus A*, **60**, 141–153.

Saravanan, R. and P. Chang, 2000: Interaction between tropical Atlantic variability and El Nino-Southern Oscillation. *Journal of Climate*, **13**, 2177–2194.

Sarmiento, J., R. Slater, R. Barber, L. Bopp, S. Doney, et al., 2004: Response of ocean ecosystems to climate warming. *Global Biogeochemical Cycles*, **18**, GB3003, doi:10.1029/2003GB002134.

Schade, L. and K. Emanuel, 1999: The ocean's effect on the intensity of tropical cyclones: Results from a simple coupled atmosphere-ocean model. *Journal of the Atmospheric Sciences*, **56**, 642–651.

Sengupta, D., B. Goddalehundi, and D. Anitha, 2008: Cyclone-induced mixing does not cool SST in the post-monsoon north Bay of Bengal. *Atmospheric Science Letters*, **9**, 1–6.

Shay, L., G. Goni, and P. Black, 2000: Effects of a warm oceanic feature on Hurricane Opal. *Monthly Weather Review*, **128**, 1366–1383.

Smith, T. and R. Reynolds, 2004: Improved extended reconstruction of SST (1854-1997). *Journal of Climate*, **17**, 2466–2477.

Sprintall, J. and M. Tomczak, 1992: Evidence of the barrier layer in the surface layer of the tropics. *Journal of Geophysical Research*, **97**, 7305–7316.

Sriver, R. and M. Huber, 2007: Observational evidence for an ocean heat pump induced by tropical cyclones. *Nature*, **447**, 577–580.

Vizy, E. and K. Cook, 2010: Influence of the Amazon/Orinoco Plume on the summertime Atlantic climate. *Journal of Geophysical Research*, **115**, D21112, doi:10.1029/2010JD014049.

Xie, S. and S. Philander, 1994: A coupled ocean-atmosphere model of relevance to the ITCZ in the eastern Pacific. *Tellus A*, **46**, 340–350.

Zedler, S., 2009: Simulations of the ocean response to a hurricane: Nonlinear processes. *Journal of Physical Oceanography*, **39**, 2618–2634.

Zhang, S., A. Rosati, and M. Harrison, 2009: Detection of multidecadal oceanic variability by ocean data assimilation in the context of a perfect coupled model. *Journal of Geophysical Research*, **114**, C12018, doi:10.1029/2008JC005261.

Zhu, T. and D. Zhang, 2006: The impact of the storm-induced SST cooling on hurricane intensity. *Advances in Atmospheric Sciences*, **23**, 14–22.

APPENDIX

If X_1 and X_2 are two sample vectors with sizes N_1 and N_2, with standard deviations S_1 and S_2 and with means $\bar{X_1}$ and $\bar{X_2}$, then the t value to check for the statistical significance of the difference of means is estimated as

$$t = \frac{\bar{X_1} - \bar{X_2}}{\sigma\sqrt{\frac{1}{N_1} + \frac{1}{N_2}}}$$

where the combined standard deviation σ is given as

$$\sigma = \sqrt{\frac{N_1 {S_1}^2 + N_2 {S_2}^2}{\nu}}$$

and the number of degrees of freedom is given as

$$\nu = N_1 + N_2 - 2$$

VITA

Karthik Balaguru received both his Bachelor of Technology and Master of Technology degrees from the Department of Ocean Engineering, Indian Institute of Technology - Madras, India in 2006. He entered the Department of Oceanography at Texas A&M University in August 2006 and earned his Ph.D. in May 2011.

Karthik may be reached at the Department of Oceanography, 3146 TAMU, Texas A&M University, College Station, Texas-77843-3146. His email is karthiknaidu@tamu.edu